ANALYSIS OF INTERACTIONS BETWEEN THE GERMLINE RNA HELICASES (GLHs) AND THEIR REGULATORS KGB-1 AND CSN-5 IN *CAENORHABDITIS ELEGANS*

A Dissertation

presented to

the Faculty of the Graduate School

University of Missouri-Columbia

In Partial Fulfillment

Of the Requirements for the Degree

Doctor of Philosophy

---

by

APRIL MARIE ORSBORN

Dr. Karen Bennett, Dissertation Supervisor

AUGUST 2006

The undersigned, appointed by the Dean of the Graduate Faculty, have examined the dissertation entitled

ANALYSIS OF INTERACTIONS BETWEEN THE GERMLINE RNA HELICASES (GLHs) AND THEIR REGULATORS KGB-1 AND CSN-5 IN *CAENORHABDITIS ELEGANS*

Presented by APRIL MARIE ORSBORN

a candidate for the degree of DOCTOR OF PHILOSOPHY

and hereby certify that in their opinion it is worthy of acceptance

_____

Karen Bennett, PhD Dissertation Supervisor

_____

Mark Hannink, PhD

_____

Catherine Krull, PhD

_____

David Pintel, PhD

_____

John Cannon, PhD

AKNOWLEDGEMENTS

For advice and support, I would like to thank all the members of the Molecular Microbiology and Immunology department. I am most grateful for the support, guidance, and encouragement of my advisor, Dr. Karen Bennett, without whose expertise this work would have been impossible. The members of my committee: Dr. John Cannon, Dr. David Pintel, Dr. Mark Hannink, and Dr. Cathy Krull have been extremely helpful and their advice and criticism have been very useful to me. The MMI office staff has been great, providing help and a smile whenever I needed it. I must thank my predecessor, Pliny Smith, who helped me learn basic techniques during my rotation and provided me with numerous reagents that have been vital in completing this work. I thank former technician Ruth Montgomery for all her help and friendship. Wensheng Li, a former post-doctoral researcher in the lab, was of immense help for the GLH-1 protein level studies and Eugene Kuzmin helped with northern analysis. A number of undergraduate researchers have helped me on various projects over the years, including Reagan Barnes, Christopher Yee, Cecelia Koetting, James Chou and Holly Boedefeld. Current members of the lab Ge Gao, Erica Racen and Tamara McEwan have been very helpful and their friendship has been invaluable. I thank my fellow MMI graduate students, past and present, for all the fun, laughs, advice, support and sharing of reagents. Last, but not least, I thank my family for standing by me, for supporting me through good and bad, for always believing in me, and my fiancé Matthew Bauer for his kindness, laughter and love.

TABLE OF CONTENTS

LIST OF ABBREVIATIONS AND GLOSSARY

N2	wild type *Caenorhabditis elegans*
L1, L2, L3, or L4	first, second, third or fourth larval stage
GLH	germline RNA helicase
KGB	kinase that GLHs bind
CSN	COP9 signalosome
ZXY	Zyxin
GST	Glutathione-S-Transferase
6-His	Sequence tag of six consecutive histidine residues
CYE	*C. elegans* Cyclin E homolog
glp	germline proliferation defective
fem	feminization
RNAi	RNA interference (dsRNA)
DTC	distal tip cell
SDM	Site directed mutagenesis
Blastomeres	cells of the early embryo
D site	MAPK docking site
Phosphodegron	Peptide sequence that when phosphorylated helps target proteins for degradation
P value	measure of significance by Student's T test, less than 0.05 is generally considered statistically significant

M+/Z-	maternal positive/zygotic negative: having a maternal contribution of a given protein but no zygotic production
M-/Z-	having neither maternal nor zygotic production of a protein
α	anti (for antibody indications)
Nomenclature:	*C. elegans* genes, mutant alleles, and RNAs are italicized (*glh-1*), proteins are in all capital letters (GLH-1). *Drosophila* genes are italicized (*vasa*) and proteins have first letter capitalized and italicized (*Vasa*)

LIST OF TABLES

LIST OF FIGURES

CHAPTER 1: INTRODUCTION

Reproduction is the fundamental biological purpose of all living creatures. Sexual reproduction facilitates species survival. The tissue responsible for continuing a species, the germline, is therefore of crucial consequence to an animal. The germline must be totipotent, able to give rise to every cell type in the organism; it is responsible for transmitting the genome to future generations by ensuring the health and viability of its offspring. The germline of the free-living, soil nematode *Caenorhabditis elegans* is an excellent model for studying reproductive biology and germline development, as will be discussed below.

Caenorhabditis elegans

C. elegans are small (1mm in length) transparent worms in the phylum *Nematoda* (Figure 1.1). *C. elegans* has many traits that make it an excellent model system. When Sydney Brenner began working with *C. elegans* in 1965, he recognized that worms were easy to maintain in the laboratory, quick growing (see *C. elegans* timeframes in Figures 1.2 and 1.3 and Table 1.1), hermaphroditic with a subset of the population composed of males, making mating and maintaining strains simple (Brenner 1974). As *C. elegans* worms are transparent, the invariant cell-fate lineage was determined from the one cell embryo, to the 959 cells of the adult hermaphrodite (Sulston et al. 1983). This cell fate map has proved invaluable for understanding the development of *C.*

Figure 1.1: Adult *C. elegans* worms. Top A. Nomarski optics of an adult *C. elegans* hermaphrodite with embryos. Scale bar 0.1mm. B. Cartoon of *C. elegans* hermaphrodite anatomy. Bottom A. Cartoon of adult male *C. elegans* anatomy. B. Nomarski optics of adult *C. elegans* male. C. Enlargement of the unilobed distal gonad. D. Ventral view of male tail; arrow cloaca, arrowhead fan. E. Tale of a fourth larval (L4) stage male (top) compared to that of a third larval (L3) stage male (bottom). Figures adapted from www.wormatlas.org

Top

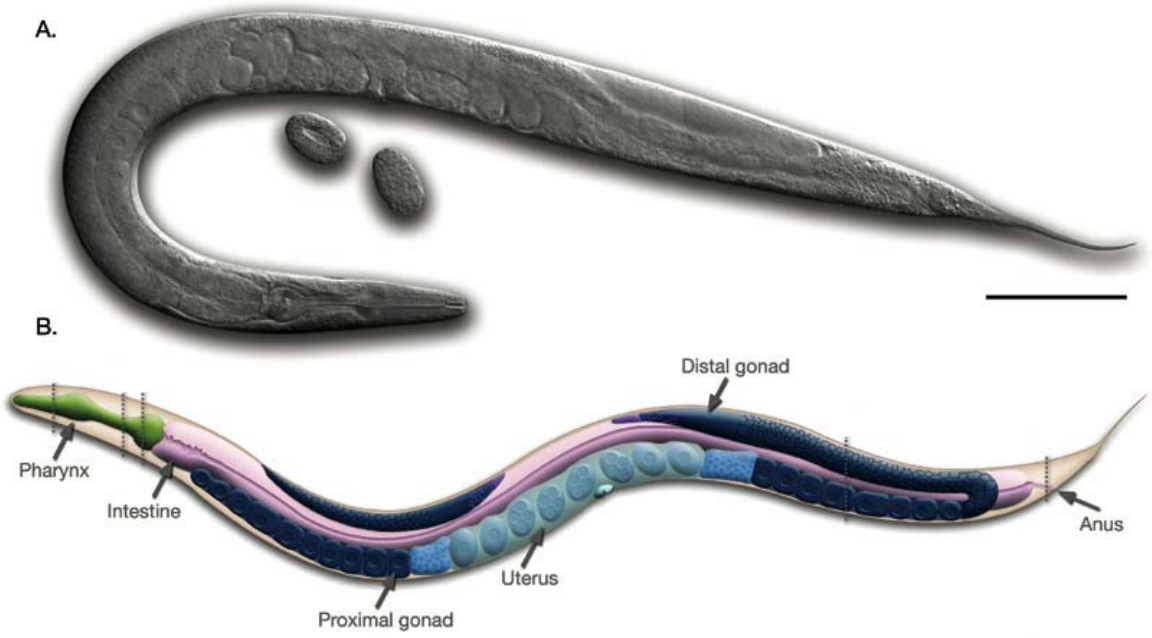
A.
B.
Distal gonad
Pharynx
Intestine
Anus
Uterus
Proximal gonad

Bottom

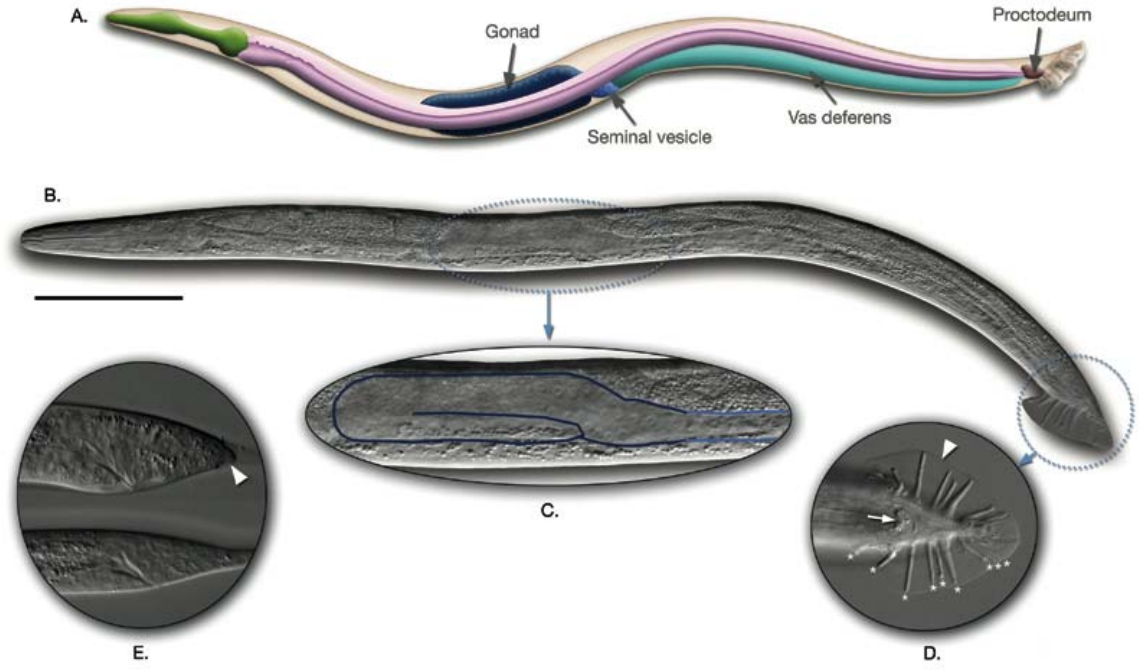
A.
Gonad
Proctodeum
Vas deferens
Seminal vesicle
B.
C.
E.
D.

Figure 1.2: Timeline of *C. elegans* embryogenesis. Numbers on line indicate number of minutes post-fertilization. Adapted from www.wormatlas.org.

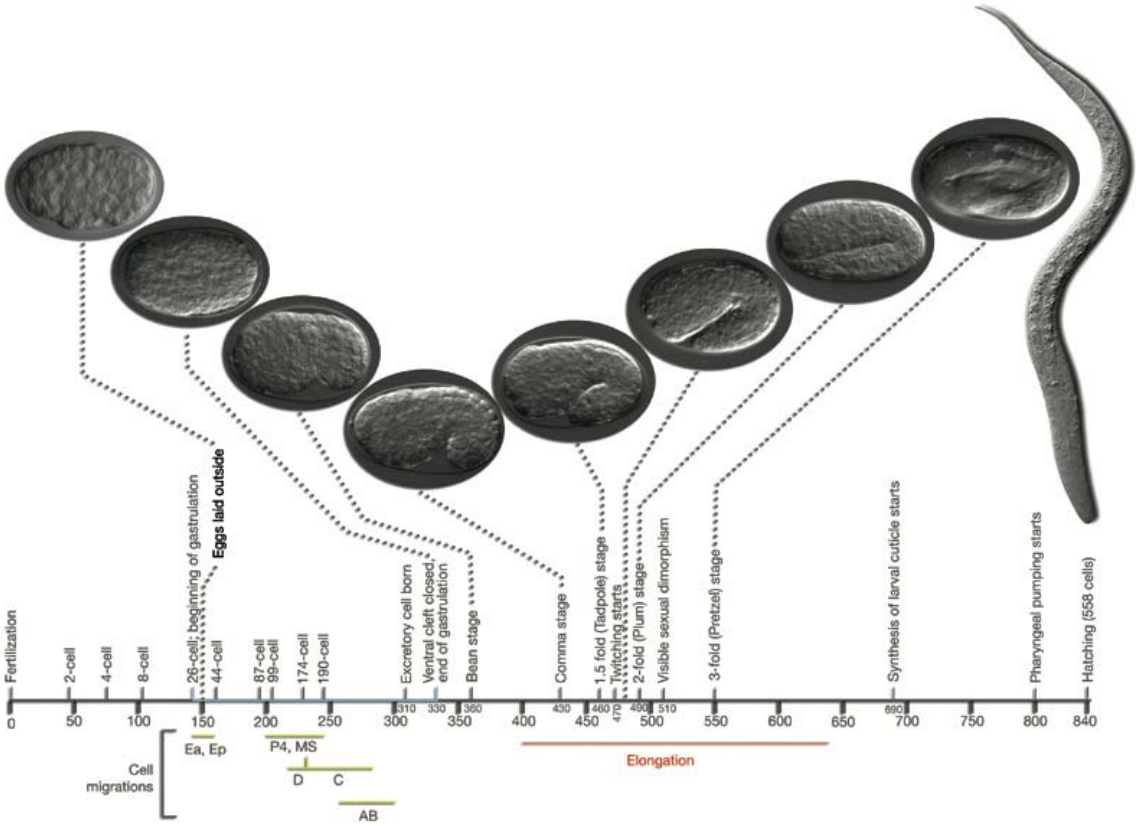

Figure 1.3: *C. elegans* life cycle. From fertilization to adult worm shown at 22°C. Alternate pathway for dauer development shown in cases of starvation, overpopulation, or temperature stress. Adapted from www.wormatlas.org.

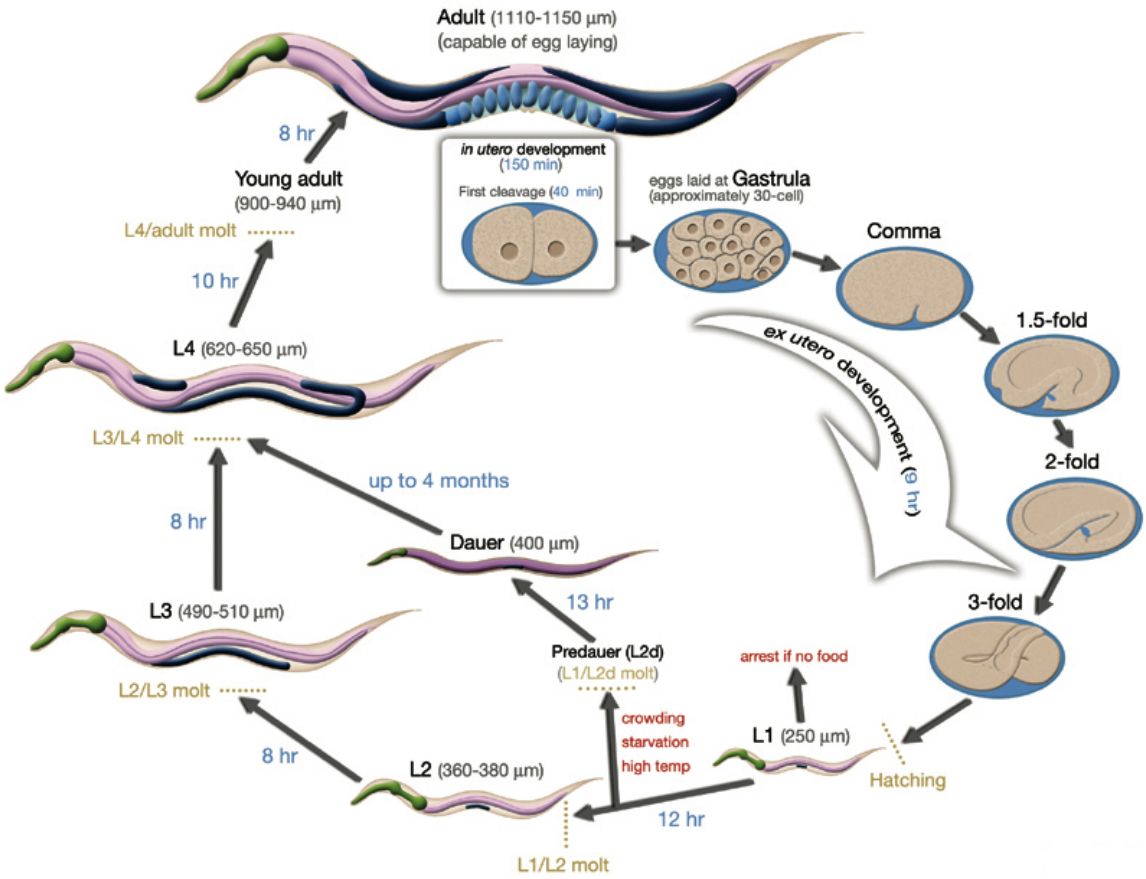

Table 1.1: *C. elegans* life cycle timeline at different temperatures. h=hours. Adapted from (Epstein and Shakes 1995).

Growth Parameters of the *Caenorhabditis elegans* Life Cycle[a]

Temperature (°C)	Embryogenesis (h)	Molts (h posthatch)				First eggs laid (h posthatch)
		L1–L2	L2–L3	L3–L4	L4–adult	
16	29[b]	24	39	54.5	74.5	94–97
20	18[b]	15	24	34	46	59–60
25	14	11.5	18.5	26	35.5	45–46

[a] Based on Hirsh *et al.* (1976, Fig. 2).
[b] Calculated by multiplying 25°C embryongenesis time by 20 and 16°C growth rate factors of 1.3 and 2.1, respectively.

elegans, and provided key evidence for programmed cell death as a normal biological process.

In addition to its physical attributes, *C. elegans* is an extremely amenable system for genetic work. The *C. elegans* genome, which is composed of six chromosomes, autosomes I-V and the sex chromosome X, was the second eukaryote and first animal to be completely sequenced (Consortium 1998). Additionally, the *C. elegans* community has a great resource in www.wormbase.org, a website and database system that catalogs information on all *C. elegans* genes and their products. The curators of wormbase are continually updating the annotation of the *C. elegans* genome, and adding sequence information for other nematode species as it becomes available. Extensive work has also been done to identify expressed genes in *C. elegans*, with a large cDNA library available to researchers. Dr. Yuji Kohara's group curates these cDNAs and has been using them to perform *in situ* analysis of all expressed genes in the worm. Images from this work are freely available to the scientific community.

The large amount of sequence information available has facilitated functional studies. The *C. elegans* Knock-Out Consortium uses reverse genetics to screen large scale mutagenized libraries of worms for deletions in requested genes. Additionally, RNA interference (RNAi) has been used widely in *C. elegans*. By injecting, feeding, or soaking worms with dsRNA we can knock-down expression of the corresponding endogenous transcript, allowing us to examine the consequences of a given protein's loss. Large scale screens have

been carried out by RNAi, and any identified phenotypes are available through wormbase (for example see (Maeda et al. 2001)).

Germline development

C. elegans is an excellent system for studying germline development. A great deal of a worm's volume is occupied by the germline (Figure 1.1), illustrating the importance of reproduction in the *C. elegans* lifecycle. The worm germline is composed of a single bi-lobed gonad, which has two equivalent U-shaped arms (Figure 1.4). The development of this organ has been studied extensively. Germline development begins in very early embryos with the birth of the P_4 cell; this cell will divide one more time during embryogenesis, giving rise to the Z2 and Z3 cells. These two cells will give rise to the entire adult germline (Figures 1.4 and 1.5). The germline cell nuclei divide mitotically, surrounding a central anucleate core, called the rachis, resulting in a syncytium in which the germ cell nuclei are only partially cellularized. By the fourth larval stage (L4), the germ cell nuclei enter meiosis and produce sperm, the sperm are then stored in the spermatheca. This is the only time during a hermaphrodite's life that sperm will be produced, so the number of sperm made at this stage limits the number of progeny that can be produced, unless mating with a male occurs.

Once sperm production is complete, the germ cell nuclei begin oocyte production. In the distal region of the germline (farthest from the vulva), germ cell nuclei continue to divide mitotically, maintaining a stem cell pool (Figure 1.4 and 1.5). The somatic distal tip cell (DTC) makes contact with the germ cell

Figure 1.4: *C. elegans* germline development. The Z2 and Z3 cells born during embryogenesis give rise to the entire adult germline. DTC= distal tip cell, sp=spermatheca. Adapted from www.wormatlas.org.

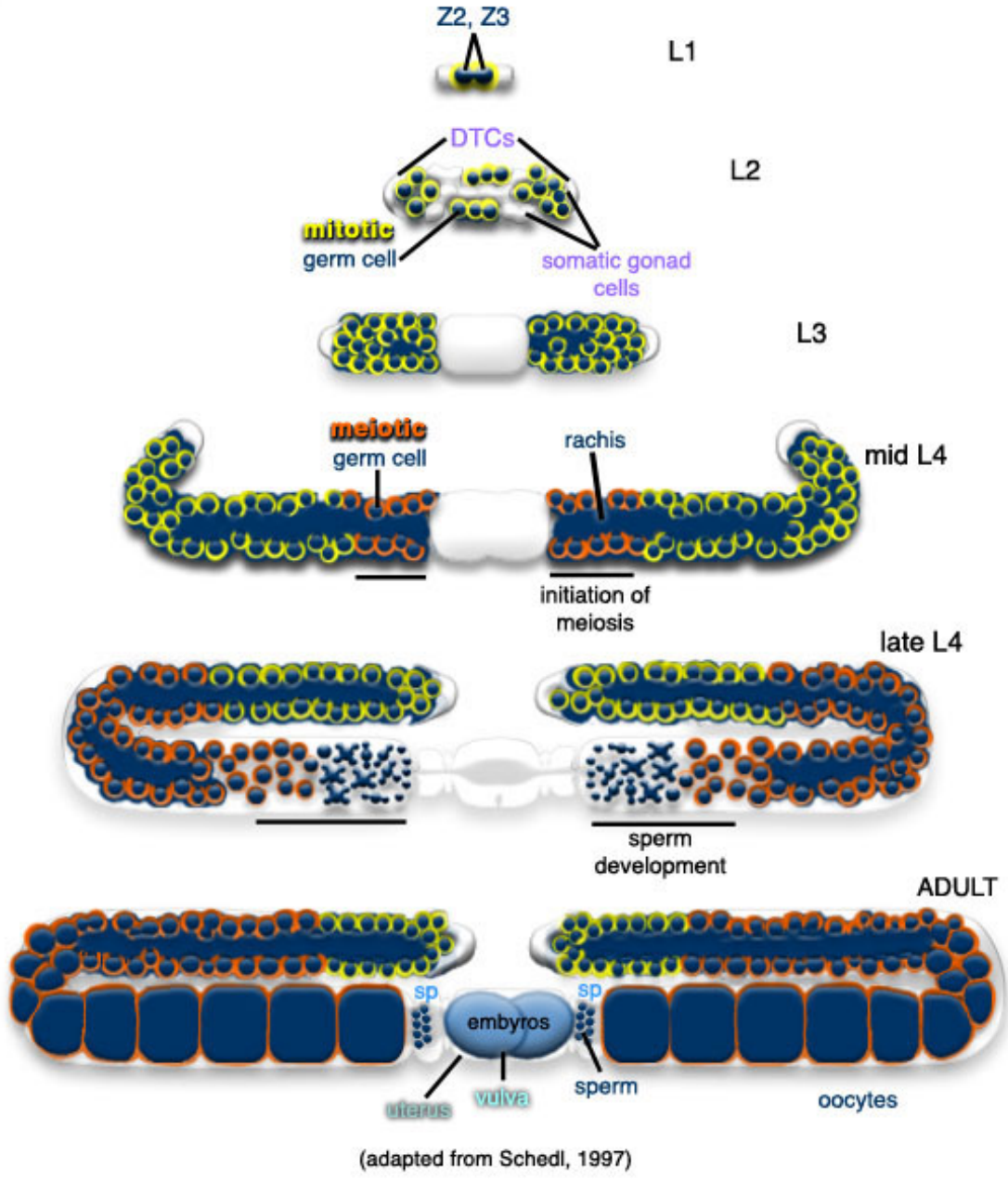

(adapted from Schedl, 1997)

Figure 1.5: DAPI staining of *C. elegans* adult germline. Top large panel: a composite image of from three gonads, showing the layout of one lobe of the adult germline, stained with DAPI to show nuclei. DG=distal gonad, DTC=distal tip cell, PCD=programmed cell death. Smaller panels: stages of mitosis and meiosis. From top left: distal end of gonad where mitosis takes place, mitotic bodies are visible as more condensed DAPI staining structures. Top right: the transition zone, where nuclei change from dividing mitotically to meiototically. A tell-tale sign of nuclei in transition is the crescent appearance where chromosomes condense on one side of the nucleus. Bottom left: pachytene stage, as condensed chromosomes re-disperse to the periphery of the nucleus, at this stage chromosomes take on “bowl of spaghetti” distribution. Bottom right: developing oocytes after pachytene progress to the diplotene stage where sister chromosomes are paired. Oogenesis concludes with diakinesis where chromosomes are at their most condensed and paired. Oocytes arrest at this stage in preparation for fertilization. Adapted from www.wormatlas.org.

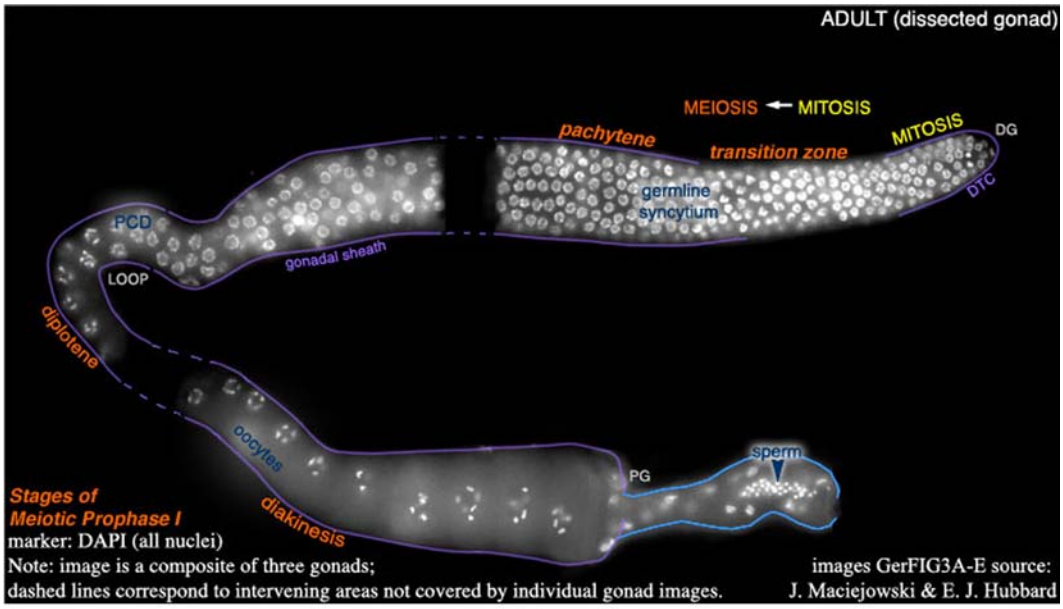
ADULT (dissected gonad)
MEIOSIS ← MITOSIS
pachytene
transition zone
MITOSIS
DG
DTC
germline syncytium
PCD
gonadal sheath
LOOP
diplotene
oocytes
PG
sperm
diakinesis
Stages of Meiotic Prophase I
marker: DAPI (all nuclei)
Note: image is a composite of three gonads;
dashed lines correspond to intervening areas not covered by individual gonad images.
images GerFIG3A-E source:
J. Maciejowski & E. J. Hubbard

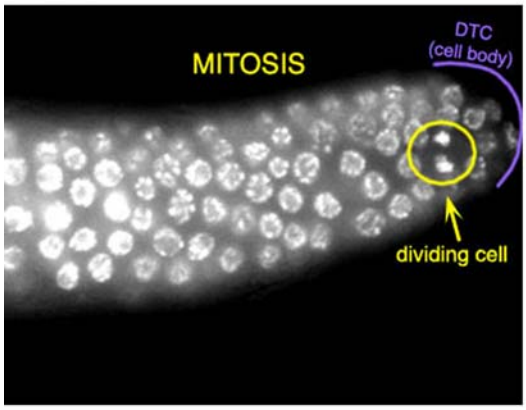
MITOSIS
DTC
(cell body)
dividing cell

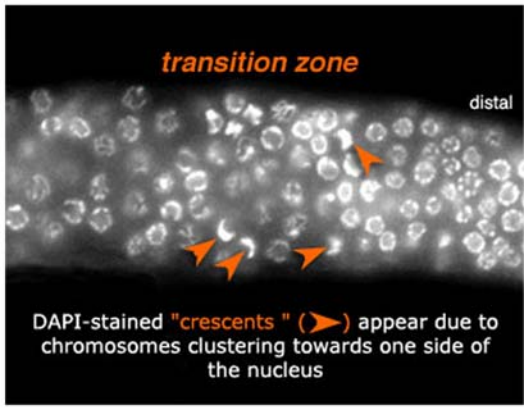
transition zone
distal
DAPI-stained "crescents " ( ) appear due to chromosomes clustering towards one side of the nucleus

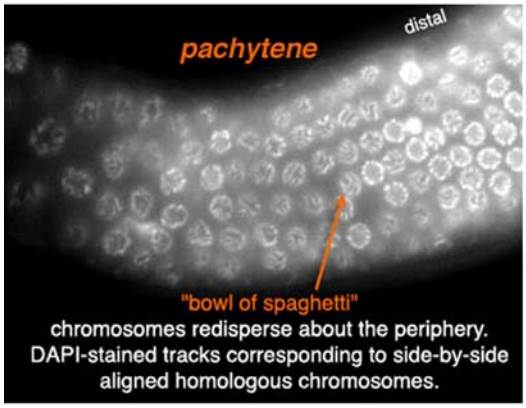
pachytene
distal
"bowl of spaghetti"
chromosomes redisperse about the periphery.
DAPI-stained tracks corresponding to side-by-side aligned homologous chromosomes.

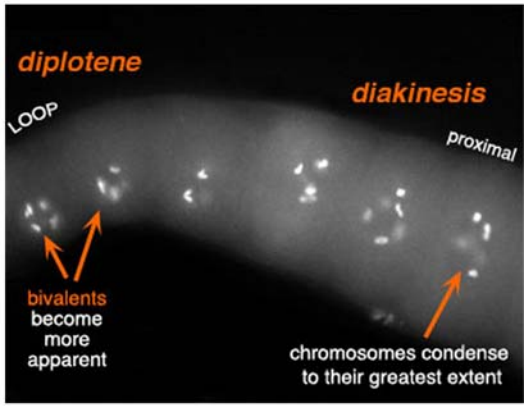
diplotene
diakinesis
LOOP
proximal
bivalents become more apparent
chromosomes condense to their greatest extent

nuclei in the distal end of the gonad and is thought to provide signals that maintain mitotic divisions (reviewed in (Crittenden et al. 2003)). After the mitotic divisions, germ cell nuclei progress proximally through the gonad, undergoing meiosis. The various stages of germ cell nuclei development are apparent by staining germlines with 4'-6'-diamidino-2-phenylindole (DAPI) a dye that stains DNA (Figure 1.5). After completion of meiosis I, oocytes cellularize, continue to grow in size and mature. Oocytes are fertilized as they pass through the spermatheca, move on to the uterus where they will divide and at approximately the 30-cell stage, be laid and continue to develop *ex utero*. The production of functional embryos, and therefore the survival of the species, depends on proper germline function, a complex process requiring coordination of many proteins.

P granules

Cell lineage fates are often determined by the proteins inherited by the cells. A germline cell fate is dictated by the inheritance of germline determinants in the form of granular structures (often referred to as germ granules) composed of proteins and RNA. In *C. elegans* these structures are referred to as P granules, and are known as polar granules in *Drosophila*, and nuage in vertebrates (Mahowald 1971; Wolf et al. 1983). P granules are deposited in oocytes and therefore consist of maternal protein; they are evenly distributed throughout the cytoplasm (Figure 1.6). As the embryo divides, P granules segregate to the germline progenitor cell. During embryogenesis, P granules are cytoplasmic until approximately the 16-cell stage, at which time they become

Figure 1.6: P granules in a *C. elegans* embryo. Left panels, Nomarski optics. Right panels, P granule staining by immunoflourescence (P granule specific antibody). A. A newly fertilized embryo shows P granules dispersed throughout the cytoplasm. B. As the embryo prepares to divide, P granules migrate to the posterior end. C. P granules are found in the P1 cell of two cell embryo. D. P granules are present only in P_2 cell of four cell embryo. E. P granules are visible in the Z2 and Z3 cells of a first larval stage (L1) worm. Size bar is 10 μm, all images taken at same magnification. Adapted from:

http://www.indiana.edu/~elegans/Photo_archive/photo_archive.html

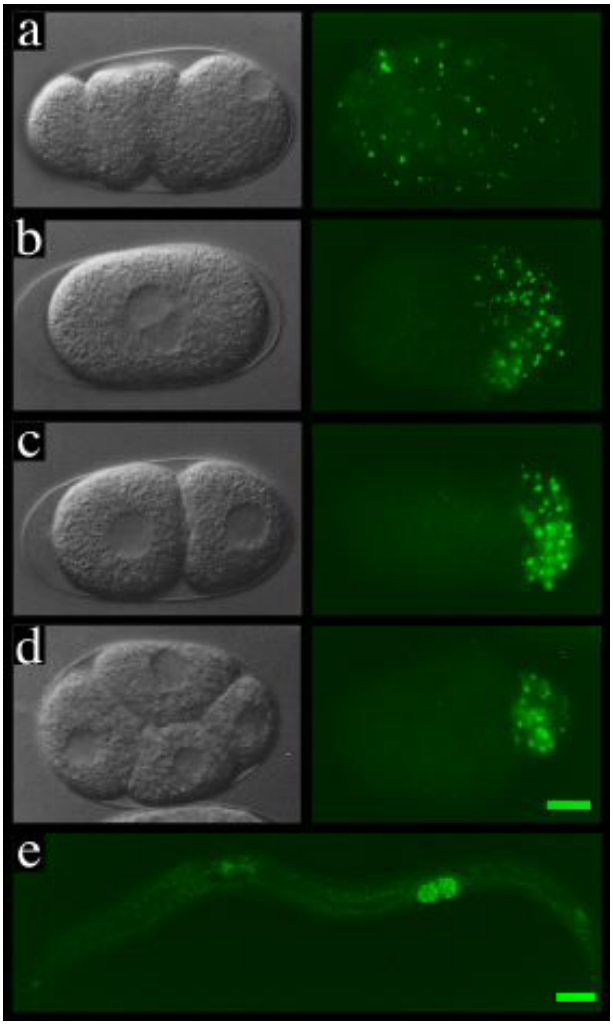

closely associated with the nuclear membrane, and make extensive contact with nuclear pores (Figure 1.7) (Wolf et al. 1983; Pitt et al. 2000). P granules continue to associate with germ cell nuclei throughout germline development, with each germ cell nucleus being surrounded with several P granules, until oocytes cellularize in the germline.

The precise function of P granules is not well understood. More studies have been carried out on the homologous structures in *Drosophila*, polar granules. It has been shown that polar granule transplantation can induce ectopic germ cell formation (Illmensee and Mahowald 1975). Although it is not known if P granules are necessary for germline formation in *C. elegans*, it has been shown that components of P granules are necessary for fertility (discussed later in this chapter). Therefore, P granule function is vital to *C. elegans* development.

The germline RNA helicase (GLH) family

To study the role of P granules in *C. elegans* development, the Bennett laboratory began to for possible P granule components. Work in *Drosophila* identified the DEAD-box RNA helicase *Vasa*, as a component of polar granules. *Vasa* has been shown to regulate the translation of mRNAs such as *nanos* (*nos*) and *gurken* (*grk*) (Hay et al. 1988; Hay et al. 1988; Lasko and Ashburner 1988; Gavis et al. 1996; Styhler et al. 1998; Tomancak et al. 1998). The vital roles of *Vasa* in translational regulation and germline determination made a search for *C.*

Figure 1.7: Electron micrograph of *C. elegans* embryo at 16 cell stage showing P granules. Left panel: section through a *C. elegans* embryo, with the P_4 cell in the bottom right corner, large electron dense granules contact nuclear membrane. Right panel: higher magnification of left panel showing just the P_4 cell shown in left panel. Two large P granules are seen associated with the nucleus. Arrowheads point to P granules contacting the nucleus on both left and right sides. Adapted from (Wolf et al. 1983)

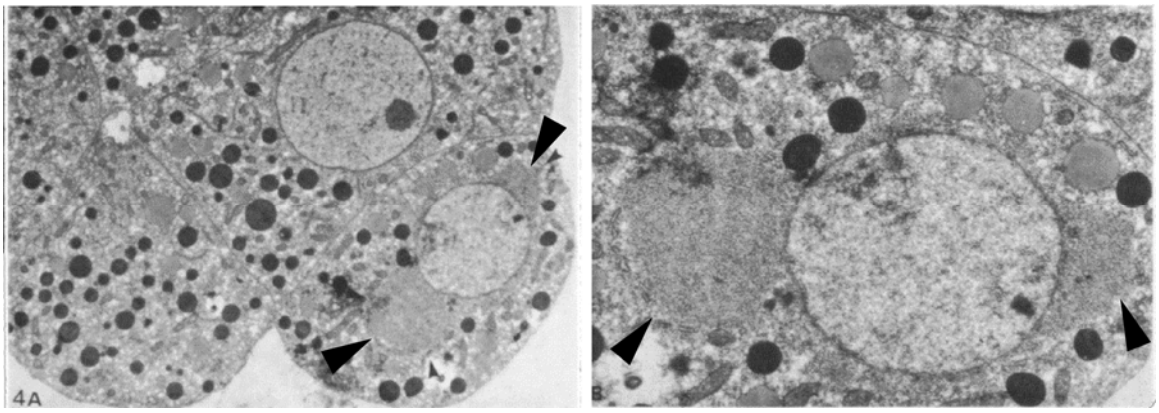

elegans homologues a logical next step to identifying *C. elegans* P granule components.

The initial searches identified one *vasa* homologue, *glh-1* (Roussell and Bennett 1993). The sequencing of the *C. elegans* genome identified three more *vasa*-like genes, *glh*-2, *glh-3* and *glh-4*, as well as a pseudo-gene *glh-4b* (Gruidl et al. 1996; Kuznicki et al. 2000). The GLHs, like *Vasa,* belong to the family of DEAD-box RNA helicases and contain nine-conserved helicase motifs, the peptide sequences that distinguish this family of proteins (Figure 1.8). Unlike *Vasa*, the GLH proteins have glycine-rich repeat regions in the N terminus (except GLH-3), and CCHC, or retroviral-like zinc fingers.

DEAD-box RNA helicases have been linked to every aspect of RNA biosynthesis (Figure 1.9) (reviewed in (Rocak and Linder 2004; Cordin et al. 2006)). On its own, the helicase core of DEAD-box proteins exhibits little substrate specificity in terms of RNA binding. It has, therefore, been postulated that the non-helicase portions of DEAD-box containing proteins may impart substrate specificity or facilitate binding to other proteins. Helicases are typically thought to unwind double-stranded stretches of nucleotides; this could well be the role of the GLHs.

Studies in the Bennett laboratory have focused on determining GLH function and have taken varied approaches to understanding this subject. A previous graduate student, Kathleen Kuznicki, identified deletion mutants in *glh-2* and *glh-3*, as well as performed RNAi with the individual *glh*s and combinatorial groups (Kuznicki 2000; Kuznicki et al. 2000). The *glh-3(um1)* deletion allele

Figure 1.8: Conserved DEAD-box RNA helicase motifs. Top: Dead-box RNA helicases are characterized by the presence of nine conserved motifs. Motifs thought to facilitate interactions with RNA substrates are indicated by arrows. The Walker motifs I and II (indicated below as motifs Ia and Ib respectively) and the Q motif are required for ATP binding. The DEAD motif interacts with Mg^{2+} and its associated phosphate groups. Bottom: Crystal structure for *Methanococcus jannaschii* DEAD-box protein. Motifs are color coded is in top panel. Adapted from (Rocak and Linder 2004).

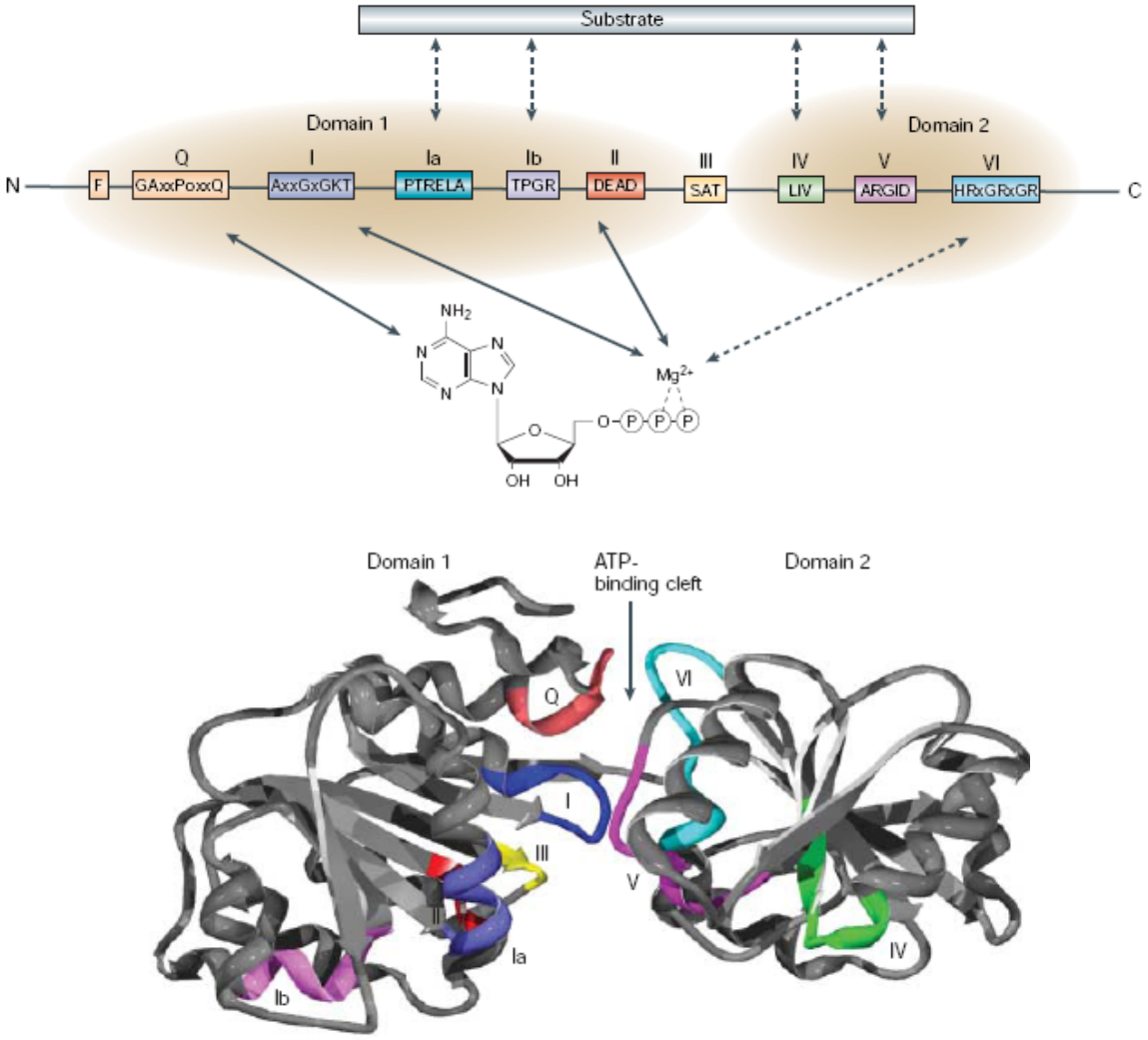

Figure 1.9: Roles of DEAD-box RNA helicases in *S. cerevisiae*. These helicases have been implicated in every aspect of RNA biosynthesis. From transcription to RNA degradation, DEAD-box proteins are crucial for normal cellular functioning. Adapted from (Cordin et al. 2006).

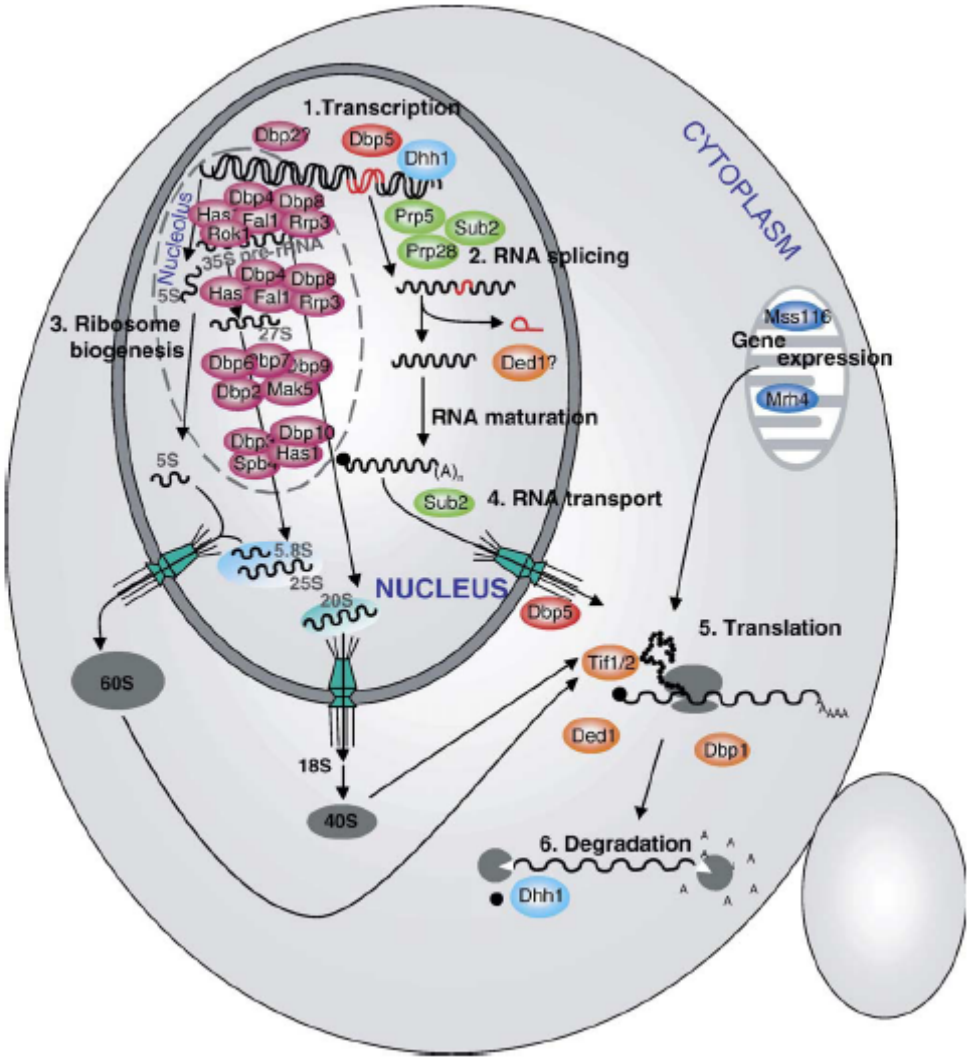

revealed that the GLHs are able to localize to P granules independently, as the loss of GLH-3 did not preclude any of the other GLH proteins from being localized to P granules (Figure 1.10). It was also found that there may be some redundancy in GLH function. Elimination of single GLH proteins at permissive temperatures had little effect on fertility (Table 1.2). The elimination of GLH-1 at the non-permissive temperature of 25°C resulted in significant sterility, as did the combinatorial loss of GLH-1 and GLH-4 at the permissive temperature of 20°C. This sterility was easily scored by a "clear gonad" phenotype when examining worms under a stereo-dissecting microscope. Dissection of these sterile worms found that they had severely under-proliferated germlines, with less than one-third the number of germ cell nuclei as their wild type (N2) counterparts (Figure 1.11). Additionally, the P granule component, PGL-1, was found to be mislocalized due to *glh-1/4* RNAi, with PGL-1 no longer present in a P granules (Figure 1.12).

The effects of *glh* RNAi on fertility are logical as the transcripts for the *glh* genes are germline-enriched (Figure 1.13 and 1.14) (Roussell and Bennett 1993; Kuznicki et al. 2000). This data confirms that the *glh*s are germline-specific. It also suggests that GLH-1 and GLH-4 play important roles in fertility, especially GLH-1 at high temperatures. The Priess laboratory found that the GLHs also serve a structural role in P granule formation. RNAi of *glh-1/2* causes P granules to drastically change in morphology, resulting in dense structures, a fraction of the size of wild type P granules (Figure 1.15) (Schisa et al. 2001).

Figure 1.10: GLH proteins localize to P granules independently. Adapted from (Kuznicki et al. 2000). A. N2 embryos reacted with αGLH-3 antibodies reveal GLH-3 is restricted to germ line progenitor cells. B. Embryos from *glh-3(um1)* mutants reacted with αGLH-3 antibodies. C. DAPI staining of embryos in panel B. D. N2 embryos reacted with αGLH-4 antibodies, GLH-4 is found both in germline and somatic blastomeres, even after affinity purification of the antibody. E. *glh-3(um1)* embryos reacted with αGLH-1 antibodies (panel 1), αGLH-2 antibodies (panel 2), αGLH-4 antibodies (panel 3) and a merged image of panels 1-3 (panel 4). F. Extruded gonad from N2 adult reacted with αGLH-3 antibodies, Inset is portion of gonad increased in magnification 3 times. G. Gonad in F with DAPI staining, arrow points to germ cell nuclei, and arrow head indicates developing oocytes. H. Extruded gonad from N2 worm reacted with αGLH-4 antibodies (panel 1), αGLH-1 antibodies (panel 2), merge of panels 1 and 2 (panel 3). Adapted from (Kuznicki et al. 2000).

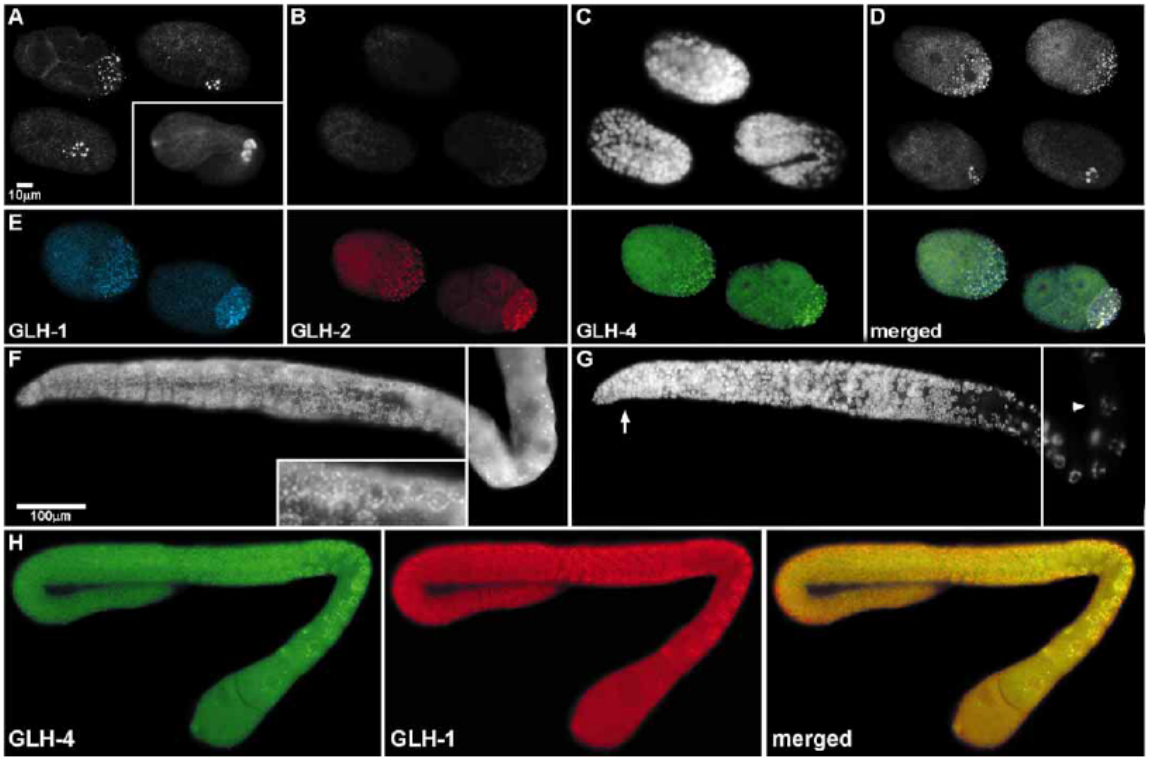
A
B
C
D
10µm
E
GLH-1
GLH-2
GLH-4
merged
F
G
100µm
H
GLH-4
GLH-1
merged

Table 1.2 Effects of *glh* RNA interference at 20°C and 25°C. Wild type worms were injected with dsRNA from *glh-1*, *glh-2*, *glh-3*, *glh-4* or combinations of the four *glh*s. The worms were purged of preformed embryos overnight, and then allowed to produce progeny at either 20°C or 25°C. The fertility or sterility of the resulting F_1 progeny was examined. Adapted from (Kuznicki et al. 2000).

	20°C		25°C	
Gene	No. of worms injected	Sterile worms in F_1 generation	No. of worms injected	Sterile worms in F_1 generation
glh-1	7	0% (0/360)	7	44% (1008/2306)
glh-2	19	0% (0/3014)	16	21% (133/623)
glh-3	14	0% (0/2371)	43	0% (0/4685)
glh-4	17	0% (0/798)	20	0% (0/876)
glh-1/2	16	4.4% (42/944)	20	23% (253/1084)
glh-1/3	10	0% (3/1340)	14	32% (285/900)
glh-1/4	60	97% (5368/5519)	69	33% (914/2774)
glh-2/3	20	0% (0/3313)	32	13% (172/1301)
glh-2/4	33	0% (0/1056)	19	15% (136/888)
glh–3/4	12	0% (0/1870)	10	0% (0/1136)
glh-1/2/3	44	4.9% (109/2234)	42	36% (1060/2945)
glh-1/2/4	7	93% (393/424)	36	38% (599/1584)
glh-1/3/4	10	92% (1376/1494)	10	31% (111/355)
glh-2/3/4	17	0% (0/approx. 1300)	39	0% (0/2015)
glh-1/2/3/4	74	93% (4078/4380)	53	14% (570/4027)

Figure 1.11: Effect of *glh-1/4* combinatorial RNAi. A. Extruded gonad from *glh-1/4* RNAi worm, stained with DAPI to visualize nuclei. B. Same gonad as in A reacted with αGLH-4 antibodies to show that RNAi knocked down GLH-4 protein. C. Another extruded *glh-1/4* RNAi gonad stained with DAPI. D. Gonad in C reacted with αGLH-2 antibodies, showing GLH-2 is present even when GLH-1 and GLH-4 are knocked down. Inset 1: proximal N2 gonad P granules visualized by αGLH-2 antibodies. Inset 2: proximal gonad of *glh-1/4* RNAi worm, reacted with αGLH-2. E. Extruded gonad from combinatorial *glh-1/2/3/4* RNAi worm, results in same phenotype seen by *glh-1/4* RNAi. Stained with DAPI to visualize nuclei. Adapted from (Kuznicki et al. 2000).

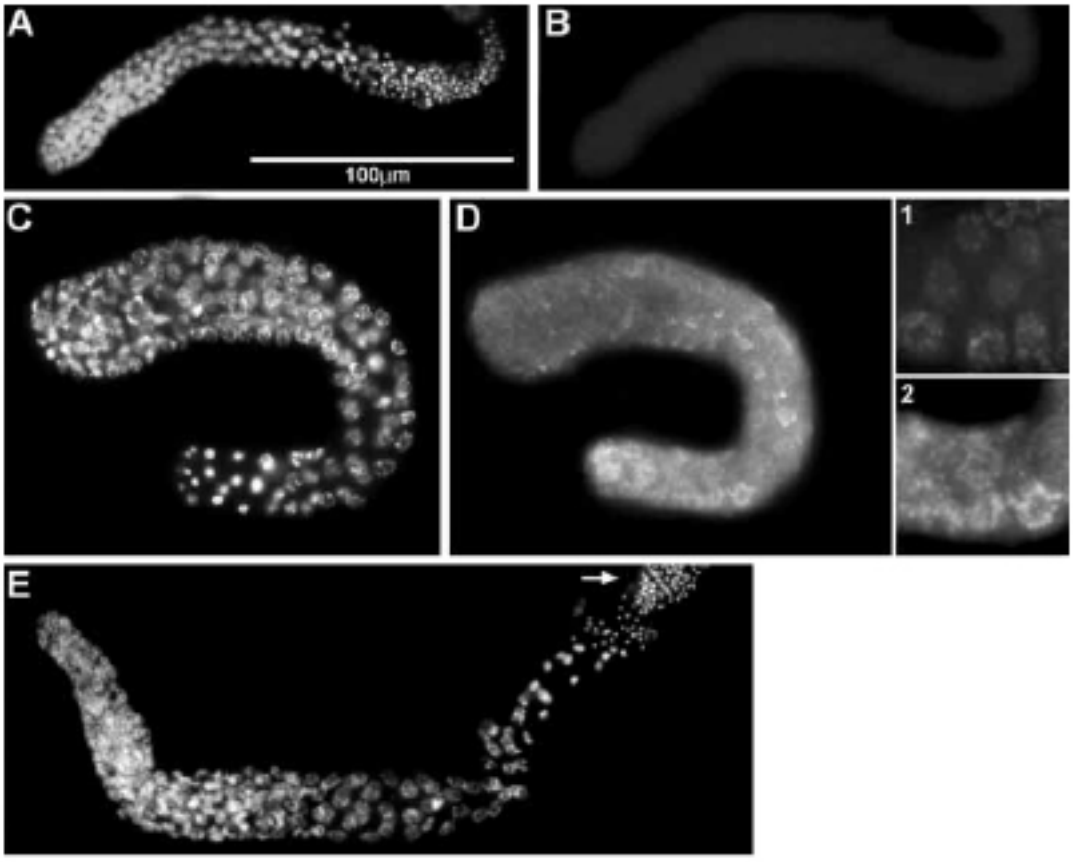

Figure 1.12: Maternal P granule components persist in *glh-1/4* RNAi embryos and PGL-1 is mislocalized in *glh-1/4* RNAi germlines. A. Embryos from worms injected with *glh-1/4* dsRNA still have GLH-4. B. Maternal GLH-1 is still found in *glh-1/4* RNAi embryos. C. The P granule component PGL-1 is found in *glh-1/4* RNAi embryos. D. Extruded germline of a *glh-1/4* RNAi worm reacted with αPGL-1 antibodies finds PGL-1 no longer in P granules, by diffusely surrounding each germ cell nuclei. Inset is a two fold magnification. E. DAPI staining of gonad in D. Adapted from (Kuznicki et al. 2000).

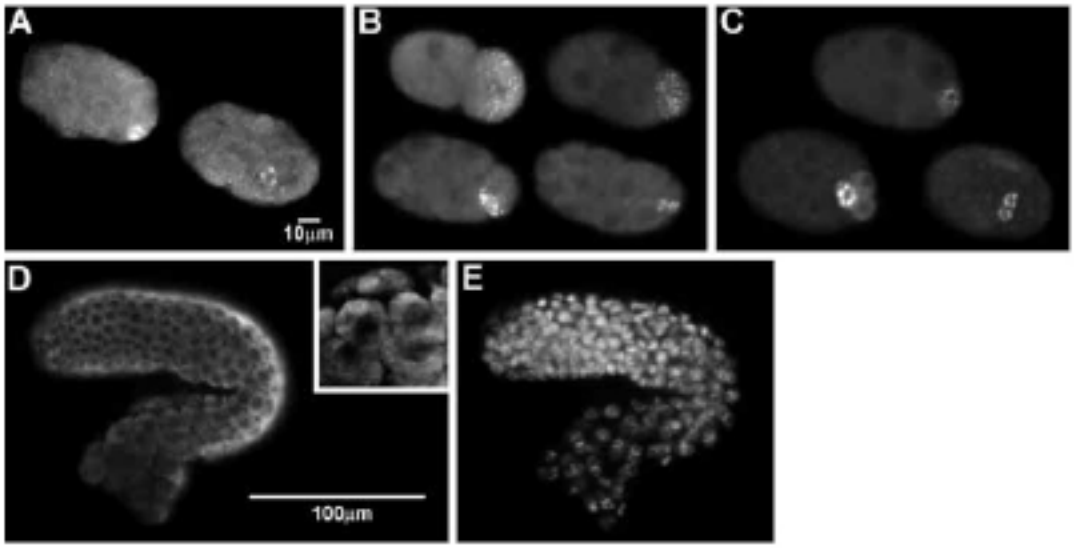

Figure 1.13: Northern analysis of *glh* gene transcript levels in germline mutants. Top: *glh-1* levels were examined in N2 and temperature-sensitive germline mutants. 15°C is permissive temperature and 25°C restrictive. At restrictive temperatures the following mutations result in: *fem-1*: many oocytes but no no sperm production, *fem-3*: overproduction of sperm but no oocytes, *glp-1*: few germ cells, only 10-20 sperm with no oocytes, *glp-4*: few germ cell nuclei, no oocytes or sperm. Adapted from (Roussell and Bennett 1993). Bottom: *glh-3* and *glh-4* transcript levels in *glp-1* and *glp-4* mutants; *vit-2* is a positive control. Adapted from (Kuznicki et al. 2000)

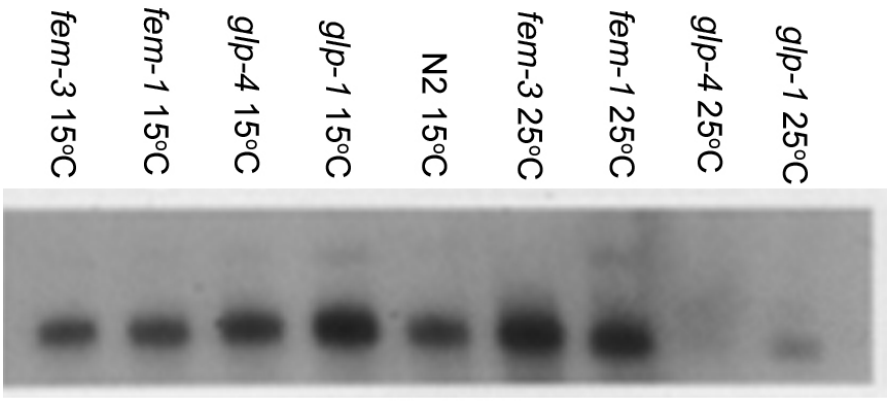

glh-1 RNA

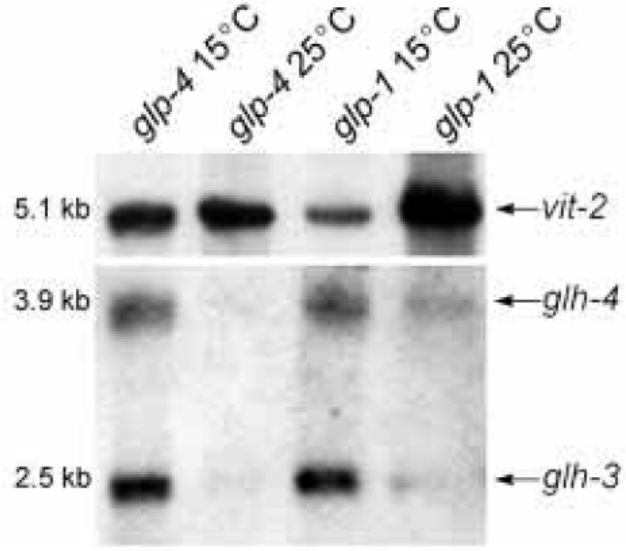

Figure 1.14: *glh-1 in situ* hybridizations. Starting in early embryos, glh-1 transcript is localized to the germline progenitor cells (dark spot in embryos in top right panel). This strong germline expression is seen in the larval stages (L1-L4) and is evident in adults. Compiled from *C. elegans* expression database.

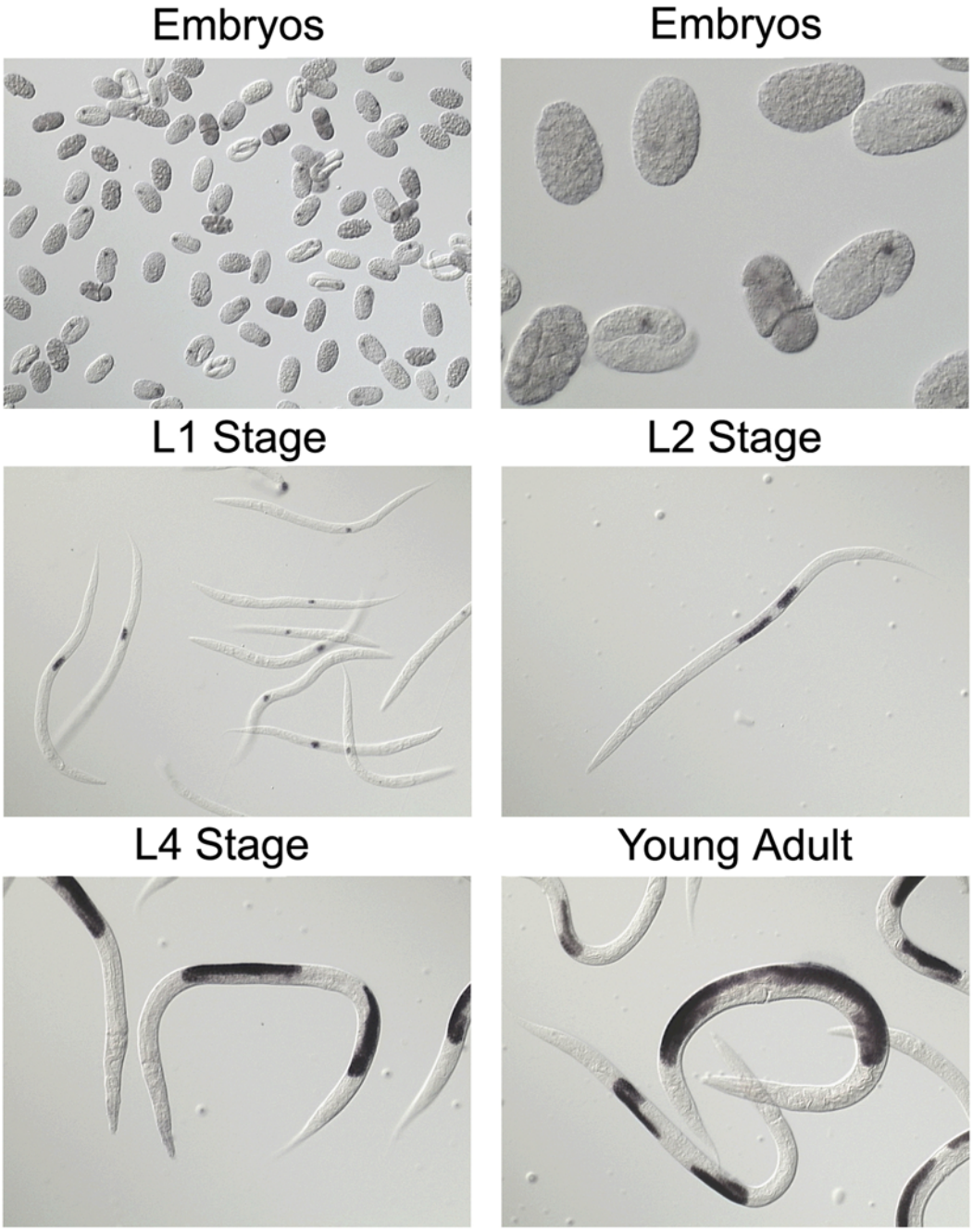

GLH interacting proteins

To further understand GLH protein function, a yeast two-hybrid screen was undertaken to identify proteins that physically interact with the GLHs. This screen was performed by previous graduate student Pliny Smith; he confirmed the positive interactors from the yeast two-hybrid screen by producing recombinant baculoviruses for several of the most promising proteins with alternate affinity tags, which were then used for GST pull-down analyses.

Although several proteins were identified as interacting with the GLHs, three of them will be considered in this work: KGB-1, CSN-5 and ZYX-1. Important roles for KGB-1 and CSN-5 were identified; these proteins will therefore be considered more extensively.

KGB-1: a kinase that GLHs bind

KGB-1 is most like kinases in the mitogen-activated protein (MAP) kinase family. This family of kinases has been well studied; the proteins are activated by a wide range of signals including cytokines and growth factors. MAP kinases (MAPKs) are often involved in stress responses. MAP kinases are generally active in signaling cascades that begin with a MAPKKK, which signals to a MAPKK that in turn activates a MAPK which can then phosphorylate its targets (Stronach 2005). In *C. elegans*, MAPKs play roles in odor response, heavy metal stress, meiotic progression, development of hypodermal cells, and protein degradation (reviewed in(Sakaguchi et al. 2004)).

Figure 1.15: P granule morphology is distorted by *glh-1/2* RNAi. A. A P granule contacting the nuclear membrane of a germ cell. B. P granules surrounding a germ cell from a *glh-1/2* RNAi worm. White arrowheads point to fibular matrix of the P granule, white arrow points to electron dense region. Black arrows point to nuclear pores. mt=mitochondria, nu=nucleus, size bar is 0.2μm. Adapted from (Schisa et al. 2001).

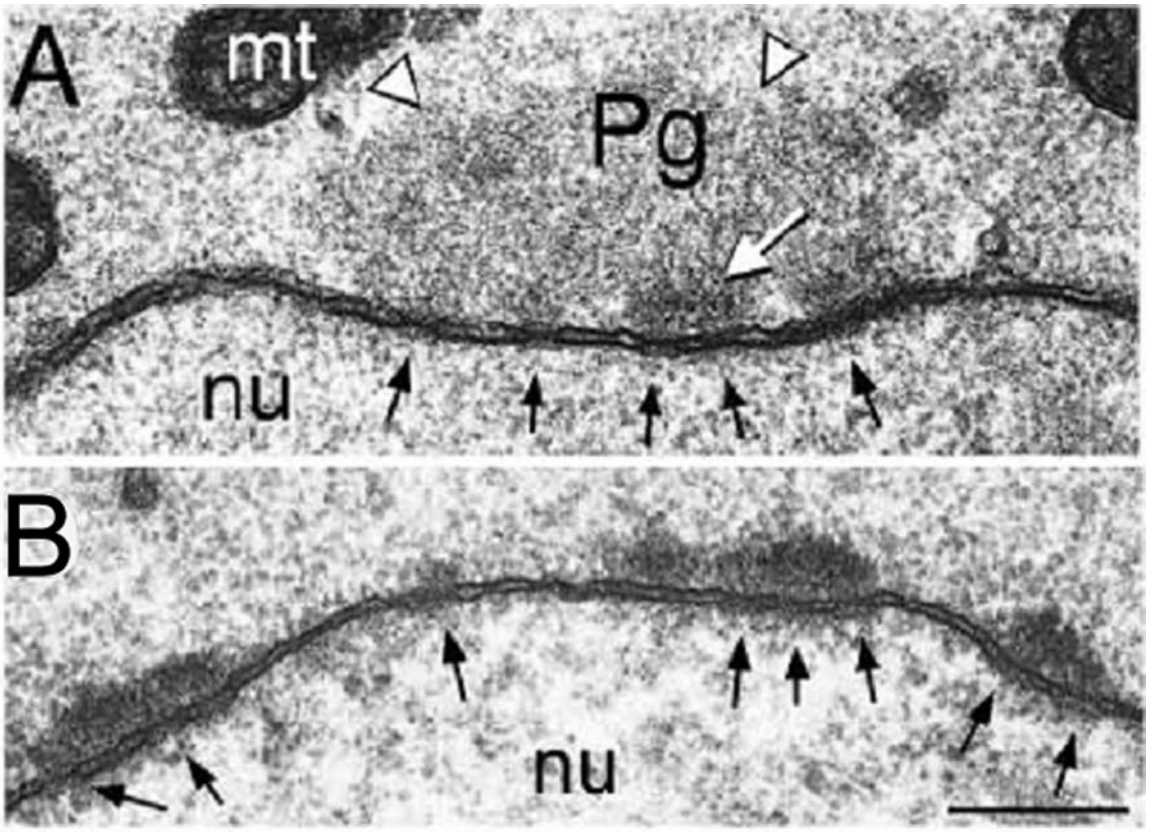

There are three subfamilies of MAPK proteins: the ERK, JNK, and p38 groups. KGB-1 is most similar to the Jun NH_2-terminal kinase (JNK) group. There are three proteins belonging to the JNK subfamily in *C. elegans*: JNK-1, KGB-1, and KGB-2, a protein with extensive homology to KGB-1. The two proteins are 86% identical and 91% similar; the *kgb-1* and *kgb-2* genes are 23 map units apart on chromosome IV. JNK proteins are characterized by a TXY activation site, which is dually phosphorylated by a MAPKK of either the MKK4 (MKK-4, ZC449.3, and VZC374L.1 proteins in worms) or MKK7 subfamilies (JKK-1 and MEK-1). Interactions between MAPK and MAPKK are thought to lead to specificity in signal response. In worms, it has been shown that JNK-1 and JKK-1 most likely compose a signaling pathway that is involved in proper neuronal functioning and locomotion. Additional scaffold proteins are thought to hold proteins in a given place or conformation, thereby contributing to JNK pathways. The putative scaffold protein UNC-16 has been linked to JNK-1-JKK-1 signaling with respect to vesicle transport (Sakaguchi et al. 2004).

Recent results have implicated the *C. elegans* JNK kinase pathways in stress related responses, such as heavy metals (Koga et al. 2000), immunity (Kim et al. 2002) and temperature (Smith et al. 2002). Response to heavy metal stress requires the KGB-1 signaling pathway, as inactivation of KGB-1 or its upstream activators, namely MEK-1, has an adverse effect on worms exposed to heavy metal stress and starvation (Koga et al. 2000). Kinase activity for KGB-1 has been demonstrated through the use of c-Jun as a substrate, which is an important finding as KGB-1 has a non-JNK typical activation site (SDY instead of

the typical TXY), which has been shown to be crucial for kinase activity (Mizuno et al. 2004). JNK kinases may use docking sites such as K/R-X-X/K/R-K/R-X(1-4)L/I-X-L/I or K/R-K/R-K/R-X(1-5)L/I-X-L/I to bind to their target substrates, which presumably allows them to phosphorylate target residues (Jacobs et al. 1999). Regulation of a protein may involve multiple factors. Motifs such as phosphodegrons can also be affected by kinases. Phosphodegrons, with a consensus of I/L-I/L/P-pT-P-notK/R, are regions when phosphorylated that can be involved in targeting proteins including Sic1 and cyclin E for degradation (Orlicky et al. 2003; Ye et al. 2004).

Our work on KGB-1 has focused on its role in fertility. In this work, we will explore the importance of KGB-1 in the germline of *C. elegans*, with particular attention to temperature stress. We find that GLH levels are misregulated in *kgb-1(um3)* mutants. We propose that this defect is evident because KGB-1 normally regulates levels of GLH proteins in the germline, most importantly in the case of elevated temperature, a stressful condition for worms. We postulate that KGB-1 may target GLH proteins for degradation to precisely regulate the amounts of GLH proteins present at any given time (this will be discussed in detail later).

Regulation of protein levels through degradation has been shown for other mechanisms of development. OMA-1 and OMA-2 are needed for *C. elegans* embryogenesis; OMA-1 is phosphorylated on two different residues by the dual specificity DYRK2 kinase, MBK-2, and another kinase GSK-3. Phosphorylation of both residues is required for *in vivo* degradation of OMA-1 (Nishi and Lin 2005). MBK-2 has also been shown to coordinate degradation of MEI-1 and

MEI-2. This regulation is essential for permitting proper establishment of the A-P axis in *C. elegans* embryos. MBK-2 function is also required for germ plasm enrichment at the posterior of the embryo before the first cell division and cytokinesis. These combined regulatory activities may allow MBK-2 to regulate protein stability in a temporal manner (Pellettieri et al. 2003). Numerous examples exist in *C. elegans* and other organisms where a protein's degradation is regulated by its phosphorylation state including: rat actin and IRS-1, human Wee1 and exonuclease 1b (Lee et al. 2004; Watanabe et al. 2004; El-Shemerly et al. 2005). In this work, we will discuss scenarios that involve KGB-1 mediated regulation of protein levels, with a focus on the GLHs, via phosphorylation that may target proteins for degradation.

CSN-5: COP9 Signalosome Subunit 5

The COP9 Signalosome (CSN) is a multi-subunit complex well conserved from plants to animals, and has been implicated in regulating protein stability through the SCF ubiquitin-ligase pathway (for review see (Cope and Deshaies 2003)). Of the eight known CSN components, CSN-5 is the most conserved and has been observed both as a part of the large hetero-octomeric CSN complex and in lower molecular weight forms, suggesting it may function outside the CSN complex. In *Arabidopsis* the two isoforms of CSN5 show differences in their locations, with the complexed CSN5 found in the nucleus and monomeric CSN5 residing primarily in the cytoplasm (Kwok et al. 1998; Oron et al. 2002).

CSN-5 has been identified as a binding partner for more proteins than the other CSN components; these partners have been identified in a variety of model organisms. CSN5 was identified as a Jun activation binding protein (CSN5 is also known as Jab1 for Jun activation-domain binding) and has been shown to interact with proteins including p27Kip1 (Tomoda et al. 1999). Evidence suggests that CSN5 can promote both degradation and stabilization of its targets (Seeger et al. 1998; Naumann et al. 1999; Bech-Otschir et al. 2001). Proteins such as p53, c-Jun, and IAA (*Arabidopsis* Auxin responsive) are degraded through CSN-mediated ubiquitinization and subsequent proteolysis by the proteasome. In contrast, the transcriptional regulators Id1 and Id3 are thought to be stabilized by their interactions with the CSN complex, and CSN5 specifically, when CSN-mediated phosphorylation is functional (Berse et al. 2004).

In *C. elegans*, the CSN complex is thought to antagonize the pathway leading to neddylation of CUL-3, leading to cycles of neddylation and deneddylation, which may allow for poly-ubiquitin chains to be added to MEI-1, a target of CUL-3. The degradation of MEI-1 is essential for the switch from meiosis to mitosis in the *C. elegans* embryo (Pintard et al. 2003). The CSN complex is also necessary for proper embryonic development in *Drosophila*; mutations in *csn5* are lethal when null, revealing defects in embryo patterning and response to DNA damage (Oron et al. 2002). Less severe mutations in *csn5* inhibit *Gurken* accumulation, reduce the number of pole cells, and cause *Vasa* protein, which is orthologous to the GLHs, to migrate more slowly when analyzed by SDS-PAGE (Doronkin et al. 2002). The CSN complex does not seem to

depend on CSN5 for its integrity, in the absence of CSN5, other subunits are still found in a multimeric complex. This suggests CSN5 is a peripheral part of the complex, however the CSN complex is non-functional when lacking CSN5 (Kwok et al. 1998; Oron et al. 2002).

Our laboratory generated antibodies to CSN-5 and found it is present in *C. elegans* in the cytoplasm and the nucleus, with particularly strong sub-nuclear localization in oocytes; this pattern was verified by other researchers (Figure 1.16) (Smith et al. 2002; Pintard et al. 2003) In *C. elegans*, *csn-5* RNA is germline-enriched but not germline-specific, with germline RNA levels being approximately 6-fold greater than those in the soma (Reinke et al. 2000; Smith et al. 2002). While the soma appears unaffected in our assays, elimination of CSN-5 using RNAi mirrors the combined loss of GLH-1 and GLH-4: sterile worms with under-proliferated gonads (Figure 1.21, panels B, D and E) (Kuznicki et al. 2000; Smith et al. 2002). The similarity of these phenotypes could indicate that CSN-5 plays a role in stabilizing GLH-1 and GLH-4, and that this regulation of the GLHs by CSN-5 contributes to fertility in worms.

Figure 1.16: CSN-5 localization and effects of *csn-5* RNAi. A. AN extruded gonad from an N2 worm reacted with αCSN-5 antibodies shows CSN-5 is present in every cell of the germline and somatic tissues (loop in top right is gut). B. Extruded gonad from a *csn-5* RNAi worm stained with DAPI, arrow points to sperm. C. Confocal image of developing oocytes showing CSN-5 localization, it is present in the cytoplasm with a strong sub-nuclear localization. D. *csn-5* RNAi gonad with αGLH-1, arrow points to region with no GLH-1 localization. E. DAPI stain of gonad in D. Adapted from (Smith et al. 2002).

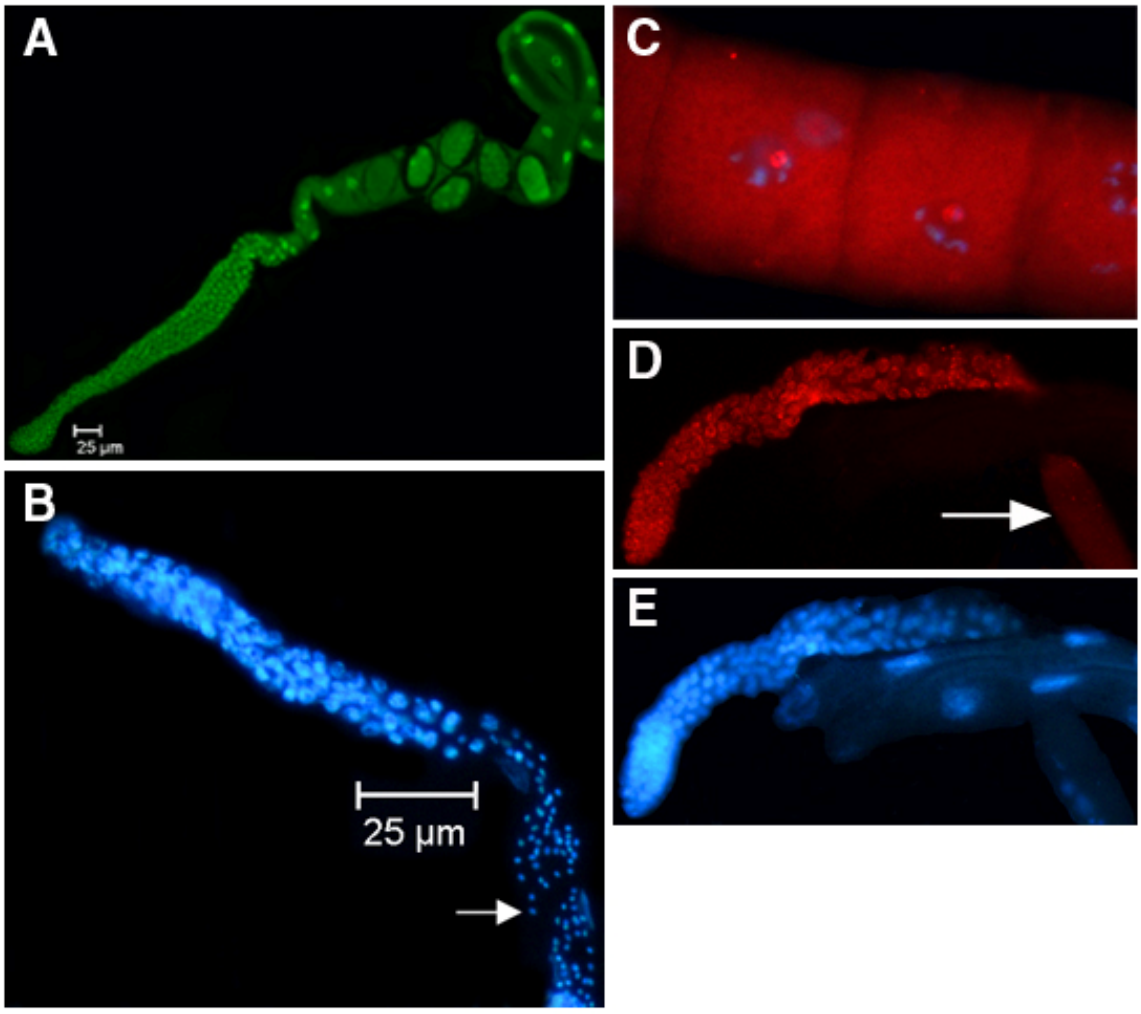

Aims of Dissertation

The goal of this work is to further understand the function of the GLH proteins and their interacting proteins KGB-1 and CSN-5 with respect to their germline functions. To address the role of KGB-1 in fertility, we examined the phenotype of *kgb-1(um3)* (referred to as *kgb-1*) mutant worms. A thorough characterization of the *kgb-1* worms is an on-going goal. We focused on aspects of the *kgb-1* phenotype with specific regard to effects on GLH proteins.

We are limited in our abilities to express proteins in the germlines of worms as repetitive elements are silenced and other methods are inefficient. Therefore, we made use of *in vitro* assays to examine molecular interactions between GLH-1 and KGB-1. We worked to elucidate the nature of the interaction between KGB-1 and GLH-1, with special consideration given to the regions of GLH-1 required for binding KGB-1. Using *in vitro* methods, we further examined the ability of KGB-1 to phosphorylate GLH-1 or target it for degradation by the proteasome. We also explored interactions between CSN-5 and KGB-1, as both proteins interact with the GLHs and seem to have roles in regulating GLH protein levels. Initial characterization of the *zyx-1(um4)* null strain (ZYX-1 is also a GLH interacting protein) was also performed in terms of effects of the mutation on fertility.

Other portions of this work focus on the functions of the GLH proteins themselves, by examining the effects of mutations in individual *glh* genes on fertility.

Chapter 2: Interactions between KGB-1 and the GLHs

Introduction

Work in the Bennett laboratory regarding the function of the germline RNA helicases (GLHs) led to a yeast two-hybrid screen, performed by Pliny Smith, which identified several GLH binding partners. He found several proteins that bound to the GLHs (Smith et al. 2002). The work presented here will focus on two GLH interacting proteins: a kinase that GLHs bind (KGB-1) and COP9 signalosome subunit 5 (CSN-5). At the time I rotated in the Bennett laboratory, Emily Coberly was in the process of a reverse genetics screen looking for deletion mutations in the *kgb-1* gene; one was found and I helped with its isolation. Pliny Smith determined the end points of the deletion using PCR and DNA sequencing. The deletion was found to eliminate approximately 1200 base pairs from the *kgb-1* gene, effectively eliminating the serine/threonine kinase domain of the predicted protein (Figure 2.1).

Initial examination of the *kgb-1(um3)* (hereafter referred to as *kgb-1*) deletion strain found that it exhibited temperature sensitive sterility at 26°C, but seemed to develop normally at the permissive temperature of 20°C. The sterility of this strain was characterized by the presence of large, endomitotically replicating oocytes (EMO) in the gonad (Figure 2.2); *kgb-1* worms produce sperm that are non-functional and seem to undergo normal mitosis (Figure 2.2 inset).

Figure 2.1: Diagram of *kgb-1* gene and KGB-1 protein. Extent of *kgb-1(um3)* deletion indicated both in the gene and protein. The exons are indicated by blue boxes, introns by the lines connecting exonds. The conserved serine/threonine kinase domain is indicated by a red box. Adapted from (Smith et al. 2002).

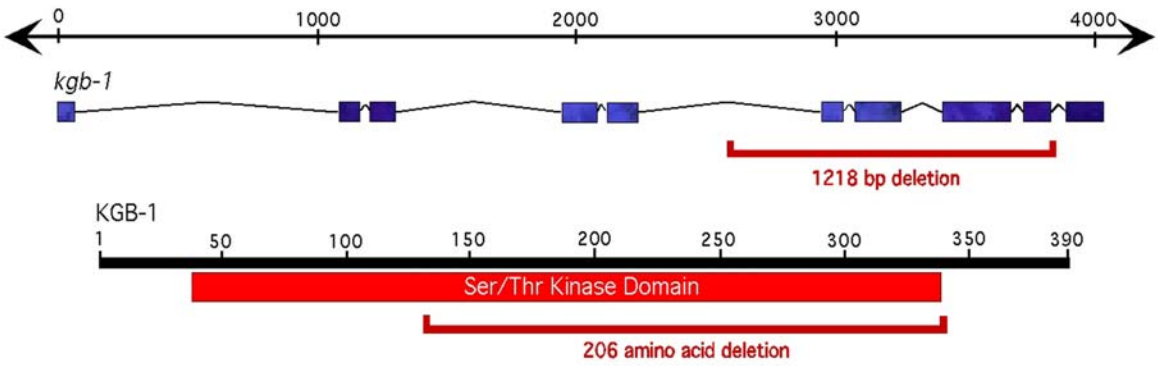

Figure 2.2: *kgb-1(um3)* grown at non-permissive temperatures exhibit endomitotically replicating oocytes (EMO). Top: *kgb-1* worms were raised at 20°C, splayed and the extruded gonads stained with DAPI to show the DNA. The dotted line to bracket indicates the transition zone from mitosis to meiosis. An asterisk indicates a developing oocyte and an arrowhead points to sperm. Bottom: *kgb-1* worms were raised at 26°C; the sterile worms were treated as above. Endomitotically replicating oocytes are indicated by arrows. Inset: mitotic figures from *kgb-1* 26°C gonad. Adapted from (Smith et al. 2002).

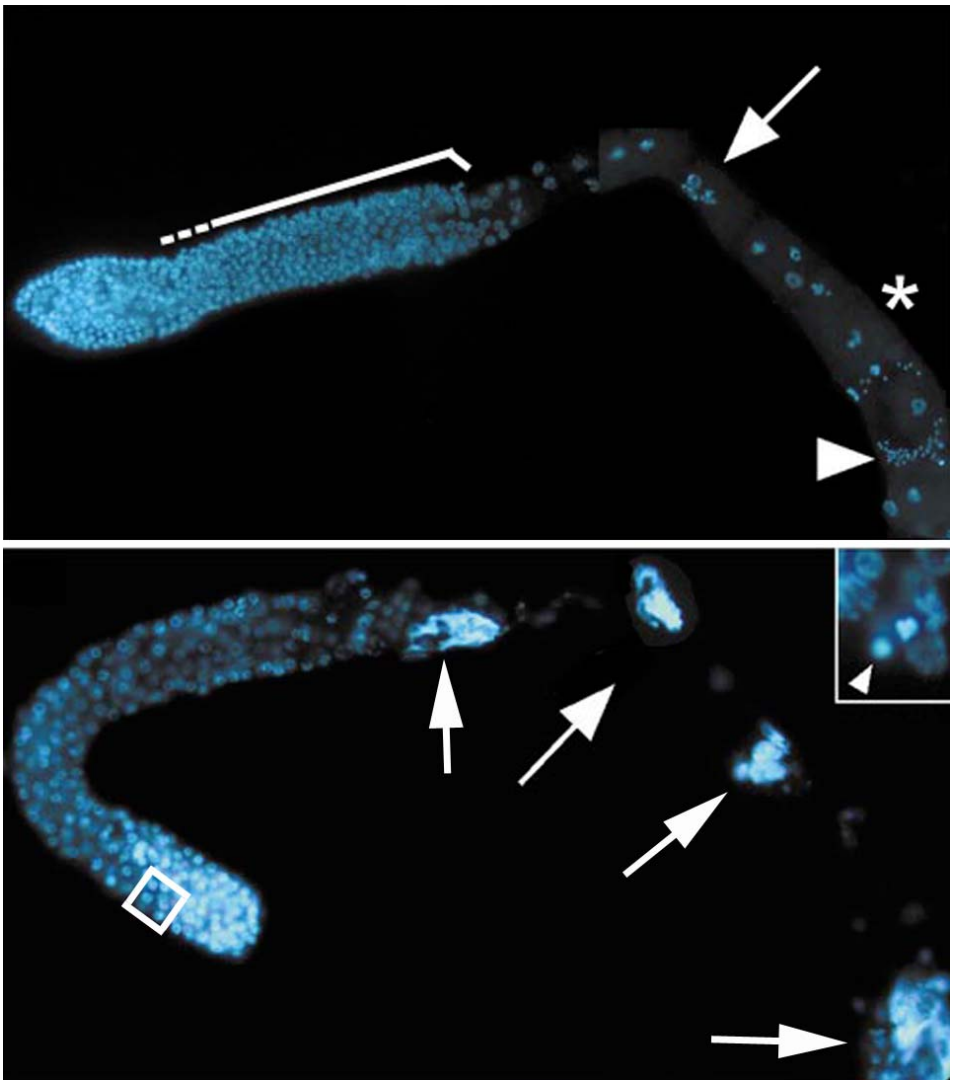

Interactions with KGB-1 and GLH proteins were independently confirmed using baculoviral expression (constructs shown in Figure 2.3). KGB-1 binds to full length GLH-1, a C-terminal truncation of GLH-1, but not an N-terminal truncation, full length GLH-2, full length GLH-3, and a C-terminal portion of GLH-4 (Figure 2.4). An ONPG colorimetric β-galactosidase assay was performed by an undergraduate researcher Lejla Mutapcic to confirm these interactions, the most robust association was seen with full length GLH-3 and KGB-1, more than 60 times greater than the negative control p53, and six fold greater than the positive control proteins SNF1 and SNF4 which are known to interact (Figure 2.5) (Ramaswamy et al. 1998; Smith et al. 2002) .

To further characterize the *kgb-1* strain, I backcrossed the strain six times against wild type (N2) worms and this strain was used for all further characterization. I determined the effects of the *kgb-1* deletion on worm fertility at permissive and non-permissive temperatures. Further analysis was done to understand the role of GLH-1 in the sterility observed in the *kgb-1* mutant. A postdoctoral fellow, Wensheng Li, performed western-blot analysis using a technique I developed to analyze the amounts of GLH protein in *kgb-1* worms. Immunocytochemistry was performed by Dr. Karen Bennett and I, to confirm the western-blot results.

Sequence analysis of GLH-1 and GLH-4 revealed the presence of a consensus MAPK docking site in GLH-1 that was not conserved in the GLH-4 sequence (Jacobs et al. 1999). An additional protein motif, the phosphodegron, was also found in GLH-1 but not in GLH-4. Phosphorylation of a protein at a

Figure 2.3: GLH 6-His constructs. GLH proteins were cloned in frame with a 6-His tag. Convenient restriction site were used to produce truncations. These constructs were used to create recombinant bacmids for GST pull-down analysis. Adapted from (Smith et al. 2002).

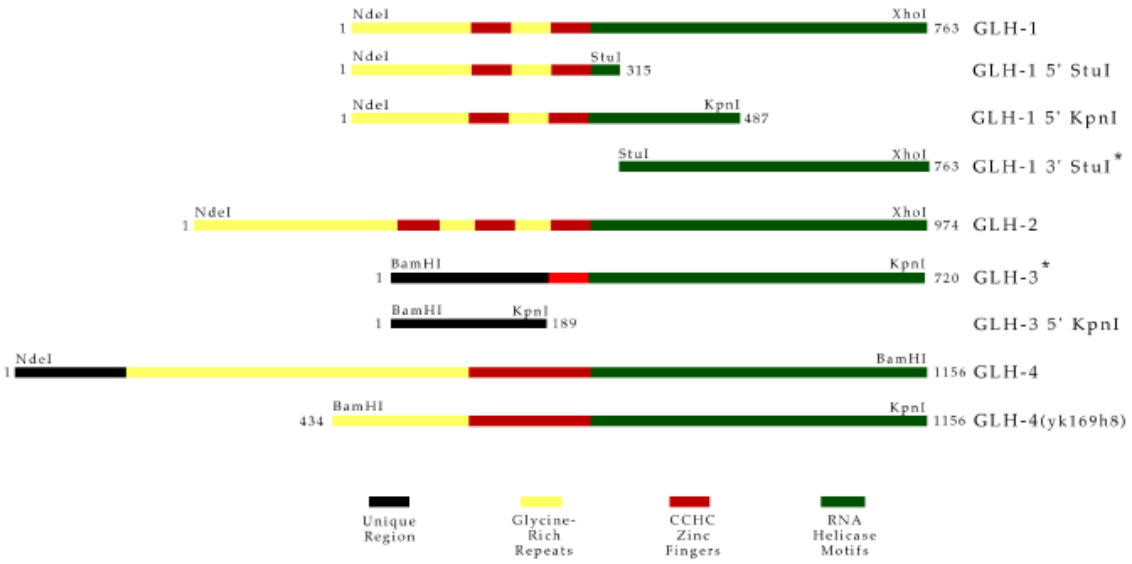

Figure 2.4: GST pull-down assays. KGB-1 GST was co-expressed with GLH-1 6-His and truncations. KGB-1 was found to bind to full length GLH-1, GLH-2, GLH-3, the C terminus of GLH-1 and GLH-4, but not the N terminus of GLH-1 or GLH-3. eGFP 6-His was used as a negative control. Adapted from (Smith et al. 2002).

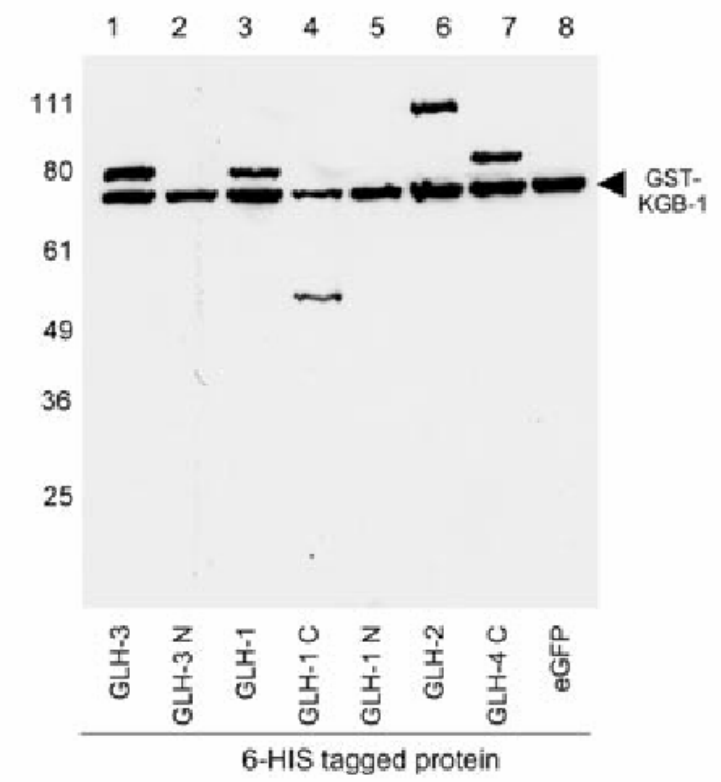

Figure 2.5: ONPG colorimetric β galactosidase assays. The positive control SNF1 and SNF4 are known to interact in yeast (Ramaswamy et al. 1998). Experiments were performed with p53 for negative controls. GLH-1 C-terminus and GLH-3 were used and their ability to interact with CSN-5, KGB-1, and ZYX-1 assayed. Adapted from (Smith et al. 2002).

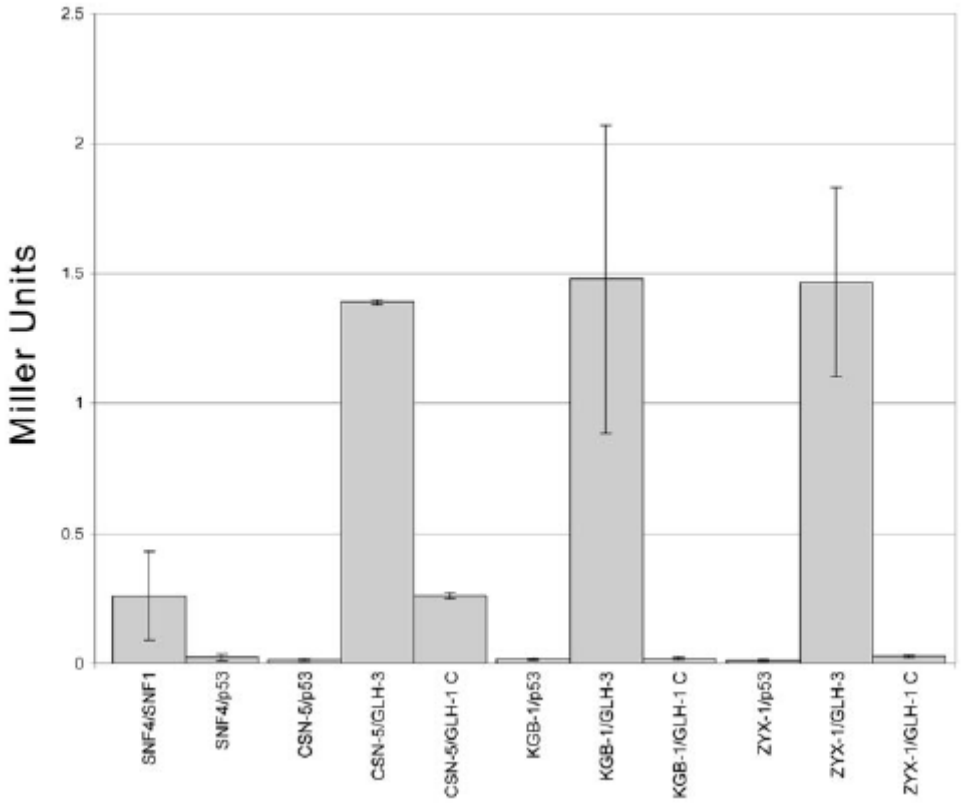

phosphodegron motif can lead to its rapid degradation (Orlicky et al. 2003). The presence of these conserved motifs provided insight into possible protein interactions and modifications that might be used to regulate GLH protein levels.

With the identification of these motifs, I made use of GLH-1 constructs lacking conserved motifs to analyze their importance for KGB-1:GLH-1 interactions. Site directed mutagenesis was also employed to determine the requirements for the MAPK docking site. Kinase assays were performed through a collaboration with Tomoaki Mizuno in the Matsumoto laboratory (Nagoya University, Japan). Proteasome inhibitor experiments were used to examine if KGB-1 might target GLH-1 for degradation *in vitro*. Further characterization of the *kgb-1* strain included germ cell counts, analysis of old worms, *glh-1* RNAi into *kgb-1* background, and attempts to analyze germ cell apoptosis.

Materials and Methods

Strains

The following *C. elegans* strains were used in this work: wild type (N2 variety Bristol), *kgb-1(um3)*, *kgb-2(km16)*, *mek-1(ks54)*, *kgb-1(um3);kgb-2(km16)*, *glh-1(ok439);glh-4(gk225)*, *kgb-1(um3);glh-1(ok439);glh-4(gk225)*, *dpy-13(cb184)*, *unc-24(cb138)*, and *unc-42(cb270)*. Some of these strains were made for this work and their construction will be described. Worms were maintained as in (Wood 1988).

Backcrossing

To generate deletion alleles, fourth larval (L4) stage hermaphrodites were mutagenized with trimethylpsoralen and subjected to UV light, this creates large chromosomal deletions (as in (Yandell et al. 1994). The screen for the *kgb-1(um3)* mutation found a break in the *kgb-1* gene. Since this type of mutagenesis is non-specific, it is likely that other double stranded DNA (dsDNA) breaks may have occurred elsewhere in the genome, resulting in extraneous mutations. These other deletions may make interpreting any phenotype difficult, and must therefore be removed. Chromosomal crossovers during meiosis should eliminate extraneous mutations in the genome, and selection for the *kgb-1(um3)* mutation by PCR allows for the maintenance of the deletion. This was achieved by crossing *kgb-1(um3)* homozygotes to wild type males six times. Wild type males were created by heat-shocking worms for six hours at 30°C, this

increases chromosomal non-disjunction, thereby increasing the number of males in the population. Wild type males can then be maintained by picking 8-20 males and placing them on a plate with one or two wild type L4 hermaphrodites. L4 stage worms were used because they have not produced oocytes, and therefore have not self-fertilized. Since male sperm out-compete hermaphrodite sperm, approximately half of the resulting progeny will be males. For backcrosses, eight to 10 wild type males were mated with one or two *kgb-1* L4 worms and the resulting progeny allowed to grow to the L4 stage. The heterozygous progeny from the initial cross were then individually plated and allowed to self-fertilize. Once reaching the L4 stage, F_2 worms were then individually plated, allowed to self-fertilize and their progeny analyzed by PCR for the *kgb-1* deletion.

Worms were harvested by pipetting 1mL of dH_2O onto the petri dish containing the F_3 generation; 150 µL of the worm/water solution was then placed into a 1.5 mL Eppendorf tube and 150 µL of proteinase K solution (50mM KCl, 10mM Tris HCl pH 8.3, 0.45% IGEPAL m (non-ionic detergent), 0.45% Tween-20, 0.01%g, 200µg/mL proteinase K) was added. The tubes were then put at -80°C to freeze the worms and crack open their cuticles. After freezing, the tubes were transferred to a 65°C shaking incubator overnight; this process allows the proteinase K enzyme to break down all the proteins in the worm, leaving behind the DNA. 9 µL of the DNA solution was treated at 85°C for 25 minutes to kill the proteinase K activity, then 1.5 µL 8mM dNTPs, 3 µL 10x PCR extension buffer (22.5mM $MgCl_2$, 500mM Tris-HCl, 140mM $(NH_4)_2SO_4$, pH 9.2), 1.5 µL 5' primer (primers were diluted 75 ng/ µL), 1.5 µL 3' primer, 0.1 to 1 µL *Taq* polymerase

and Nanopure treated dH_20 to a total of 30 µL were added. Each plate was screened in triplicate with two sets of primers. The inner primer set would produce a larger band in wild type worms and a smaller band in *kgb-1* worms; the deletion primer set would produce a band in wild type worms, but fell within the *kgb-1* deletion and therefore produced no band in the *kgb-1* mutant. The primers were as follows:

kgb-1 5' inner 5'ATAATCCGTCTACTAAACGCG3'

kgb-1 3' inner 5'GAAATGTCGTGGTCGGCTTG3'

kgb-1 5' deletion 5'CTTGGAAATGTGCCGAAACC3'

kgb-1 3' deletion 5'CGGCAGAAAATTGGTATCAGG3'

The PCR samples were denatured for one minute at 95°C, reduced to 94°C for 30 seconds and then to 58°C for one minute then to 70°C for 2.5 minutes; the reactions were cycled 35 times and stored at 4°C upon completion. 10 µL of the resulting PCR product was analyzed by electrophoresis on a 1% agarose gel made with 1XTBE (0.089M tris-borate, 0.089M boric acid, 0.002M EDTA). An example of a back cross gel is shown in Figure 2.6.

Brood counts

To analyze effects on fertility, the number of offspring produced by *kgb-1* worms was determined at 15°C, 20°C, or 26°C. A portion of starved plates (an NGM plate that had been seeded with OP50 *Escherichia coli*, all of which had been eaten as the worms reproduced) of either wild type (N2) or *kgb-1* worms was placed (chunked) onto fresh plates with OP50 *E. coli*, and worms allowed to

Figure 2.3: PCR results from *kgb-1(um3)* backcross. Samples of F2 progeny of a kgb-1(um3) backcross were analyzed by PCR using primers that fall outside of the deletion (outers) results in a band smaller than wild type (blue arrows). PCR with primers inside the deletion (inners) results in no band being produced with the mutant strain (green arrows); however, a band is present in reactions with wild type and heterozygous worms.

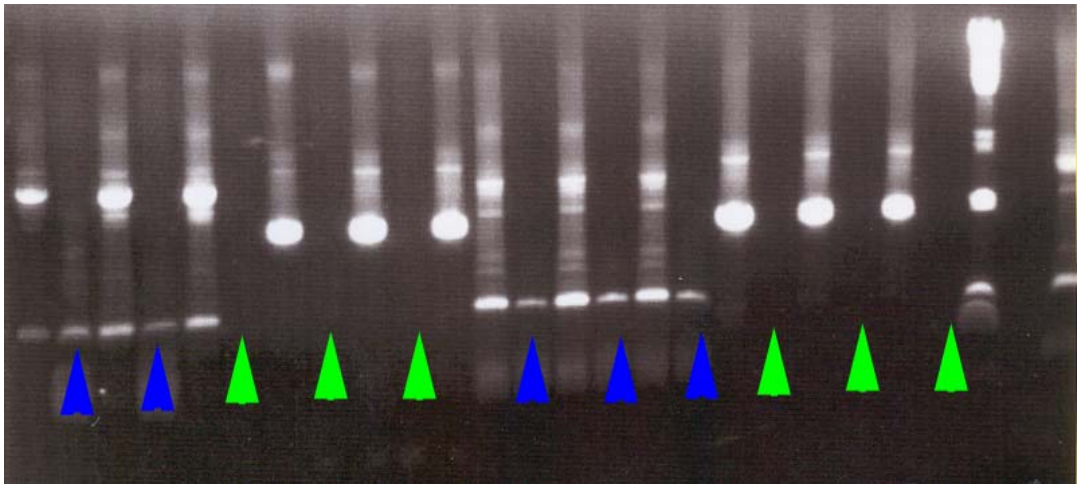

grow to the L4 stage. Individual L4 worms were plated on seeded NGM agar plates and allowed to grow for 5 days at 20°C or 7 days at 15°C, the F_2 progeny were then counted. Since *kgb-1* worms are sterile at 26°C, the procedure for this temperature was slightly different; L4 worms that had been grown at 20°C were shifted to 26°C and their F_1 progeny were then individually plated at the L4 stage. The resulting F_2 progeny were counted. The brood count data was processed in Microsoft® Excel and significance determined using a Student's T-Test.

Western blot analysis

To analyze GLH levels in the *kgb-1* strain, worms were either maintained at 20°C, or grown at 20°C and shifted to 26°C either as L1s or L4s. Worms were grown on 60x15mm petri dishes containing NGM agar (0.05M NaCl, 1.7% agar, 0.25% peptone 1 µg/mL cholesterol, 1mM $CaCl_2$, 1mM $MgSO_4$, 25mM potassium phosphate). The NGM plates were seeded with 100 µL of an overnight culture OP50 *E. coli* grown in LB; the plates were placed at 37°C overnight to grow a lawn of bacteria for the worms to eat. Worms were grown to the L4 stage in mixed population either at 20°C or 26°C and then individual L4 hermaphrodites were picked onto fresh plates and allowed to grow one to five more days at the appropriate temperature. The worms were washed off with M9 solution (22mM KH_2PO_4, 22mM Na_2HPO_4, 86mM NaCl), put onto plates without food to clean them and then picked individually into 70µl M9 solution. 25µl of 4X protein loading dye (125mM Tris HCl pH6.8; 10% glycerol, 2% SDS; 5% 2-β-mercaptoethanol, 0.000125% bromophenolblue) and 5µl of 50X Complete

Protease Inhibitor Cocktail (Roche, Indianapolis, IN) were added to each sample, and the tubes quick-frozen in liquid N_2. The tubes were then boiled for ten minutes and the proteins analyzed using 8%SDS-PAGE, transferred to nitrocellulose membranes which were blocked in 5% non-fat reconstituted dry milk in 1xPBS overnight. The blots were then incubated with rabbit antibodies generated to GLH-1 N terminal peptide sequence CMSDGWSDSESAAKAKTGFGSGG or GLH-4 N terminal peptide CMSFSDDGWGAEAEVKVAEKVP diluted 1:1000 in 1xPBS, or anti β-tubulin (Sigma) monoclonal antibodies at 1:10000 in 1xPBS for one hour at 37°C. The blots were then washed four times for ten minutes per wash with PBS 0.2% Tween-20. Secondary goat anti rabbit (for GLH-1 and GLH-4 antibodies) or goat anti-mouse (for β-tubulin) conjugated to horseradish peroxidase (ICN Biomedicals, Irvine, CA) were then diluted 1:10000 in PBS and incubated with the blots for one hour at room temperature. The blots were then washed six more times in PBST, incubated with 15 mLs each SuperSignal® West Pico Chemiluminescent Substrate (Pierce) stable peroxide solution and luminal/enhancer solution for five minutes. The blots were then exposed to autoradiography film. The blots were scanned and processed in Adobe Photoshop. For quantitation the films were treated as above but incubated with 5 mLs each SuperSignal® West Dura Chemiluminescent Substrate (Pierce, Rockford, IL) stable peroxidase and luminol/enhancer solutions, exposed to a BioRad imaging screen overnight, and scanned by BioRad FX phosphoimager. The intensity of the resulting bands was quantitated using QuantityOne software,

with wild type values set to one and all other strain values determined in relation to wild type.

Northern blot analysis

To determine RNA levels of *glh-1*, *glh-4*, and *kgb-1* at 20°C and 26°C starved wild type or *kgb-1* L1 larvae were transferred to 150x15mm plates that had been seeded with 1 mL overnight culture of OP50 in LB. The worms were then allowed to grow to the adult stage, washed off the plates with M9 and collected in 50 mL conical tubes. The worms were then allowed to gravity settle on ice, the M9 aspirated off, fresh M9 added, and the worms were incubated at the appropriate temperature on a rocker for 30 min to clear the bacteria from their guts. Worms were transferred to glass round bottomed tubes and total RNA was then collected as in (Reinke et al. 2000). For every 1 mL of packed worms, 4 mL of Trizol reagent (Invitrogen, Calsbad, CA) was added, and the tube vortexed vigorously for two minutes, flash frozen in liquid N_2, and thawed at 37°C. This procedure was repeated once. 2 mL of $CHCl_3$ for every 1 mL of packed worms was added to the thawed Trizol solution. The tube was shaken for 15 seconds by hand and allowed to sit for three minutes at room temperature. The tube was then centrifuged at 3000 rpm at 4°C for 15 minutes. The aqueous layer was carefully removed and deposited into a fresh tube, to which an equal volume of isopropanol was added, along with glycogen to aid in pellet formation. The tube was mixed well and incubated at room temperature for ten minutes. The solution was again centrifuged at 3000 rpm and 4°C for five minutes. The isopropanol

was removed from the pellet which was washed with 75% ethanol, centrifuged as before, and the pellet dissolved in 0.5 mL of DEPC treated dH_2O or deionized formamide. The concentration of RNA was determined by OD_{260}. The samples were then stored at -80°C for further use.

To determine transcript levels, total RNA from wild type and *kgb-1* grown at 20°C or 26°C was analyzed as in (Chomczynski and Sacchi 1987). Equal amounts of each total RNA sample were run on 1.25% MOPS-acrylamide (40mM MOPS, 10mM NaOAc, 7% formaldehyde) gels and transferred to nylon membranes (HybondN+, Amersham Piscataway, NJ). Probes were generated using Stratagene Prime-It II kit (Stratagene, La Jolla, CA) according to manufacturer's protocol using cDNA fragments for *glh-1*, *glh-4*, and the *C. elegans eIF4A* gene, and a PCR product for *kgb-1*. Membranes were exposed to autoradiography film for 2 hours to overnight; films were scanned and processed in Adobe Photoshop. The blotting procedure was carried out by Eugene Kuzmin.

GST pull-down analysis

Reagents and procedures used in these processes were as previously described (Smith 2001; Smith et al. 2002). To summarize, HighFive cells (Invitrogen, Carlsbad, CA) were co-infected with recombinant baculovirus containing a bacmid in which the protein to be tested was cloned in frame with either a GST or 6-Histidine (6-His) sequence tag (Figure 2.7). The virus was allowed to replicate and produce protein for ~72 hours and then the cells were harvested and lysed in PBS or 300mM LiCl with 1% Triton X-100, 1mM PMSF,

and 1X Complete Protease Inhibitor Cocktail (Roche, Indianapolis, IN). To enhance cell lysis, the cells were frozen and thawed on ice. The lysed cells were centrifuged at 10,000*g* for 10 minutes to remove insoluble materials. 800-1000µL of cleared lysates were incubated with 50µL of Glutathione Uniflow Resin (BD Biosciences, Palo Alto, CA) in PBS (50:50 volume) that had been pre-blocked overnight in 3% BSA in PBS and thoroughly washed. The proteins were incubated with the resin for two hours on a rotating wheel at 4°C, then washed with 1ml of 1XPBS, 1% Triton X-100 for 10 minutes; this wash was repeated five more times. After removing the final wash solution, the proteins were eluted using 50mM Tris with 10mg/mL of reduced glutathione. An equal volume of 4X protein loading dye was added, the proteins were boiled and analyzed using SDS-PAGE and western-blot analysis using αGST antibodies at 1:10000 dilution, and αHis antibodies at 1:2000 dilution (Santa Cruz Biotechnology, Inc., Santa Cruz, CA) and goat-α-rabbit secondary antibodies conjugated to horseradish peroxidase (ICN, Costa Mesa, CA) at 1:10000 dilution; all antibodies were diluted in 1XPBS. Blots were developed using Supersignal West Pico chemiluminescence (Pierce, Rockford, IL) and exposed to film for autoradiography. Films were scanned and processed using Adobe Photoshop.

Site directed mutagenesis

GLH-1 was cloned in frame with a 6-His in the pFastBac plasmid as previously described (Smith et al. 2002). Primers to delete the entire docking (D) site, or to separately mutate each of the consensus leucine at positions 588 and

589 and the lysine at 581 to asparagine were generated using the parameters from the Stratagene Quick Change® II Site Directed Mutagenesis Manual. The primers for the mutagenesis were were:

5’ D site deletion 5’GATGCGAAAGAAGCGAGCTGGGAATCGATATCGA3’

3’ D site deletion 5’TCGATATCGATTCCCAGCTCGCTTCTTTCGCATC3’

SDM *glh-1* KN 5’ (aa 581)

5’ATGCGAAAGAAGCGAGAACAAGGACAAACTTCTAGA

SDM *glh-1* KN 3’ (aa 581)

5’ CTCTAGAAGTTTGTCCTTGTTCTCGCTTCTTTCGCAT

SDM 5’ L588W *glh-1*

5’GAAGAAGGACAAACTTCTAGATGTGCTGGGAATCGATATCGACAG

SDM 3’ L588W *glh-1*

CTGTCGATATCGATTCCCAGCCACTCTAGAAGTTTGTCCTTCTTC

SDM 5’ L589W *glh-1*

5’GGACAAACTTCTAGAGCTTTGGGGAATCGATATCGACAGTT3’

SDM 3’ L589W *glh-1*

AACTGTCGATATCGATTCCCCAAAGCTCTAGAAGTTTGTCC

Site directed mutagenesis (SDM) was performed using PCR as per the Stratagene published protocol (Stratagene, La Jolla, CA) (Figure 2.7). Previously, Pliny Smith had cloned *glh-1* in frame with a 6-His tag in pFastBac entry vector, this plasmid was named PAT 8-1. This plasmid was used for site directed mutagenesis. For SDM PCR 2 µL PAT 8-1 (5 ng/µL) was mixed with 5 µL *Pfu* Turbo 10x reaction buffer, 1 µL 5’ SDM primer (125ng/µL), 1 µL 3’ SDM

Figure 2.7: Diagram of Quick Change Site Directed Mutagenesis (Stratagene) procedure used to produce recombinant GLH-1 bacmids for GST pull-downs.

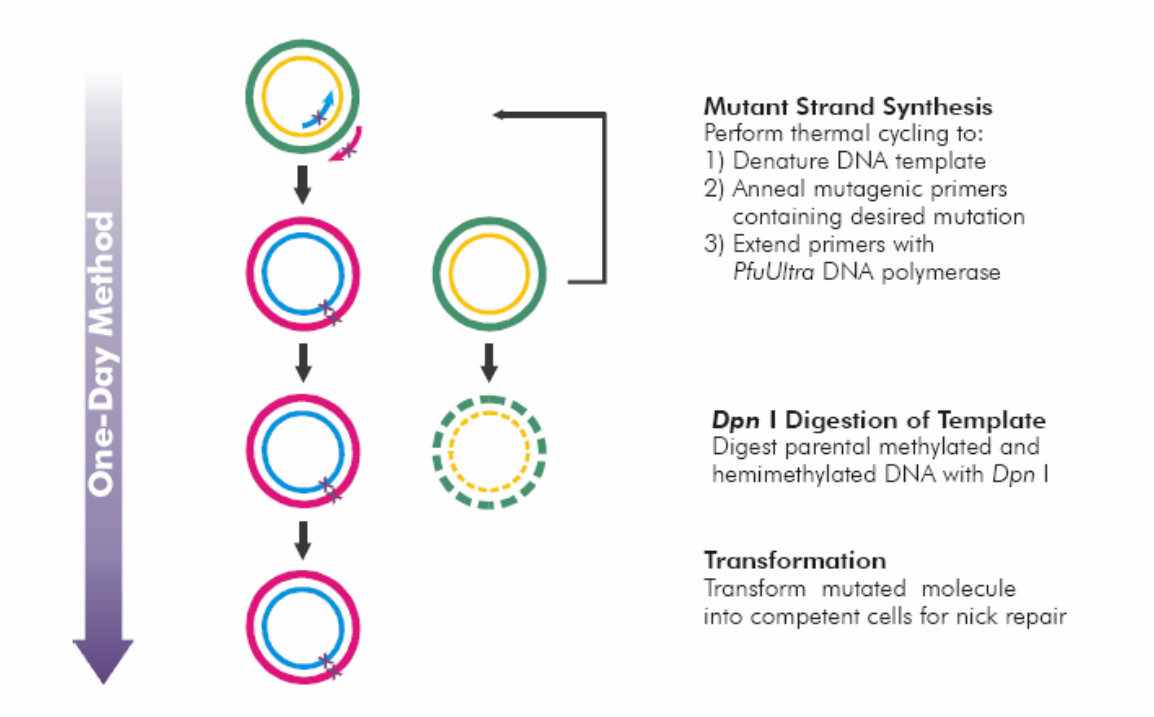

primer (125 ng/μL), 3 μL 8mM dNTs, 37 μL dH20 and 1 μL *Pfu* Turbo polymerase. The reaction was placed in a thermocycler and incubated at 95°C for 1 minute, then cycled at 95°C for 50 seconds, 60°C for 50 seconds, and 68°C for 7 minutes (1 minute per kilobase of plasmid) 18 times. A final 7 minute extension at 68°C followed and the reaction was stored at 4°C. After PCR was finished, 1 μL DpnI (10 units/μL) was added to the reaction and incubated at 37°C for one hour, this digests the methylated or hemi-methylated non-PCR generated plasmids. Bioline Gold α-select competent cells (Bioline, Boston, MA) were then transformed. The cells were thawed on ice and 25 μL of cells were put into pre-chilled 12x75mm snap cap tubes (Fisher Scientific, Hampton, NH). To the cells, 2 μL of the appropriate PCR reaction was added and the tubes were incubated on ice 30 minutes, heat shocked at 42°C for 45 seconds, then placed on ice for 2 minutes. 450 μL of 2xYT media was added to each tube, and the reactions were incubated at 37°C for one hour, with shaking at 225 rpm. The reactions were then plated on LB plates supplemented with ampicillin (150 μg/mL) and the plates placed at 37°C overnight. The next day, individual colonies were picked into 5 mL of LB media with ampicillin, and allowed to grow overnight at 37°C with shaking at 225 rpm. 3 mL of each sample was centrifuged at 7000 rpm for five minutes, media removed, and cells resuspended in 200 μL 50mM Tris-HCl, pH 7.5 and 10mM EDTA by vortexing. The cells were then lysed by adding 200 μL 0.2M NaOH with 1% SDS and the solutions mixed by inverting; the reaction was then neutralized through the addition of 200 μL 0.7M potassium acetate; 7% glacial acetic acid. The tubes were centrifuged at 14000 rpm for 10

minutes and the cleared lysates added to a column containing 1 mL Celite resin slurry in 7M guanidine hydrochloride; a vacuum was applied to the columns and they were washed twice with 3 mL 200mM NaCl, 20mM Tris-HCl pH 7.5, 5mM EDTA with 50% ethanol. After the final wash, the columns were centrifuged briefly to remove any residual wash solution. 20 µL TE buffer (10mM tris, 0.1mM EDTA pH 8.0) that had been warmed to 50°C was added to each column; one hour later the columns were placed in fresh 1.5 mL Eppendorf tubes and spun for 30 seconds at max speed (14000 rpm) using a table top centrifuge. The concentration of DNA was determined using $O.D._{260}$ and, to verify the mutations, the clones were sequenced using the primer 5' *glh-1* SDM seq 5'CTACGTCATGATTGCAATCGAC3' which lies 5' to the D site sequence to verify the mutations.

Baculovirus generation

Entry clones were (pFastBac plasmids) transformed into DH10Bac cells (Invitrogen) (Figure 2.7). Snap cap tubes were pre-chilled, and DH10Bac cells were thawed on ice; 100 µL of cells were placed in each tube with 5 µL of *glh-1* SDM clones in pFastBac (derived from PAT 8-1) (200 pg/µL) was added to the cells and the tube swirled to combine. The cells were incubated on ice 30 minutes, heat shocked at 42°C for 45 seconds and placed on ice for 2 minutes. To each tube 900 µL SOB medium was added and the cells were incubated at 37°C for 4 hours at 225 rpm. 40 µL each of X-gal (20 mg/mL) and 0.2M IPTG were spread on each LB plate with kanamycin (50 µg/mL), gentamycin (7

μg/mL), and tetracycline (10 μg/mL) and transformation reactions spread on these plates. The plates were incubated at 37°C for 48 hours. White colonies were picked into 5 mL of LB media with kanamycin (50 μg/mL), gentamycin (7 μg/mL), and tetracycline (10 μg/mL) and incubated at 37°C overnight. The bacmids were isolated by centrifuging 3 mL of overnight culture, removing media and resuspended cells in 300 μL of 50mM Tris-HCl pH 8.0, 10mM EDTA, 100 μg/mL RNAse A by vortexing. The cells were lysed by adding 300 μL 0.2M NaOH, 1% SDS and tubes inverted. 300 μL of 3M potassium acetate pH 5.5 was added to neutralize and tubes put on ice 10 minutes. The tubes were then centrifuged at 14000 rpm for 10 minutes and the cleared lysates transferred to a fresh tube containing 500 μL 100% isopropanol, and the tubes centrigued again for 10 minutes at 14000 rpm. The ispropanol was aspirated and the pellet washed with 500 μL 70% ethanol. After centrifuging for five minutes at 14000 rpm, the ethanol was removed, the pellet dried for five minutes and resuspended in 40 μL TE.

The resulting transgenic baculoviral genomes (bacmids) were transfected into High-Five cells according to manufacturers' directions. For transfections, $9x10^5$ cells were plated per well of six well, 35mm plate, with 2 mL of insect cell media (Biowhittaker or GellGro) supplemented with 8% FBS and 0.8 mg/mL gentamycin. Cells were allowed to attach for at least one hour. For each sample, 1 μg of bacmid DNA was diluted in 100 μL of unsupplemented Insect cell media, 6 μL of CellFectin reagent (Invitrogen) was combined with 100 μL unsupplemented insect cell media and the DNA and CellFectin solutions mixed

and incubated at room temperature for 45 minutes; 800 µL of unsupplemented Insect cell media was then added to the DNA/CellFectin solution. The media was removed from each well of insect cells and the DNA solution added. The cells were incubated with the DNA solution for five hours at 27°C. The DNA solution was then removed and 2 mL of supplemented Insect cell media added to each well. The cells were then incubated at 27°C for up to five days, until cells showed signs of infection. The cells were harvested along with the media in 15 mL conical tubes, with the cells previously removed by centrifugation at 500 rpm for 5 minutes. The cleared media was kept as the passage one (P1) viral stock and the cells were lysed in 200 µL 1xPBS with 1% Triton X-100, 1x complete protease inhibitor (Roche), and 1mM PMSF and the lysates analyzed for protein production by western-blot as described in the GST pull down section. The P1 viral stock was then amplified by infecting a 25 cm flask of HiFive cells with 200 µL of P1 virus, incubating at 27°C for up to five days. The cells were then harvested and the P2 viral stock clarified as above. This P2 stock was further amplified by adding 1 mL P2 stock to a 75 cm flask of HiFive cells and allowed to grow 3 to 5 days. Again the virus was harvested as above, and used for infections and GST pull downs.

Immunocytochemistry

Immunocytochemistry was performed as in (Kuznicki et al. 2000; Smith et al. 2002). Wild type and *kgb-1* worms were grown at 26°C from the L1 stage or 20°C their whole life. Two or more days after L4, the adult worms were splayed

onto gelatin-coated slides, and the gonads were dissected into M9 buffer. The slides were quick-frozen on dry ice. For GLH-1 images, the tissues were fixed in 3% formaldehyde/0.1 M K_2HPO_4 pH 7.2 for one hour at room temperature, followed by a quick wash in PBS, a five minute incubation in methanol at -20°C, two additional rinses in PBS and one in H_2O. For PGL-1 images, the slides were fixed first for 15 minutes in -20°C methanol, then for 15 minutes in -20°C acetone. All slides were air dried and blocked with 1.5% ovalbumin and 1.5% BSA in PBS; they were then incubated overnight at 4°C with αGLH-1 antibody (rabbit) against the N-terminus of GLH-1 (Gruidl et al. 1996) that had been diluted 1:500 in PBS or αPGL-1 antibody diluted 1:3000 in PBS (a gift of the Strome laboratory, Indiana U.). The tissues were washed four times in PBST (PBS with 0.05% Tween 20) at 15°C; they were blocked again before adding Alexa Fluor488-conjugated goat anti-rabbit secondary antibody (Molecular Probes, Eugene OR) that had been diluted 1:3000 in PBS. The slides were again incubated at 4°C for four hours and then washed six times in PBST, with DAPI at 0.01 μg/ml added in the penultimate wash; they were rinsed in H_2O, and air dried. Gelutol (Elvanol, Dupont Chemicals, Wilmington, DE) was applied to the slide, a coverslip was added and the gelutol allowed to harden overnight. GLH-1, PGL-1, and DAPI staining of nuclei were recorded with a Spot CCD camera attached to a Zeiss Axioplan microscope. All GLH-1 and PGL-1 images were taken at the same exposure of 0.5 seconds.

Germ cell counts

Individual wild type and *kgb-1* worms were grown as in the Western analysis section above at 26°C to two days past the L4 stage. Worms were picked into 3% formaldehyde, 0.1 M K_2HPO_4 pH 7.2 and fixed for five minutes, washed with 1xPBS, 0.02% Tween-20, and post-fixed in ice cold methanol for five minutes at -20°C. The worms were then washed one time with 1xPBS, 0.02% Tween-20, then incubated with 0.02% Tween-20 plus DAPI at 0.01 μg/ml for 10 minutes. The worms were then washed two more times as above, once with nanopure water, and gelutol mounting media added. The worms were put onto slides with cover-slips and the gelutol allowed to harden overnight. Individual germ cells were then counted using a Zeiss Axioplan microscope at 100x; the data was processed in Microsoft® Excel and analyzed by the Student's T Test.

Mating rescue

We mated older (3 days beyond the L4 stage) *kgb-1 and* wild type worms raised at the permissive 20°C temperature with wild type males and the number of progeny produced were counted.

RNA interference

To generate *glh-1* dsRNA, primers were generated corresponding to the helicase region of the *glh-1* gene with a T7 polymerase amplification site added to the 5' end of the primer. The primers were:

glh-1 5’ helicase:

5’GTAATACGACTCACTATAGGGCCCAAATTTACAACGAGGG3’,

glh-1 3’ helicase:

5’GTAATACGACTCACTATAGGGCTGGATATAGTCATCAATG3’.

A cDNA clone of *glh-1* was amplified using *glh-1* helicase primers (PCR parameters same as in backcrossing section) and the resulting PCR product used to produce dsRNA. dsRNA was generated using an Ampliscribe T7 transcription kit (Epicentre Technologies, Madison, WI). In a 1.5 mL Eppendorf tube, 8 µL of PCR product were combined with 2 µL of 10x reaction buffer, 1.8 µL each dUTP, dGTP, dCTP, and dATP, 2 µL DTT and 2 µL T7 polymerase. This mixture was incubated at 37°C overnight. To clean up the transcription, 115 µL DEPC treated H_2O was added to the tube, along with 18 µL 5M NH_3OAC, and 3 µL 0.5M EDTA. 150 µL of phenol:choloroform:isoamyl alcohol at 25:24:1 was added and the sample vortexed and then centrifuged for one minute. The aqueous (top) solution was moved to a fresh tube and 150 µL chloroform:isoamyl (24:1) alcohol added, vortexed, and centrifuged again for one minute. The aqueous layer was again moved to a fresh tube and 150 µL isopropanol added; the sample was then placed at -20°C for 30 minutes. The tube was then centrifuged at 14000 rpm for 15 minutes and supernatant removed, leaving behind the RNA pellet, to which 600 µL of 70% ethanol was added and the tube centrifuged again at 14000 rpm for 15 min. The ethanol was then removed and the pellet allowed to dry for 5 minutes, then resuspended in 20 µL of 10mM Tris, 0.1mM EDTA. The dsRNA was backfilled into glass needles (Sutter, CA) and

young adult worms raised at 20°C were injected and incubated at 26°C; the worms were purged overnight of any embryos or oocytes present before injection and were switched to a new plate. The F_1 progeny were individually plated, and plates examined for the presence of progeny or for sterility (often indicated by clear gonad phenotype) three to five days later.

Proteasome inhibitor experiments

HighFive cells (Invitrogen, Carlsbad, CA) were grown and infected as in GST pull-down analysis above. Cells were allowed to grow for 18 hours after infection at 26°C and treated with 1μM MG132 (Calbiochem, San Diego, CA) for five hours. The cells were then harvested and treated as in GST pull-down analysis above. The proteins were analyzed by western blot analysis using the αHis antibody diluted 1:2000 in PBS (Santa Cruz Biotechnology, Inc., Santa Cruz, CA) to examine total GLH-1 6-His levels.

Kinase assays

Recombinant GST-GLH-1 was generated as described above in GST Pull Down section. This protein was then shipped to Nagoya University and the immunoprecipitation and protein kinase assays were performed by Tomoaki Mizuno, as described previously (Sakaguchi et al. 2004).

SYTO-12/acridine orange staining

SYTO-12 staining was performed as previously described (Gumienny et al. 1999). Wild type and *kgb-1* worms were raised at 26°C from the L1 stage. Worms were age matched and plated at the L4 stage and allowed to grow for two more days. To each plate of worms, 300 µL of 33 µM SYTO-12 in M9 solution was placed on the plate surface. The plates were covered with aluminum foil and incubated at 26°C for four hours. The worms were then picked onto fresh seeded plates for 45 minutes to purge any bacteria in the gut. 150 µL of M9 with 5 mM levamisole was placed on a slide with an agarose pad and the worms picked into the liquid and examined using a Zeiss Axioplan microscope.

Acridine orange staining was carried out as above, but using 2mM acridine orange in M9 and allowing the worms to incubate for one hour and processed as above, as previously described (Hermann et al. 2005).

Generation of *kgb-1(um3); glh-1(ok439); glh-4(gk225)*

As a summer project, undergraduate intern James Chou (University of Maryland, Baltimore) helped to produce the *kgb-1(um3);glh-1(ok439);glh-4(gk225)* triple mutant. The *glh-1(ok439);glh-4(gk225)* double mutant had been constructed by undergraduate researcher Chrisopher Yee. Since the *glh-1(ok439);glh-4(gk225)* exhibits significant sterility when homozygous for both mutations, this strain is maintained by using the balancer chromosome gHT2 (which balances the region chromosome 1 including *glh-1* and *glh-4*) which includes a marker for GFP in the pharynx and is easily screened using a

fluorescent stereo-microscope; the gHT2 balancer is lethal as a homozygote. To produce the triple mutant, two crosses were performed. First, hermaphrodites heterozygous for the gHT2 balancer were mated to *kgb-1(um3)* homozygous males. Worms expressing gHT2 were selected; these should be heterozygous both for gHT2 and the *kgb-1* deletion. The worms were allowed to self fertilize, individual F_2s plated and screened for the *kgb-1* deletion as described in the Backcrossing section. Homozygous *kgb-1(um3)* hermaphrodites heterozygous for gHT2 were then mated to *glh-1(ok439);glh-4(gk225)* males balanced with gHT2. F_1 progeny expressing gHT2 were individually plated, allowed to self fertilize and screened as above for homozygous *kgb-1* deletion and the presence of the *glh-1(ok439)* deletion (Figure 2.8).

Comparison of adult and embryo proteins

Wild type and *kgb-1(um3)* worms were grown in 5% X1666 (a strain of *E. coli*) liquid culture until the adult stage. The worms were then gravity settled on ice, washed two times with M9 buffer and settled again. 500 µL aliquots of adults were placed into 1.5 mL Eppendorf tubes and flash frozen in liquid N_2. The remaining adults were treated with an alkaline hypochlorite solution (0.25M NaOH, 1.5% NaOCl) to dissolve the worm cuticle, leaving behind any embryos. The eggs were then washed six times with M9, 500 µL (~$2x10^6$ eggs) samples collected in 1.5 mL Eppendorf tubes, and the eggs flash frozen in liquid N2. Protein samples were stored at -80°C until used. Adults and embryos were then thawed in either Buffer 1 (25mM Hepes, 300mM NaCl, 1.5mM $MgCl_2$, 1% Triton

Figure 2.8: PCR selection for *kgb-1(um3),glh-1(ok439);glh-4(gk225)*. Hermaphrodites from the second cross exhibiting gHT2 were harvested and screened (reactions in triplicate) with primers from *kgb-1* backcrossing. Presence of inner band and absence of deletion band confirmed homozygousity of worms.

M *kgb-1* inner *kgb-1* deletion

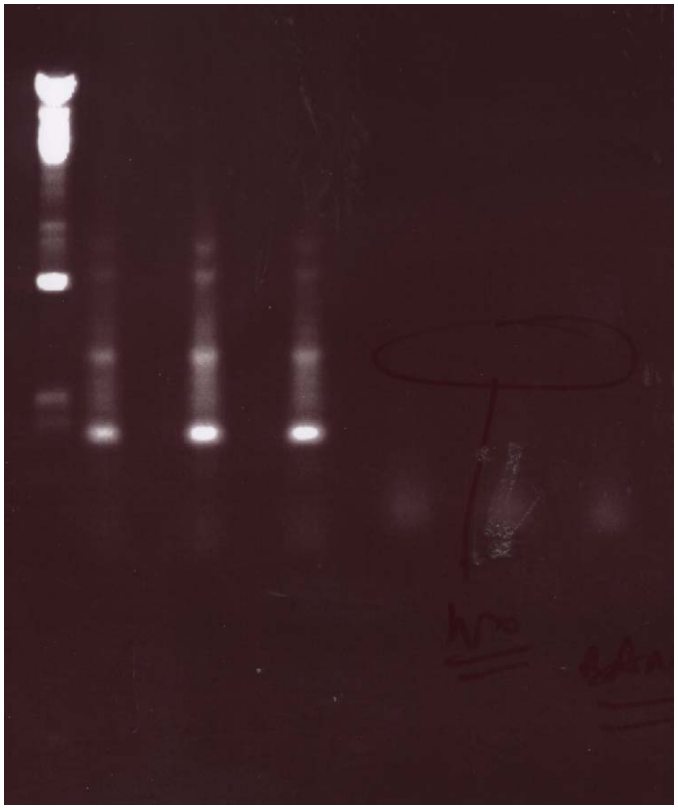

X-100, 0.1mM DTT, 0.2mM PMSF, and 1x Complete Protease Inhibitor (Roche)) (Jonas and Privalsky 2004), Buffer 2 (1x NEB Buffer 3 (50mM Tris, 10mM $MgCl_2$, 1mM DTT, pH 7.9), 1x Complete Protease Inhibitor (Roche), and 1mMPMSF), or Buffer 3 (1x λ Protein Phosphatase Buffer (NEB, Ipswich, MA), 1x Complete Protease Inhibitor (Roche), 1mM PMSF). The worms or embryos were then lysed by four passages through a French Pressure Cell Press (American Instrument Co., Silver Springs, MD) at 900 lb/in^2, with the protein cleared by centrifugation. This protein was then either frozen, 150 µL samples treated with 2 µL calf intestinal phosphatase (NEB) at 37°C for 1 hour or λ protein phosphatase (NEB) at 30°C for 30 minutes. Protein homogenates were then mixed with 20 µL 8x protein loading dye, boiled for 10 minutes, and analyzed by SDS-PAGE (8% acrylamide:bis gels 39:1) and western blotting, as described above.

Generation of *kgb-1(um3); kgb-2(km16)* double mutant

The *kgb-1(um3)* strain was isolated in the Bennett laboratory and described in (Smith et al. 2002), the *kgb-2(km16)* was isolated by the Matsumoto laboratory and described in (Sakaguchi et al. 2004). To generate the double mutant, Wensheng Li performed the following experiments. Males from the *kgb-1(um3)* strain were mated with hermaphrodites from the *kgb-2(km16)* strain. Individual F_1 progeny were plated, as were their F_2 progeny. The F_2 progeny were grown to adults, washed off the plates and 150µL of worms/H_2O solution was added to 150µL proteinase K solution (50mM KCl, 10mM Tris HCl pH 8.3,

0.45% IGEPAL, 0.45% tween-20, 0.01% gelatin, 200µg/mL proteinase K). The worm/proteinase K mixture was frozen at -80°C to crack open the worm cuticle, then incubated at 65°C overnight to digest the worm protein, leaving behind the DNA. The following primers were used to screen for the presence of both mutations: forward 5'GGTCTACCAGAGTTTGTGGGGAATC3' and reverse 5'GATAGCCTTGCACTTCGTTG3' using PCR parameters indicated in Backcrossing section. These primers will produce two products one for *kgb-1* (999 bps) and one for *kgb-2* (1248 bps) with wild-type DNA, the lack of both bands indicates both *kgb-1(um3)* and *kgb-2(km16)* mutations were present. Since *kgb-1* and *kgb-2* are within 23 map units of each other.

Results

Brood size is reduced in *kgb-1(um3)* worms

The sterility observed in *kgb-1* worms at 26°C led us to examine the impact of the *kgb-1* deletion on worms grown at other temperatures. After the strain had been backcrossed six times to N2 males, individual *kgb-1* and N2 worms were age matched and L4 worms individually plated at 15°C, 20°C, and 26°C. The number of progeny produced by each worm was analyzed and the average and standard deviation were determined at each temperature for each strain. A Student's T Test was performed to determine if the differences in numbers of progeny produced by *kgb-1* and N2 worms were statistically significant.

We found that at 20°C, which is considered a permissive temperature, *kgb-1* worms have a slightly reduced brood size compared to N2, but this difference is not statistically significant (Table 2.1). In contrast, at 15°C, *kgb-1* brood sizes are only 60% that of N2, and the difference is significant, with a P value of <0.001. At 26°C, *kgb-1* worms are greater than 95% sterile; the few fertile worms have very small brood sizes, with 33 individually plated worms producing only 20 progeny (less than one progeny per worm). In comparison to wild type, *kgb-1* worms produce 0.005% as many progeny, a statistically significant difference (P value <0.001). At 25°C, approximately 40% of *kgb-1* worms are sterile (Smith et al. 2002).

Table 2.1: Brood counts in N2 and *kgb-1* worms. Individual L4 worms from each strain were age matched and individually plated. F_1 offspring were counted four to seven days after plating depending on temperature. *P_0 L4 animals were shifted to 26°C; the F_2 broods of F_1 adults were determined. P value was determined by comparing brood counts of *kgb-1* with N2 worms grown at same temperature using a Student's T test. s.d.= standard deviation

Strain	Growth Temp.	Total # F_1 progeny/ # P_0 worms counted	Average progeny ± s.d	% of wild type at same temperature	% Sterility	P value
kgb-1(um3)	15°C	3084/33	93±40	60%	0%	<0.001
	20°C	4776/30	159±71	93%	0%	0.13
	26°C*	20/33	0.6±2	0.005%	85%	<0.001
N2	15°C	5884/38	154±39			
(wild type)	20°C	5678/33	172±80			
	26°C*	1332/11	132±37			

Sterility of *kgb-1* worms cannot be rescued by wild type sperm

To determine if *kgb-1* worms are sterile due to the production of nonfunctional sperm at 26°C, we mated *kgb-1* worms with N2 males and found that no progeny were produced. We also examined *kgb-1* male worms at 26°C by mating them with *dpy-13*, *unc-24*, and *unc-22* homozygous recessive hermaphrodites, all of which exhibit an obvious movement defect that is easily scored. No cross progeny (those exhibiting wild type movement) were observed; this suggests that *kgb-1* males are either unable to mate at 26°C or the sperm they produce at this temperature are non-functional (Smith et al. 2002).

GLH-1 levels are increased in *kgb-1* worms

The sterility phenotype of *kgb-1* worms at 26°C led us to examine the cause of this sterility. As KGB-1 is known to bind the GLHs, both by yeast two hybrid and GST pulldown analysis, we wondered if disruption of the *kgb-1* gene would have effects on the GLHs. To examine this we analyzed the levels of GLH-1 and GLH-4 in *kgb-1* worms grown at 26°C from the L1 stage compared to N2. The difference was striking; GLH-4 levels seemed similar between N2 and *kgb-1* worms, but GLH-1 levels were drastically increased in *kgb-1* worms (Figure 2.9A). The same experiment was performed with worms grown one, two, or three days past L4, and GLH-1 levels were quantitated; wild type levels at one day past L4 were established as a value of one, and all levels determined relative to this (Figure 2.9B). In N2 worms, GLH-1 levels decrease as the worms age, but this same reduction was not seen in *kgb-1* worms. GLH-1 levels were

Figure 2.9: Levels of GLH-1 are increased in *kgb-1* worms at 26°C. A. N2 and *kgb-1* worms raised at 26°C from the L1 stage to 3.5 days past L4 were picked and equal numbers of worms examined for GLH-1 and GLH-4 proteins. B. *kgb-1* and N2 worms were grown at 26°C from L1 stage, age matched, and grown one, two and three days past L4 stage. Equal numbers of worms were analyzed. This graph is a compilation of three different, but identical experiments, standard error bars are shown. Significant differences from wild type levels are indicated by as asterisk. N2 levels at day one past L4 were set to one and all values determined relative to this level. A representative blot was examined using αtubulin antibodies and is shown below.

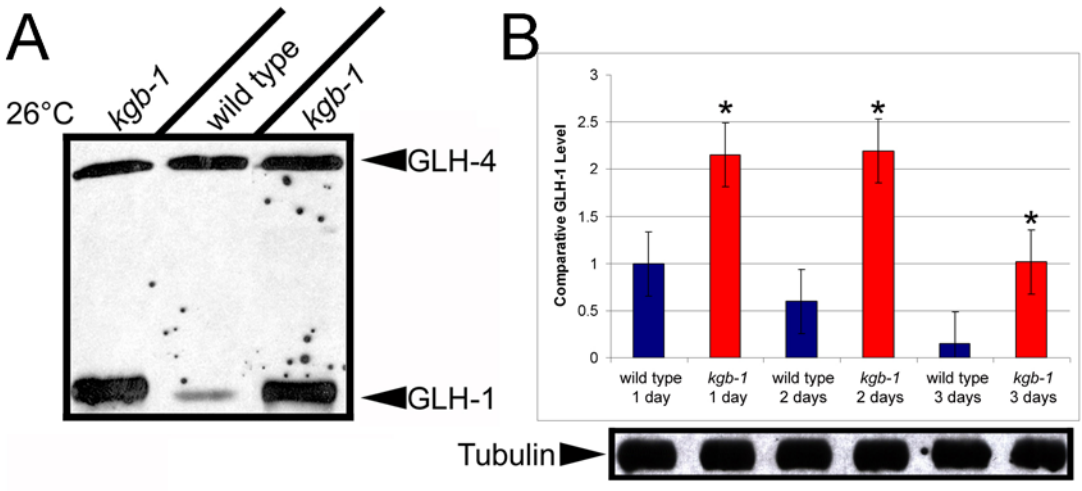

increased by seven-fold in *kgb-1* mutants, compared to their wild type counterparts.

Similar experiments were performed with *kgb-1* and N2 worms at 20°C. Again, GLH-4 levels were similar between N2 and *kgb-1*; GLH-1 levels were increased in *kgb-1* worms grown at 20°C, but not as drastically as at 26°C (Figure 2.10A). GLH-1 levels were quantitated at one, three, and five days past L4 (Figure 2.10B). Again, GLH-1 levels decreased in wild type worms as they aged, but remained high in *kgb-1* worms, but the only significant increase was seen at three and five days past L4, as worms are reaching old age.

To corroborate the western blot analysis, *kgb-1* and N2 worms were raised at 26°C and analyzed by immunocytochemistry for GLH-1. When treated identically, it was clear that GLH-1 levels in *kgb-1* worms were much higher than in N2. Extruded gonads from N2 and *kgb-1* worms were examined for GLH-1, and images taken with identical camera exposures (Figure 2.11 C and D). Upon closer examination, it was evident that the structure of P granules were perturbed in the *kgb-1* mutants. Increased magnification showed that while N2 worms exhibit well-organized P granules that form discrete structures, with each germ cell nuclei having several discrete P granule aggregates surrounding it, *kgb-1* worms have a great deal more GLH-1 and, consequently, larger P granules (Figure 2.11 E and F). These large P granules are non-distinct; they completely surround the germ cell nuclei and fill much of the space between the nuclei. Instead of punctate structures, *kgb-1* P granules are diffuse and disorganized.

Figure 2.10: GLH-1 levels are increased less dramatically at 20°C in *kgb-1* worms. A. Western blot analysis of N2 and *kgb-1* worms grown at the permissive temperature (20°C) 3 days past L4 stage. GLH-1 and GLH-4 levels were examined. B. N2 and *kgb-1* worms were raised at 20°C, age matched, and analyzed by western blot at one, three, and five days past L4 stage. The graph is the result of three different, but identical experiments. Significant difference from wild type is indicated by an asterisk. N2 levels at 1 day past L4 were set to one and all other levels determined relative to this value. Standard error bars are shown. Below, a representative blot was reblocked and examined with αtubulin antibodies.

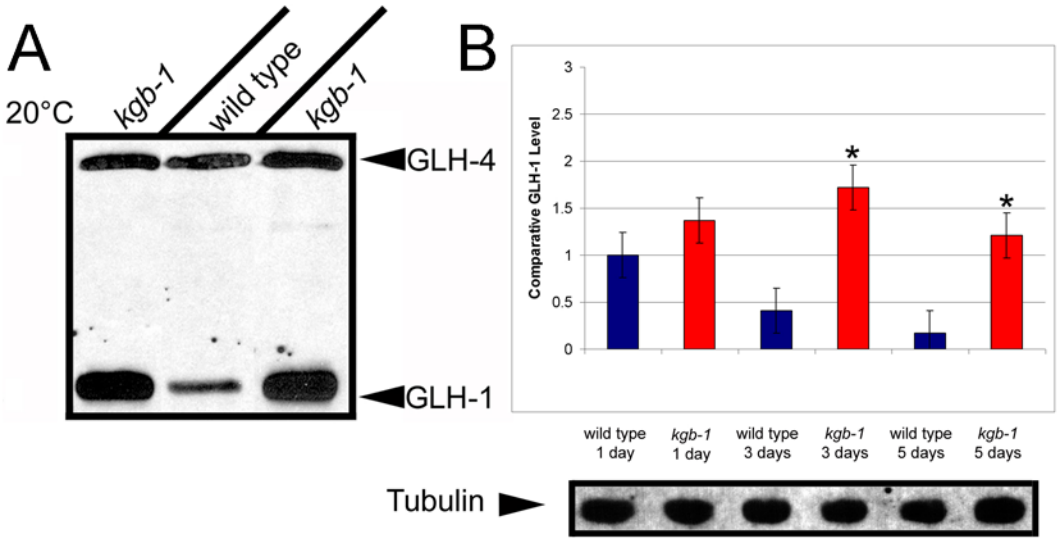

Figure 2.11: GLH-1 levels are increased in *kgb-1* extruded gonads. N2 and *kgb-1* worms were grown at 26°C from the L1 stage, age matched at L4 stage, and analyzed 2 days later. A. Gonad from N2 worm extruded and stained with DAPI to visualize nuclei. A germ cell in pachytene stage is indicated by an arrowhead, an asterisk marks a germ cell in diakinesis. B. Gonad from *kgb-1* worm treated as in A. Arrows point to EMO oocytes. C. Same gonad as in A reacted with antibodies against GLH-1. A portion of the mitosis to meiosis transition zone is indicated by a box, this corresponds to portion of gonad seen in E. D. Same gonad as in B reacted with αGLH-1 antibodies. Portion of the gonad is indicated by a box corresponds to F. Figures C and D were taken with the same camera exposure. All figures A through D were taken at 400x magnification. E. 1000x magnification of gonad in C showing GLH-1. F. 1000x magnification of gonad in D showing GLH-1. Figures E and F were taken with the same camera exposure.

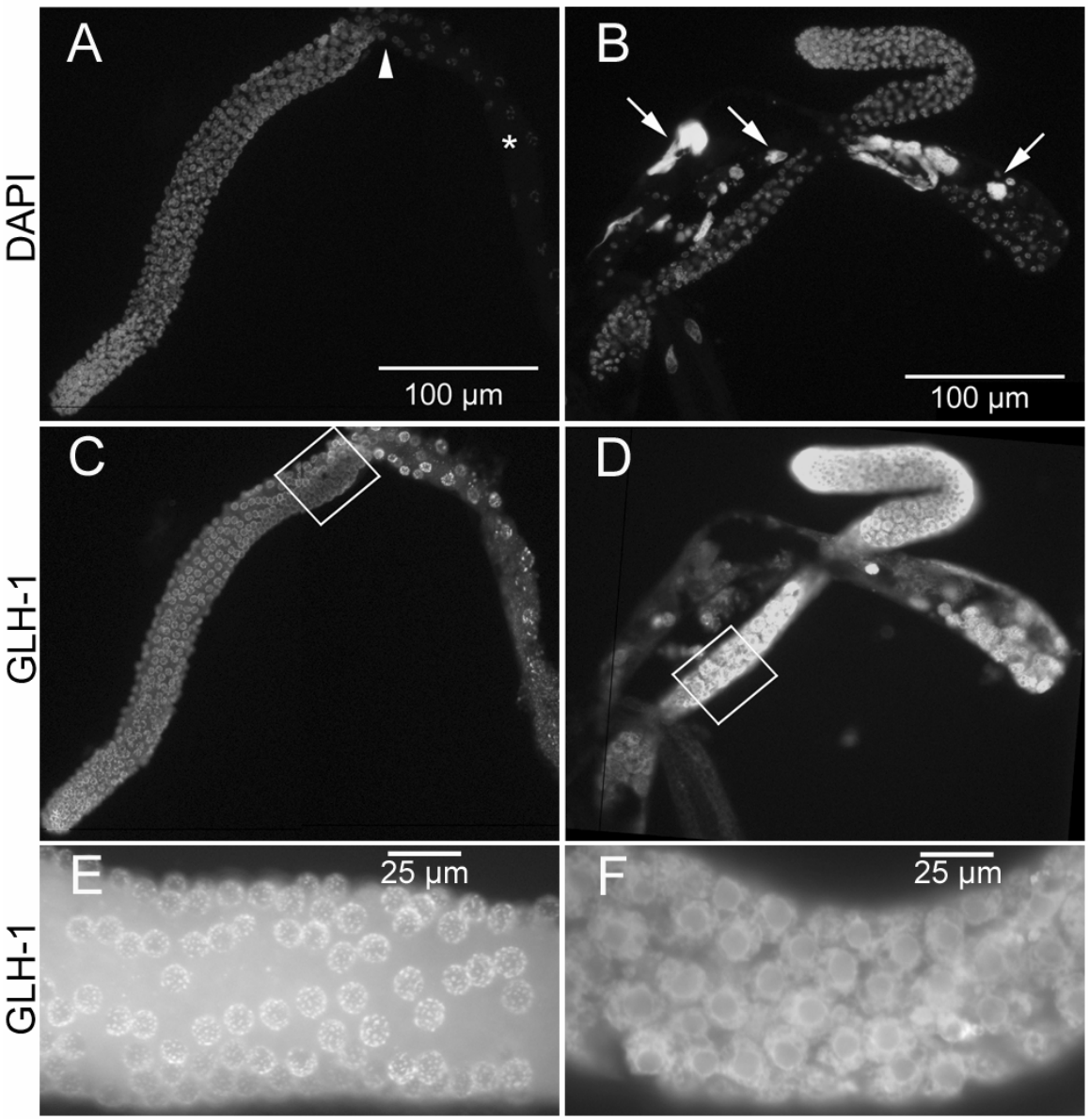
A
B
DAPI
100 µm
100 µm
C
D
GLH-1
E
F
25 µm
25 µm
GLH-1

Western blot analysis of old worms also revealed excess GLH-1 in *kgb-1* worms, those five days past L4, at 20°C (Figure 2.12E). We found *kgb-1* worms did exhibit higher GLH-4 levels, as well as higher GLH-1 levels, compared to wild type worms. At this stage, all the sperm produced have been expended through fertilization, and old age is thought to be a relatively stressful condition, much like high temperature. For this reason, we examined another P granule component in *kgb-1* worms raised to old age at the permissive temperature. N2 and *kgb-1* extruded gonads were reacted with an antibody against PGL-1 (P granule defective-1), a constitutive component of P granules, known to depend on GLH-1 for its localization (Kawasaki et al. 1998). We found that PGL-1 levels were also increased in *kgb-1* old worms compared to N2 worms raised to the same age and temperature (Figure 2.12 A and C). At this late stage, *kgb-1* worms even exhibit abnormal endomitotically replicating oocytes (EMO) as indicated by the disrupted morphology of the nuclei, their increased size, and (Figure 2.12D).

Transcripts of *glh-1* and *glh-4* are not increased in *kgb-1* worms

To determine if the increased GLH-1 levels observed in *kgb-1* worms were due to a change in transcript abundance, northern blot analyses were performed using total RNA from N2 and *kgb-1* worms grown at 20°C and 26°C (Figure 2.13). Transcript levels of *glh-1*, *glh-4*, *kgb-1*, and *eIF4A* (loading control) were examined. We saw little difference in amounts of *glh-1* or *glh-4* either between 20°C and 26°C samples or between N2 and *kgb-1* samples. We also detected no *kgb-1* transcript expressed in the *kgb-1* worm, either at 20°C or

Figure 2.12: P granule components are increased in old worms. A. An extruded gonad from an old wild type (N2) worm grown at 20°C for 4 days beyond L4 was reacted with PGL-1 antibodies. B. DAPI staining of gonad in A. C. An extruded gonad from an old *kgb-1* worm (treated as in A). D. DAPI staining of gonad in C. Images A and C were taken with the same camera exposure. E. N2 and *kgb-1* worms were raised at 20°C and grown to five days past L4 stage, with GLH-1 and GLH-4 levels analyzed by western blot.

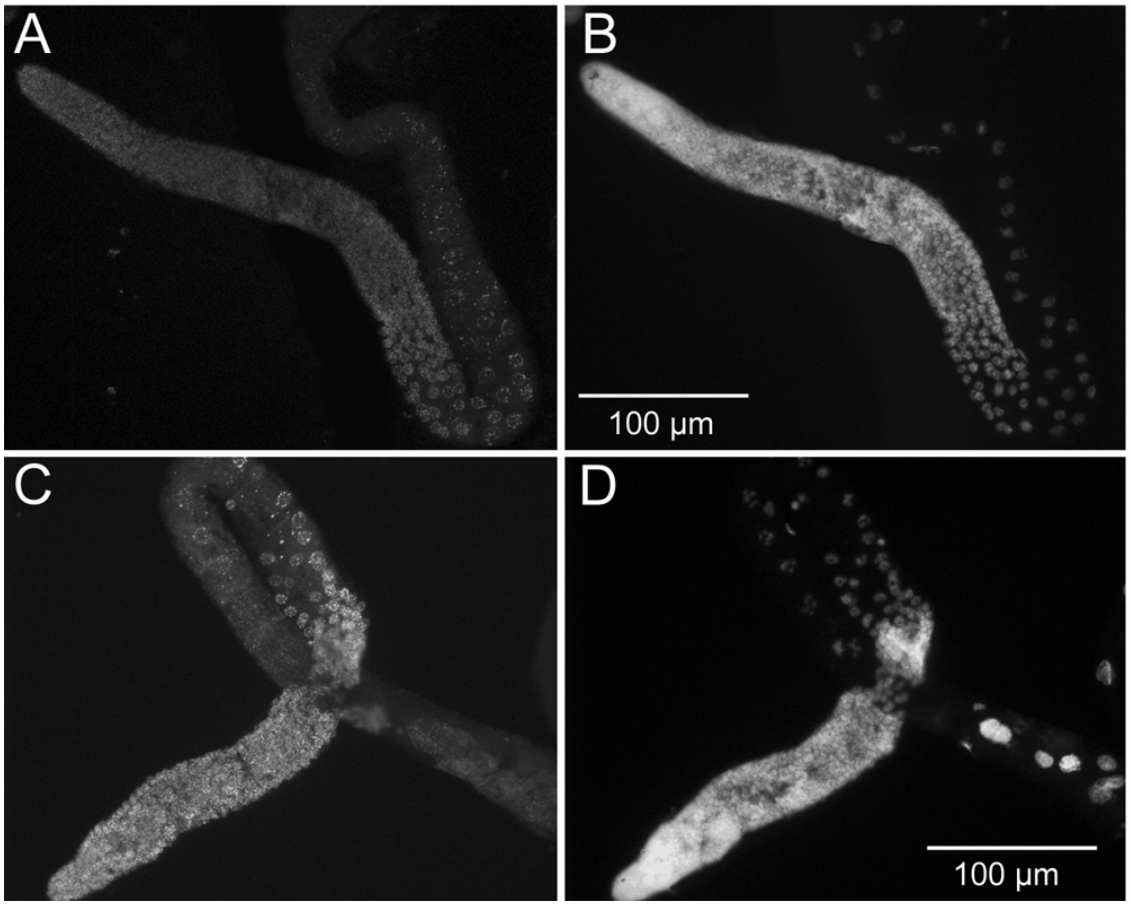
A
B
100 µm
C
D
100 µm

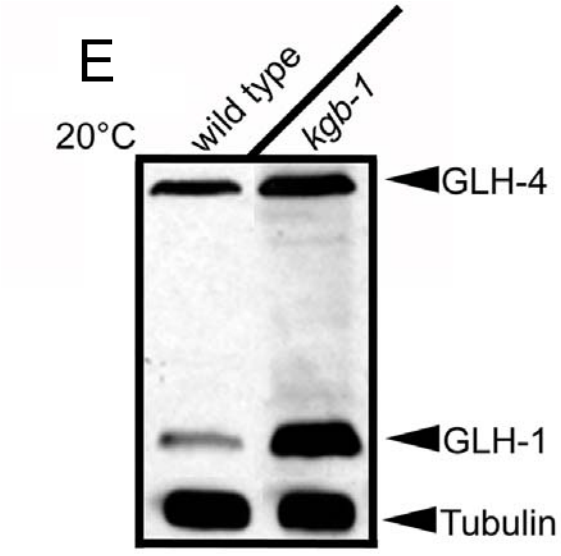
E
20°C
wild type
kgb-1
GLH-4
GLH-1
Tubulin

Figure 2.13: Northern analysis of N2 and *kgb-1* worms grown at 20°C and 26°C. Levels of *glh-4*, *glh-1*, and *kgb-1* transcripts were analyzed. *eIF-4A* serves as a loading control.

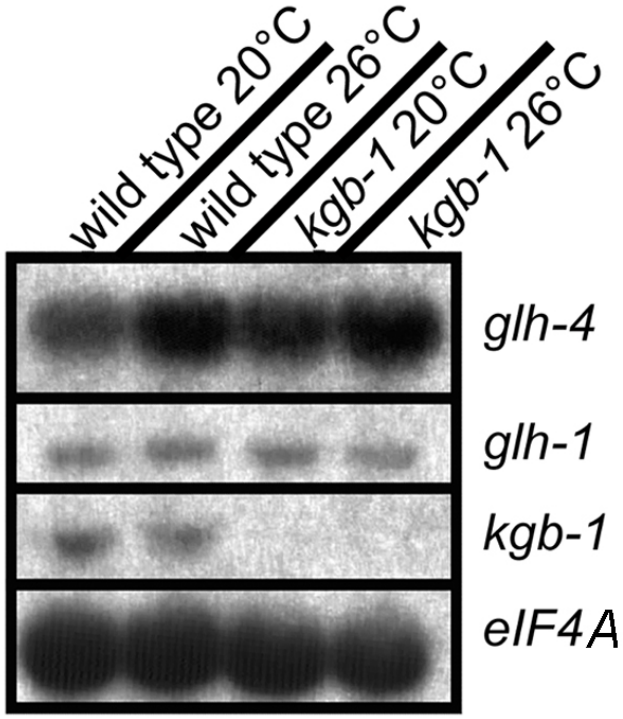

26°C, as we predicted, indicating that the *kgb-1* strain is indeed a null. Taken together, these results indicate that the increases in GLH-1 observed in *kgb-1* worms are due to a regulation of GLH-1 by KGB-1 at the protein level and not due to changes in transcription.

Gonads of *kgb-1* worms are larger than wild type

The gonads of *kgb-1* worms are severely affected, having EMO oocytes and excess GLH-1. It also seemed that *kgb-1* gonads were relatively larger than their wild type counterparts (Compare sizes of gonads in Figure 2.2 and 2.11 in which the *kgb-1* gonad is wrapped back upon itself). To address gonad size, the number of nuclei in gonads from N2 and *kgb-1* worms grown to two days past L4 at 26°C were counted. We found that *kgb-1* worms had 22% more germ cell nuclei than N2 worms (Table 2.2), with an average of 510 germ cell nuclei in *kgb-1* and 419 in N2; this difference is statistically significant (P value <0.04).

KGB-1 binding to GLH-1 requires the MAPK docking site

To determine why GLH-1 and GLH-4 might be regulated differently in the *kgb-1* strain, we examined the two proteins for the presence of conserved regulatory motifs. Alignments of the C-termini of the proteins revealed the presence of a consensus MAPK docking (D) site and phosphodegron in GLH-1 (Tables 2.3 and 2.4) (Jacobs et al. 1999; Orlicky et al. 2003). These sites are conserved in GLH-4, with GLH-4 matching a second consensus alternate of the MAPK D site (Table 2.3 line 2) more closely, but still possessing a single

Table 2.2: Germ cell counts of N2 and *kgb-1* worms 2 days past L4 at 26°C.

Avg.=Average, Diff.=Difference.

Strain	Avg. # Germ Cell Nuclei	# Gonads Counted	% Diff.	P value
N2	419	10		
kgb-1	510	6	+22%	<0.04

Table 2.3: C-terminal alignment of GLH-1 and GLH-4 protein sequences. GLH-1 and GLH-4 proteins were aligned using BLASTP. Identical amino acids are indicated by their single letter identifier, similar amino acids are indicated by a +. The phosphodegron is highlighted in yellow with non-consensus residues indicated by red text and underlined. The MAPK docking site is highlighted in red with non-consensus amino acids indicated by white text and underlined. The endpoint of the *glh-1(ok439)* truncation is indicated by an arrow.

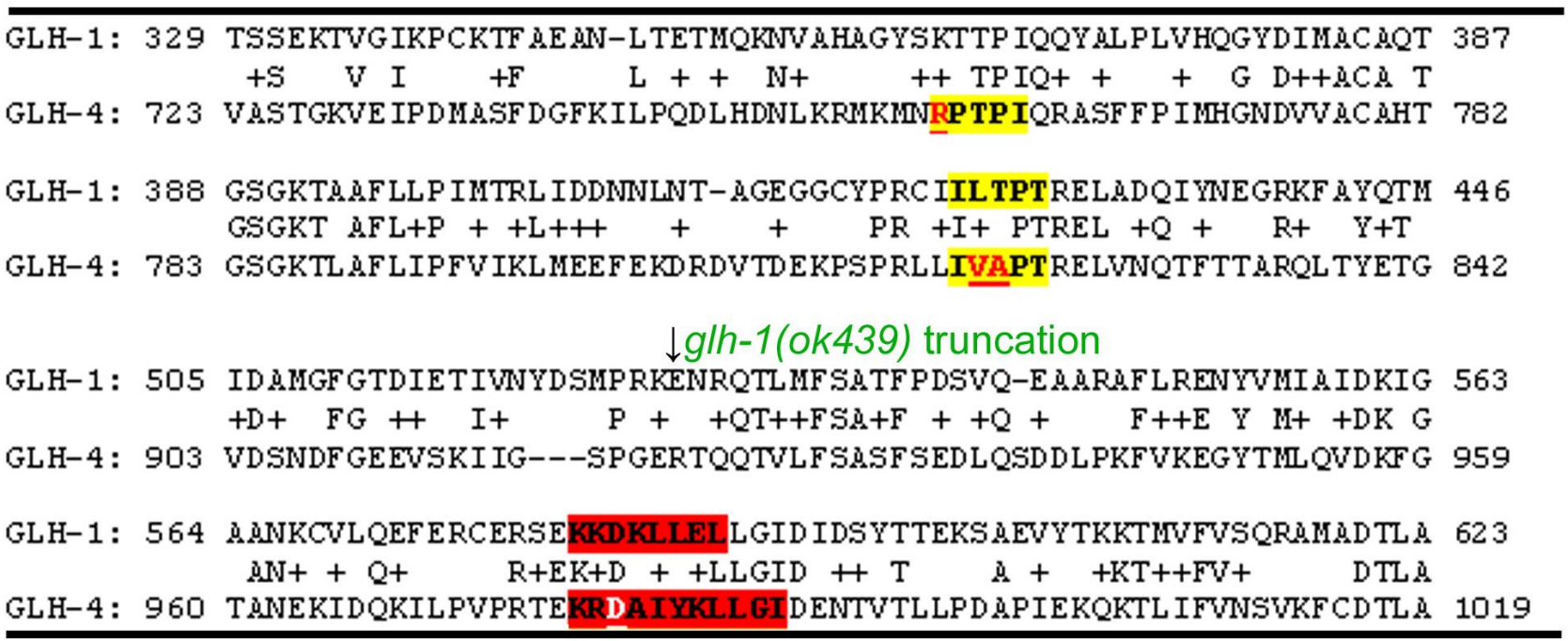
GLH-1: 329 TSSEKTVGIKPCKTFAEAN-LTETMQKNVAHAGYSKTTPIQQYALPLVHQGYDIMACAQT 387
+S V I +F L + + N+ ++ TPIQ+ + + G D++ACA T
GLH-4: 723 VASTGKVEIPDMASFDGFKILPQDLHDNLKRMKMNRPTPIQRASFFPIMHGNDVVACAHT 782
GLH-1: 388 GSGKTAAFLLPIMTRLIDDNNLNT-AGEGGCYPRCIILTPTRELADQIYNEGRKFAYQTM 446
GSGKT AFL+P + +L+++ + + PR +I+ PTREL +Q + R+ Y+T
GLH-4: 783 GSGKTLAFLIPFVIKLMEEFEKDRDVTDEKPSPRLLIVAPTRELVNQTFTTARQLTYETG 842
↓glh-1(ok439) truncation
GLH-1: 505 IDAMGFGTDIETIVNYDSMPRKENRQTLMFSATFPDSVQ-EAARAFLRENYVMIAIDKIG 563
+D+ FG ++ I+ P + +QT++FSA+F + +Q + F++E Y M+ +DK G
GLH-4: 903 VDSNDFGEEVSKIIG---SPGERTQQTVLFSASFSEDLQSDDLPKFVKEGYTMLQVDKFG 959
GLH-1: 564 AANKCVLQEFERCERSEKKDKLLELLGIDIDSYTTEKSAEVYTKKTMVFVSQRAMADTLA 623
AN+ + Q+ R+EK+D + +LLGID ++ T A + +KT++FV+ DTLA
GLH-4: 960 TANEKIDQKILPVPRTEKRDAIYKLLGIDENTVTLLPDAPIEKQKTLIFVNSVKFCDTLA 1019

Table 2.4: Consensus MAPK docking site and phosphodegron motif. MAPK docking site based on (Jacobs et al. 1999). Phosphodegron motif based on (Orlicky et al. 2003).

MAPK docking site	K/R-X-X/K/R-K/R-X(1-4)L/I-X-L/I or K/R-K/R-K/R-$X_{(1-5)}$L/I-X-L/I
Phosphodegron	I/L-I/L/P-pT-P-notK/R

mismatch. The corresponding GLH-4 phosphodegron is two amino acids from consensus, and most critically, with the threonine which is phosphorylated converted to an alanine. GLH-4 does possesses an alternate site that better matches the phosphodegron (Table 2.4 first yellow highlighted site), but it is still one residue from consensus.

To examine the role of the docking site, we first made use of truncations of the GLH-1 protein that were generated by convenient restriction sites (Figure 2.3). We performed GST pull downs with three truncations of GLH-1, one that eliminates a N-terminal portion of GLH-1; the others are two C-terminal constructs, one of which lacks both the phosphodegron and the D site and the other lacks only the D site. We found that KGB-1 could bind the N-terminal truncation construct. However, KGB-1 was not able to bind either construct that lacked the D site (Figure 2.14).

To further examine the role of the D site, site directed mutagenesis was used to mutate individual residues and to delete the entire site. Consensus residue lysine 581 was first changed arginine (K581N); this construct was then used to mutate either leucine 588 (within the D site) or leucine 589 (right next to the D site) to tryptophan (L588W and L589W respectively). In another construct, the entire D site was deleted (indicated by no D site). These three constructs were then used in GST pull downs, as described above. We find that neither the K581N/L588W nor the K581N/L589W mutations completely abrogates GLH-1 binding to KGB-1 (Figure 2.15 lanes 2 and 1 respectively). Although the K581N/L588W construct is severely decreased in its binding efficiency (compare

Figure 2.14: KGB-1 cannot bind GLH-1 truncations lacking MAPK docking site. A. A diagram depicting the GLH-1 protein is shown. Numbers indicate amino acid residues. The MAPK docking site is indicated by a red box and the phosphodegron by a green box. B: An input blot for a pull-down experiment reacted with antibodies against the GST and 6-His tags, indicating all proteins were produced and present in the cell lysates used for GST-pulldowns. Lane one: full-length GLH-1 6-His co-expressed with KGB-1 GST. Lane two: KGB-1 GST with eGFP 6-His, negative control. Lane three: the second construct (aa 1-315) in top panel with KGB-1 GST. Lane four: GLH-1 (aa 315-763) with KGB-1 GST. Lane five: GLH-1 (aa 1-487) with KGB-1-GST. C. Western-blot of GST-pulldown experiments, lanes same as in part B. Binding performed as in GST pull-down analysis methods section.

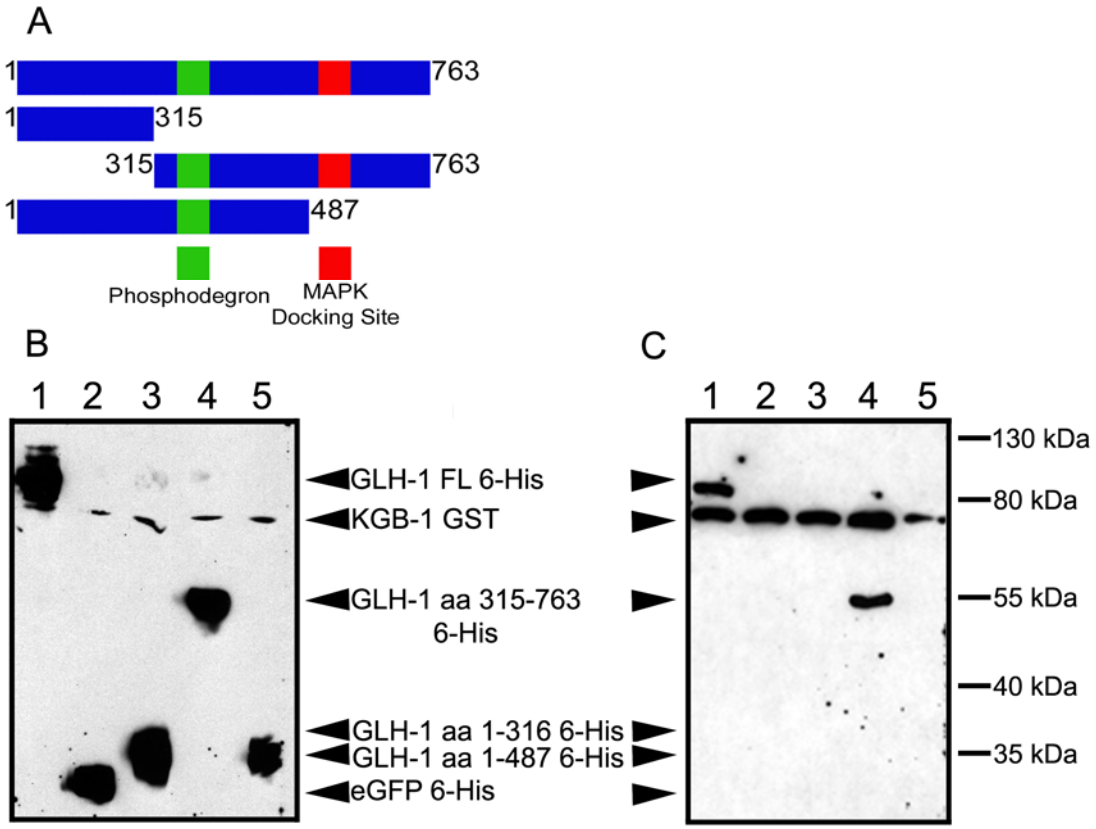
A
1
763
1
315
315
763
1
487
Phosphodegron
MAPK
Docking Site
B
1 2 3 4 5
GLH-1 FL 6-His
KGB-1 GST
GLH-1 aa 315-763
6-His
GLH-1 aa 1-316 6-His
GLH-1 aa 1-487 6-His
eGFP 6-His
C
1 2 3 4 5
130 kDa
80 kDa
55 kDa
40 kDa
35 kDa

lanes 2 and 4 of Figure 2.15), the K581N/L589W binds better than wild type GLH-1 (compare band intensities for Figure 2.15 lanes 1 and 4). Deletion of the entire D site (Figure 2.15 lane 3) drastically inhibits GLH-1 binding to KGB-1; upon long exposures, a faint band can be seen (not shown), indicating that KGB-1 can still bind GLH-1 lacking the D site. This indicates that, although the D site is crucial for the KGB-1:GLH-1 interactions, other sites may be involved. This is consistent with previous results, as GLH-4, which lacks a consensus D site, has been shown to bind to KGB-1 (Smith et al. 2002).

KGB-1 can utilize GLH-1 as a phosphorylation substrate in vitro

Previous results have shown that KGB-1 is able to phosphorylate the heterologous substrate c-Jun via in vitro kinase reactions (Mizuno et al. 2004). These studies indicated that even with the non-consensus activation site of SDY rather than TPY, KGB-1 is a functional kinase. We therefore examined the ability of KGB-1 to phosphorylate GLH-1 (Figure 2.16). On its own, KGB-1 phosphorylates GLH-1 only weakly; similarly, phosphorylation of c-Jun by KGB-1 alone is limited (Figure 2.16 lane 1). However, when KGB-1 is first activated by the *C. elegans* MAPK kinase MEK-1, it phosphorylates GLH-1 at much higher levels; the same is true for c-Jun (Figure 2.16 lane 2). The phosphorylation of KGB-1 by MEK-1 reduces the electrophoretic mobility of KGB-1 (a slower migrating band is resolved). By mutating the ATP binding site of KGB-1 (lysine 67 changed to arginine), KGB-1 is not activated by MEK-1 (Figure 2.16 bottom panel) and fails to phosphorylate either GLH-1 or c-Jun (Figure 2.16

Figure 2.15: GST pull-downs with KGB-1 and GLH-1 after site directed mutagenesis. Lane 1: 6-His tagged GLH-1 K581N/L589W with KGB-1-GST. Lane two: 6-His tagged GLH-1 K581N/I588W with KGB-1 GST. Lane three: 6-His tagged GLH-1 lacking D site (aa 581-588) with KGB-1 GST. Lane four: KGB-1-GST and full-length GLH-1-6-His. Binding was performed as in GST pull-down analysis methods section.

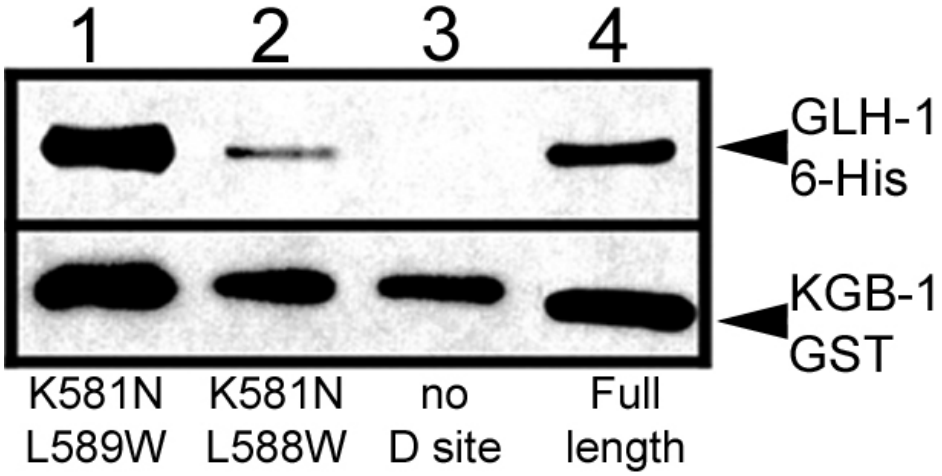

Figure 2.16: KGB-1 can phosphorylate GLH-1 *in vitro*. *In vitro* kinase reactions were carried with GST-GLH-1 (top panel) and GST-c-Jun (second panel), HA-KGB-1 (third panel) and Flag-MEK-1 (fourth panel). In lane 1, basal levels of GLH-1 and c-Jun phosphorylation are seen when incubated with KGB-1 alone. Lane 2 shows phosphorylation levels of GLH-1 and c-Jun when KGB-1 is activated by MEK-1. A mutated, constitutively inactive form of KGB-1 was used in lane 3. The top two panels are audioradiograms, the bottom two panels are western blots.IP: immunoprecipitation, IB: immunoblot.

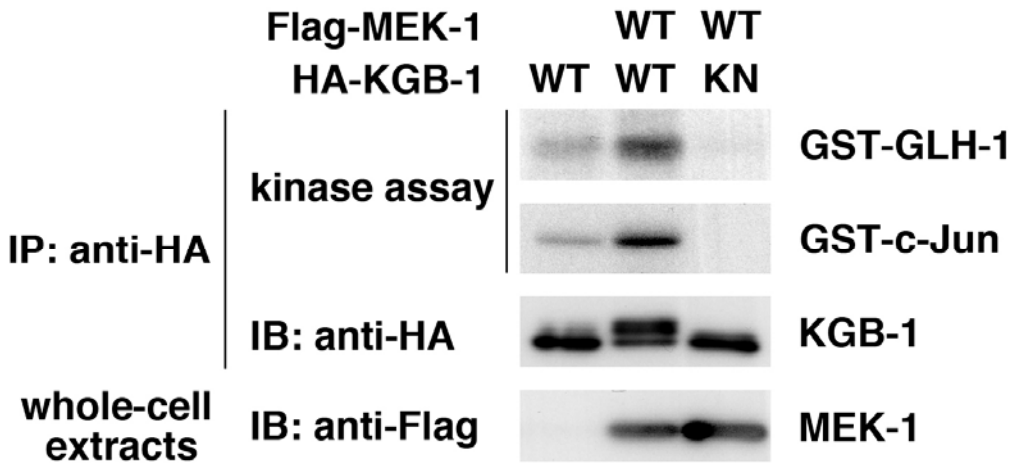

lane 3). This work indicates that, at least *in vitro*, KGB-1 is able to use GLH-1 as a phosphorylation substrate.

KGB-1 targets GLH-1 for degradation in a proteasome dependent manner

To examine the means KGB-1 might use to regulate GLH-1 levels, we devised an experiment to assess levels of GLH-1 when expressed with KGB-1 or other proteins, and analyzed the effect of proteasomal function on these levels. Using our baculoviral system, we expressed GLH-1 independently, or in conjunction either with KGB-1, CSN-5 or GST alone. All experiments were done in duplicate with one sample receiving the proteasome inhibitor MG132 18 hours after infection and one sample not. After the addition of MG132, all samples were allowed to produce protein for five more hours, harvested, and GLH-1 levels examined. We found that in the presence of KGB-1, GLH-1 was found at much lower levels when compared to GLH-1 when expressed alone, with CSN-5 or GST alone (Figure 2.17 Top panel; compare lanes 1 and 7 to other lanes). When protein degradation was blocked through MG132 proteasome inhibition, GLH-1 accumulated when expressed with KGB-1 (Figure 2.17 Top; lanes 6 and 7) but remained constant in the presence of CSN-5 and GST alone. This suggests that KGB-1 is able to target GLH-1 for degradation by the proteasome in insect cells.

A similar experiment was performed using N2 whole adult worm extract. Worms were lysed, the protein cleared by centrifugation, and MG132 was added

Figure 2.17: KGB-1 mediates GLH-1 degradation in a proteasome dependent manner. Top: HighFive cells were infected with 6-His tagged GLH-1 6-His alone, GLH-1-6-His and CSN-5 GST, GLH-1 6-His and KGB-1 GST, or GLH-1 6-His and GST alone. Total levels of GLH-1 are shown. αTubulin loading control shown. Bottom: GLH-1 in N2 extracts is degraded by the proteasome. Whole worm extracts were generated and either incubated alone at room temperature for five minutes, or with the addition of MG132 under the same conditions.

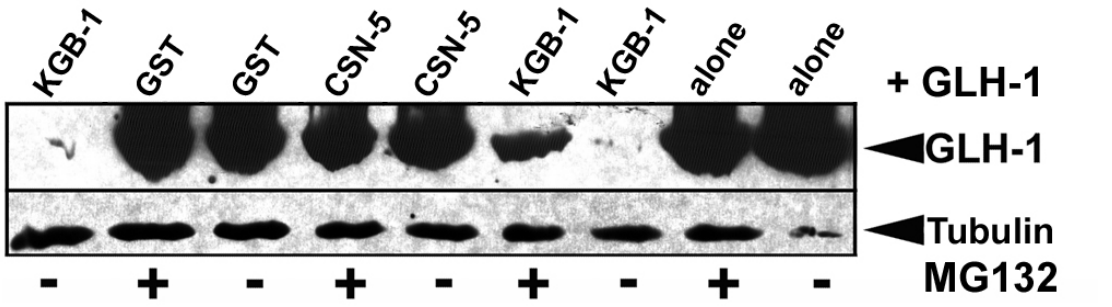

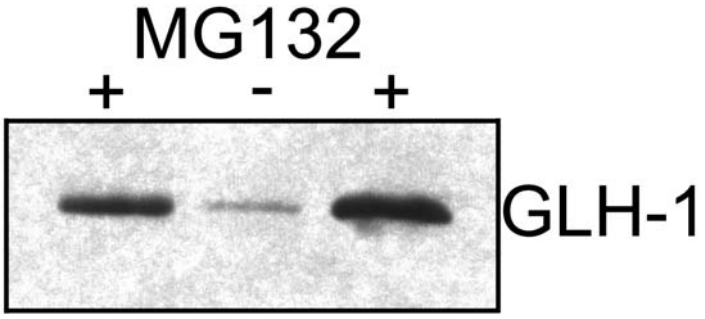

to half the samples. The proteins were then incubated at room temperature for five minutes and amounts of GLH-1 analyzed by western blot. In these extracts, GLH-1 levels are higher when treated with MG132 compared to untreated samples analyzed identically (Figure 2.17 bottom). This indicates that *in vivo*, GLH-1 may be degraded by the proteasome. This experiment was only performed one time and will require additional verification.

GLH-1 levels are increased in *mek-1(ks54)* and *kgb-1(um3);kgb-2(km16)* mutants

KGB-1 contains a unique, non-consensus activation site (SDY instead of the typical TDY site); the only other MAPK with this site is the *C. elegans* protein KGB-2, a protein with extensive similarity to KGB-1. Protein comparisons show KGB-1 and KGB-2 are 91% similar and 86% identical, allowing for the possibility of redundant functions. It is likely that *kgb-1* and *kgb-2* are the result of a genomic duplication, as they are both located on chromosome IV approximately 23 map units apart.

Even with such extensive similarity, KGB-1 and KGB-2 do not have entirely redundant functions, as KGB-2 is not able to compensate for the lack of KGB-1 in *kgb-1* worms. No obvious germline defects have been detected in *kgb-2* mutants (our unpublished results). A double mutant was created, carrying both *kgb-1(um3)* and *kgb-2(km16)* alleles (*kgb-1;kgb-2*). In addition, previous studies have shown that KGB-1 is activated by the MAPK kinase MEK-1 (Mizuno et al. 2004). If KGB-1 is activated exclusively by MEK-1, it would be expected that

GLH-1 levels would be affected in *mek-1(ks54)* mutants as they are in *kgb-1* worms. To test the *kgb-1;kgb-2* double and *mek-1(ks54)* mutant, GLH-1 levels were compared for *kgb-1*, *kgb-2*, *kgb-1;kgb-2*, and *mek-1(ks54)* worms two days past L4 at 26°C (Figure 2.18). This experiment was repeated three times with quantitation and the average increase compared to wild type was determined.

Only a modest increase is seen in the *kgb-2* mutant compared to wild type (40% increase), while *kgb-1* worms show a much greater increase (2.9 fold). The double *kgb-1/2* mutant shows an additive increase (4.5 fold increase), suggesting that normally both KGB-1 and KGB-2 regulate GLH-1 levels, which KGB-1 being the more crucial of the two proteins. Additionally, a modest increase was seen in *mek-1* mutants (70% fold). This suggests that, although MEK-1 may activate KGB-1, it is likely not the only MAPK kinase involved in KBG-1 activity. This is logical as *C. elegans* has many more MAPKKs than MAPKs (Sakaguchi et al. 2004; Stronach 2005). A complex regulatory system with more than one signaling cascade maybe necessary for GLH regulation.

glh-1 RNAi into *kgb-1* worms partially rescues sterility

To determine if excess GLH-1 protein is responsible for the sterility phenotype observed in *kgb-1* worms at 26°C, we tried to decrease GLH-1 levels using RNA interference (RNAi). In N2 worms, *glh-1* RNAi results in sterile worms at 26°C with small, under-proliferated gonads (Kuznicki et al. 2000). To decrease GLH-1 protein, *glh-1* dsRNA was injected into N2 and *kgb-1* worms raised at 20°C. The worms were then transferred to 26°C and purged overnight

Figure 2.18: GLH-1 levels are also increased in the *mek-1(ks54)* strain and in the *kgb-1(um3);kgb-2(km16)* double mutant. *mek-1(ks54)*, wild type, *kgb-1(um3), kgb-2(km16)*, and *kgb-1(um3);kgb-2(km16)* worms were grown at 26°C for two days past L4 and total GLH-1 levels were assayed by western blot analysis of protein homogenates from 120 worms of each strain. The quantification below the figure reflects the average of three separate experimental values for each mutant strain, with wild type levels set to one.

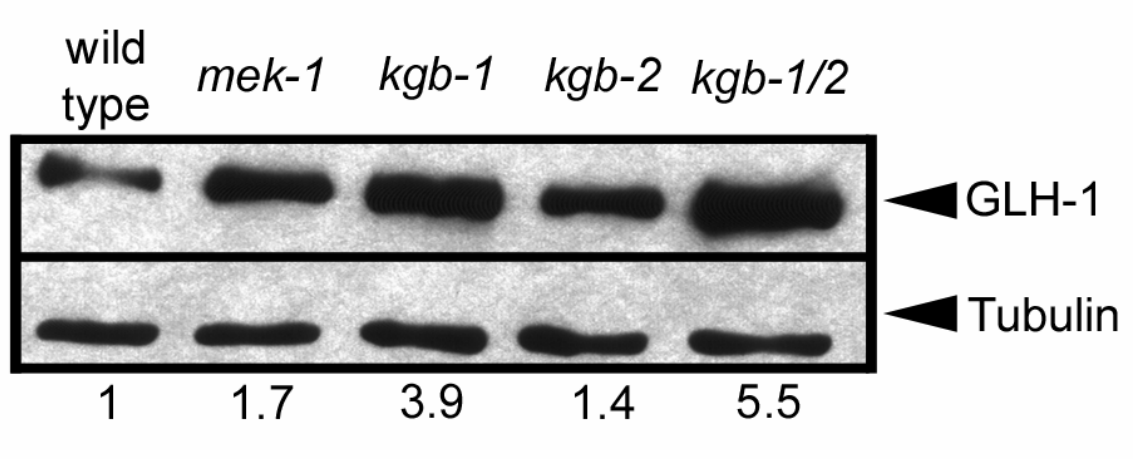

to eliminate oocytes that had formed prior to injection. The progeny of the injected worms were then examined for fertility. We find that *kgb-1* worms are significantly more fertile (18%) than their non-injected *kgb-1* counterparts (7%) when injected with *glh-1* dsRNA ($p<0.001$) (Table 2.5). Two independent but identical experiments were performed to gather this data.

GLH-1 migrates differently in embryos and adults

Phosphorylation of a protein will sometimes cause changes in protein migration; numerous western blots revealed no migration difference in GLH-1 protein from N2 and *kgb-1* adult worms (Figures 2.9, 10, and 18). We did, however, observe differences in the migration rates of GLH-1 protein derived from N2 adults and embryos (Figure 2.19 Top), but GLH-4 does not show the same difference (Figure 2.19 Bottom). Relative abundance of GLH-1 and GLH-4 protein showed opposite distributions in embryos and adults. When starting with identical volume of embryos or adults, GLH-1 is more abundant in adults than embryos, requiring three to four fold more embryonic lysate than adult protein to visualize similar levels (Figure 2.19 Top 40 µL of adult protein compared to 150 µL). In contrast, GLH-4 is relatively more abundant in embryos with three to four fold more adult than embryonic protein required for similar levels by western blot (Figure 2.19 Bottom 150 µL of adult protein compared to 40 µL of embryos).

Similar experiments were performed using protein extracts from both N2 embryo and adult proteins, as well as *kgb-1* adults and embryos. Even in the embryos of the *kgb-1* background, we still see a shift in migration of GLH-1

Table 2.5: Removal of excess GLH-1 from *kgb-1(um3)* increases fertility. Wild type and *kgb-1* worms were raised at 20°C until they were gravid, and were injected with *glh-1* dsRNA. Injected worms were placed at 26°C and purged overnight. The resulting F1 progeny were examined for fertility. A Student's T test found *kgb-1* worms significantly more fertile than their non-injected counterparts ($p<0.0059$) when subjected to *glh-1* RNAi. Asterisk indicates samples compared in a Student's T test.

glh-1 RNAi	# sterile F_1s (total F_1s)	# injected	% fertile F_1s
wild type (N2)	106 (114)	17	7%
wild type (N2) no RNAi	0 (20)		100%
kgb-1(um3)	101 (123)	26	18%*
kgb-1(um3) no RNAi	279 (289)		3%*

Figure 2.19: GLH-1 and GLH-4 migration in N2 adults and embryos. N2 adults and embryos were lysed in phosphate buffer 1. Top: A western blot was run to optimally resolve the migration of GLH-1 (~80 kDa) appropriate amounts of adult and embryo proteins to give similar intensities for GLH-1. Bottom: A different western blot than in the top panel, the blot was performed to optimally resolve the migration of GLH-4 (~120 kDa), appropriate amounts of adult and embryo proteins were loaded to give similar intensities for GLH-4.

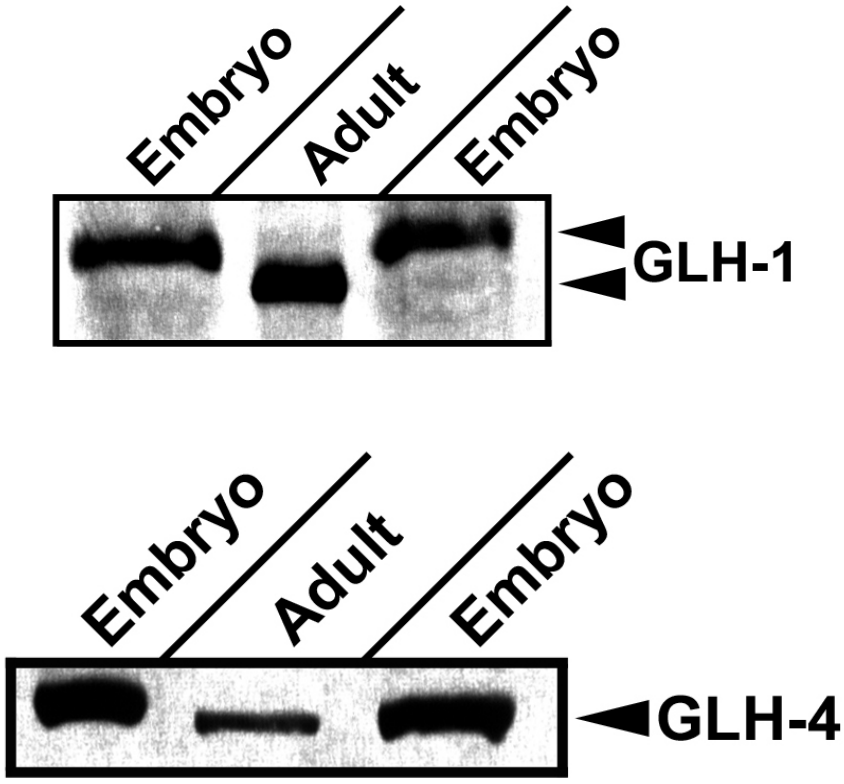

protein similar to that seen in N2 embryos when compared to adults (Figure 2.20).

GLH-1 in embryos is sensitive to degradation

To address the changes in GLH-1 migration in adults and embryos, phosphatase assays were performed. N2 adult and embryo protein was treated with λ protein phosphatase and incubated at 30°C for 30 minutes. We found that while adult GLH-1 protein could withstand these treatments, GLH-1 from embryos was undetectable even under mock treatments (Figure 2.21, two different attempts at same experiment). To be sure that just GLH-1 was degrading and not all other proteins in the embryos, the blots were re-examined using antibodies generated to GLH-4 and αTubulin. Both of these proteins were detectable in embryo extracts at similar levels, whether or not the proteins had been placed at 30°C or frozen immediately after generation (input), although GLH-4 levels may be regulated oppositely, with GLH-4 in adults more susceptible to degradation that in embryos (Figure 2.21 bottom).

The fact that GLH-1 from embryos could not withstand the time necessary to prepare proteins for the 30 minute incubation at 30°C made it impossible to determine if phosphatase treatment eliminated the shift in GLH-1 protein. Therefore, we are not able to examine the nature of the migration shift seen in embryos compared to adults; it may be due to phosphorylation or some other protein modification, but it does not seem to depend exclusively upon KGB-1.

Figure 2.20: GLH-1 migration in N2 and *kgb-1* adults and embryos. Embryos and adults from both N2 and *kgb-1* worms were lysed in phosphate buffer 1, analyzed by western blot, and GLH-1 size was examined.

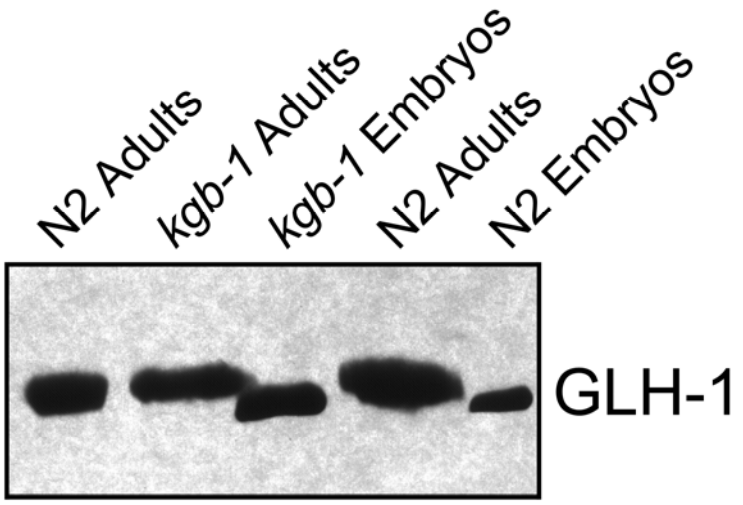

Figure 2.21: GLH-4, GLH-1 and Tubulin in N2 adults and embryos treated with phosphatase. Top: N2 adults and embryos were lysed in phosphatase buffer 2. A + indicates addition of λ protein phosphatase, - indicates no phosphatase added. Lanes with neither + or – indicates input proteins, not treated at 30°C. The blot was first examined for GLH-1, then reblocked and reexamined with αGLH-4 and αTubulin antibodies. Bottom: N2 adults and embryos were lysed in phosphate buffer 1. A + indicates addition of CIP, - no CIP added. Input proteins were frozen in dye immediately after clearing by centrifugation. Blot was examined for GLH-1 and GLH-4 proteins. Middle band in adult input lane is a likely GLH-4 degradation product. Both panels were loaded with protein amounts optimized for GLH-1, not GLH-4; too little GLH-4 was present in the adult lanes of the top panel for detection. A: adult, E: embryo.

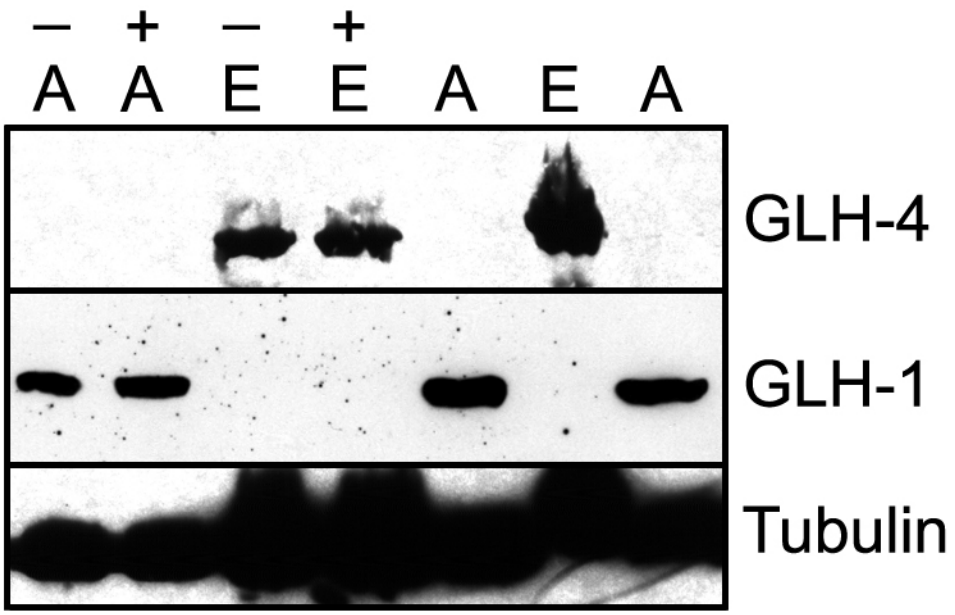
– + – +
A A E E A E A
GLH-4
GLH-1
Tubulin

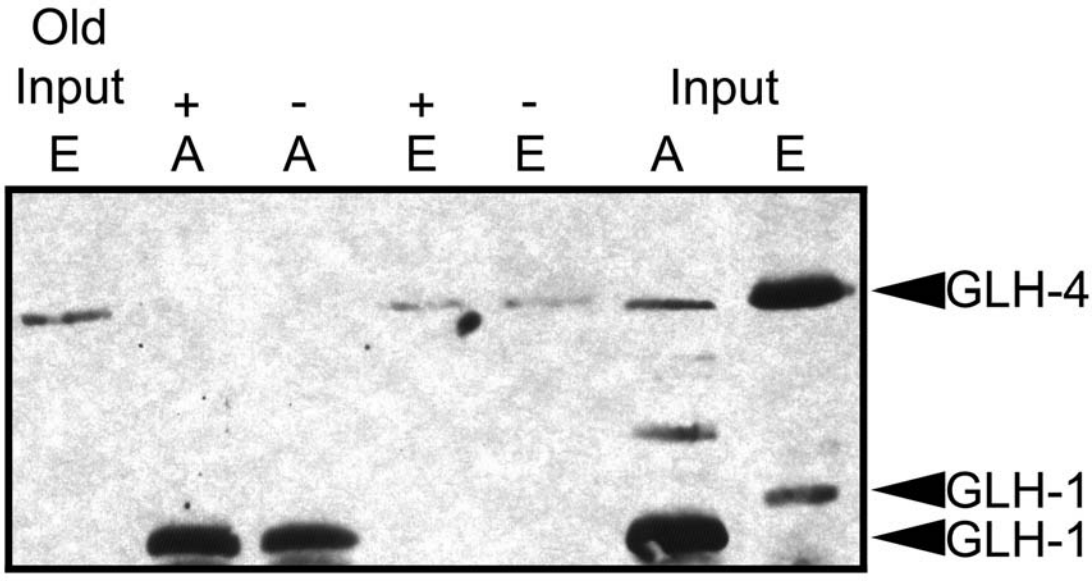
Old
Input
+ - + -
Input
E A A E E A E
GLH-4
GLH-1
GLH-1

Examination of *kgb-1(um3); glh-1(ok439); glh-4(gk225)* mutant

Mutants containing three genetic lesions, *kgb-1(um3); glh-1(ok439); glh-4(gk225)*, were generated. Our goal was to determine if elimination of GLH-1 and GLH-4 in the *kgb-1* background would restore fertility. However, the triple mutants exhibited pleiotrophic phenotypes. They mostly resembled *glh-1/4* double mutants when grown at 20°C (Figure 2.22 panel B, although some triple mutants did have larger gonads, but were sterile (Figure 2.22 panel C). Some of the triple mutants did produce dead eggs, with the some gonads having EMO oocytes (Figure 2.22 panels C and D). The *glh-1(ok439)* strain is not a protein null (as considered in Chapter 4), which may make interpretation of any phenotypes related to this strain difficult. Unfortunately, due to a freezer malfunction, this strain has been lost, so further examination will require the long process of regeneration.

Acridine orange and SYTO 12 staining of N2 and *kgb-1* worms

The endomitotic replicating oocytes (EMO) observed in the *kgb-1* mutant led us to wonder if there were other defects in normal germline processes in these worms. To address this possibility, *kgb-1* and N2 worms were stained with acridine orange or SYTO-12, two vital dyes that stain apoptotic cells (Gumienny et al. 1999; Hermann et al. 2005). Wild type worms usually show very few (0-2) dying cell corpses. These dying cells can often be identified by Nomarski optics as they form “buttons” on the gonad before they are engulfed by the somatic sheath. The dying germ cell nuclei are usually quite small (Figure 2.23). In

contrast, *kgb-1* worms show very large structures that stain with both acridine orange and SYTO-12 (Figures 2.23). Additionally, acridine orange and SYTO-12 staining structures seem more frequent in *kgb-1* worms, with nearly every *kgb-1* worm having these structures, whereas only 4 out of 20 N2 worms were identified with SYTO-12 or acridine orange staining corpses. Further analysis will be required to understand these structures.

Figure 2.22: DAPI staining of N2 and *kgb-1(um3); glh-1(ok439); glh-4(gk225)* triple mutants. A. Extruded gonad from an N2 worm raised at 20°C stained with DAPI to visualize nuclei. B. Extruded gonad from a sterile *kgb-1(um3); glh-1(ok439); glh-4(gk225)* triple mutant. C. Extruded gonad from a *kgb-1(um3); glh-1(ok439); glh-4(gk225)* triple mutant that produced only dead embryos. D. Enlargement of portion of Panel C in box. Arrows point to sperm, arrowheads point to possible EMO oocytes, asterisks indicated bivalent chromosomes in developing oocytes.

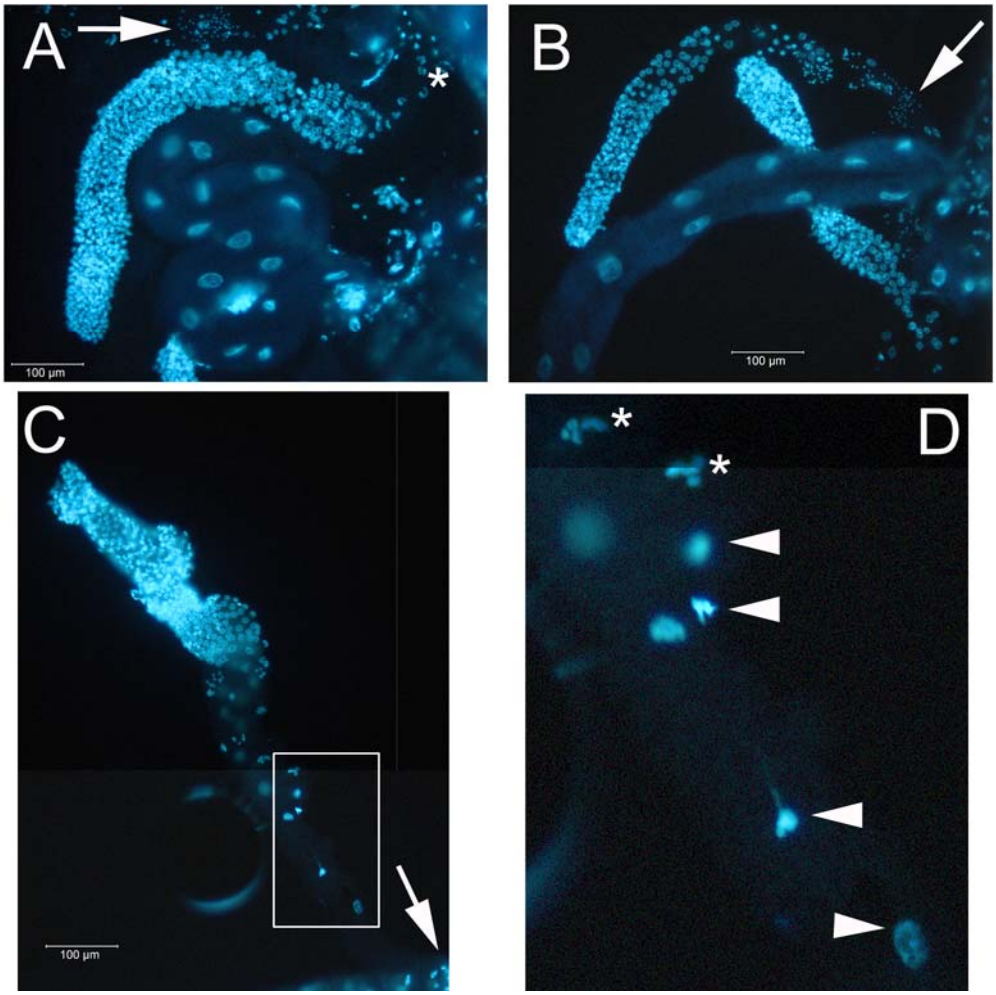

Figure 2.23: Acridine orange and SYTO-12 staining of N2 and *kgb-1* worms. Top: N2 and *kgb-1* worms were raised at 26°C from L1 and stained with acridine orange two days past L4 stage. Worms were visualized by Nomarski optics (to reveal obvious cell corpses), and using fluorescence to show dying cells. Bottom: As in top panel, N2 and *kgb-1* worms were raised at 26°C and stained with SYTO-12 to reveal dying cells. Arrows point to dying cells.

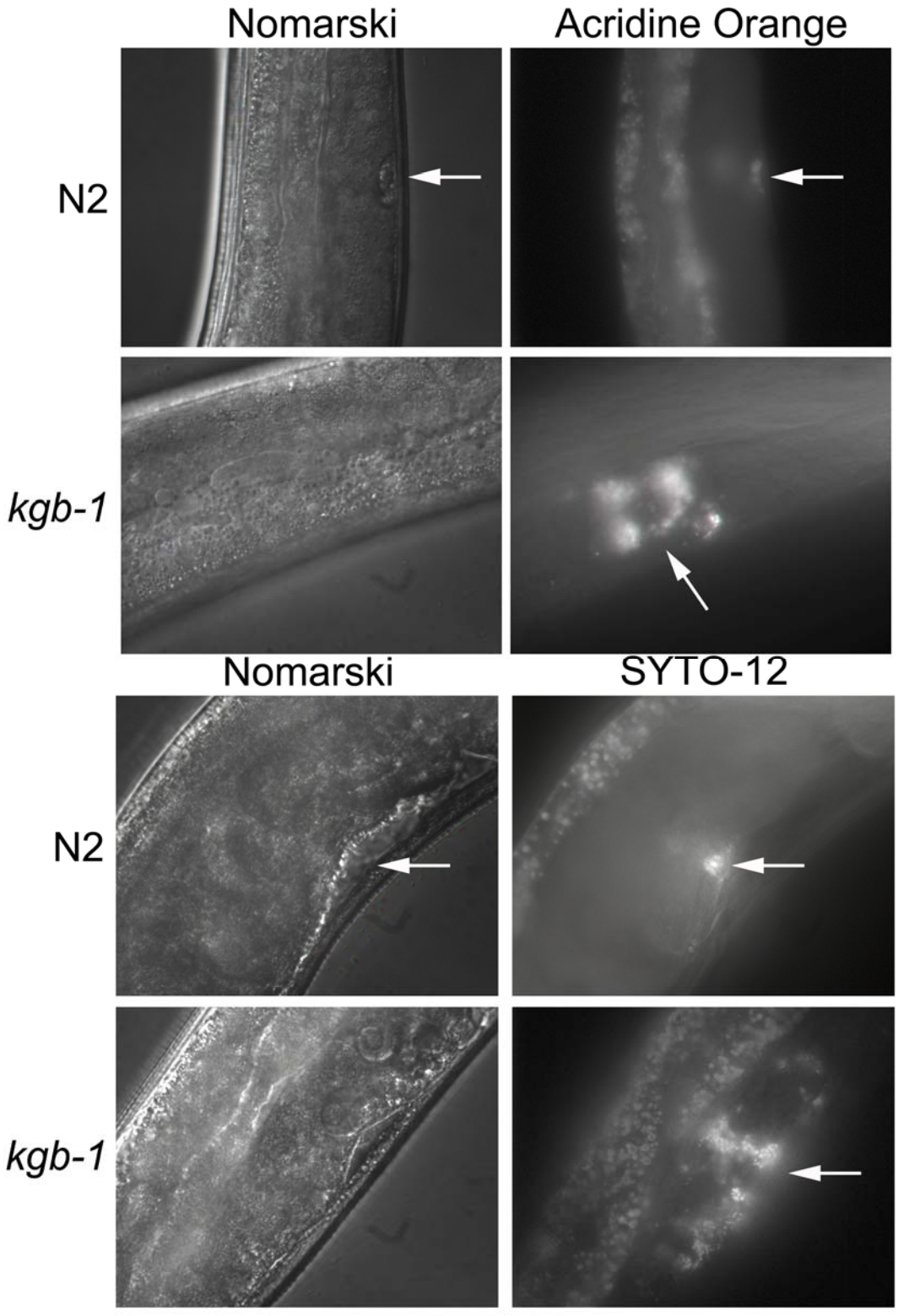
Nomarski
Acridine Orange
N2
kgb-1
Nomarski
SYTO-12
N2
kgb-1

Discussion

Mutation of the *kgb-1* gene has drastic effects on the fertility of *C. elegans*. When *kgb-1* worms are raised at 26°C, they are sterile, producing large gonads with EMO and more germ cell nuclei than N2 worms treated identically (Figures 2.2 and 2.11, Table 2.2). Fertility is also affected at colder temperatures; *kgb-1* worms produce only 60% the number of progeny as their wild type counterparts raised at 15°C. No significant change in brood size is observed at the permissive temperature of 20°C (Table 2.1). Not only hermaphrodites are affected by the *kgb-1* deletion; *kgb-1* males are not able to fertilize hermaphrodites at 26°C. These results point to potential roles for KGB-1 protein in the stressful conditions of high and low temperature.

Regulation of protein levels is vital for cellular functioning and development; control of protein amounts through degradation is known to play a role in developmental processes. Kinases regulate degradation of proteins required for development. In *C. elegans* the dual specificity kinase MBK-2 coordinates the degradation of the MEI-1, MEI-2 and OMA-1 proteins, permitting establishment of the A-P axis during embryogenesis (Pellettieri et al. 2003; Nishi and Lin 2005). Additional *C. elegans* proteins are regulated through degradation; the transcription factor PIE-1 is degraded in a coordinated manner. As the embryo divides, PIE-1 is enriched in germline progenitor cells, and excluded from somatic cells. PIE-1 has two CCCH zinc fingers (ZF1 and ZF2); ZF1 is required for PIE-1 to be degraded in the soma, and ZF2 is required for PIE-1 to be

enriched in the germline. POS-1 and MEX-1, *C. elegans* embryonic P granule components, also contain PIE-1-like ZF1 domains, and are therefore degraded in somatic cells during embryogenesis (Reese et al. 2000). Taken together this suggests that localized and coordinated degradation is important during *C. elegans* embryogenesis.

Our data suggests that the degradation of GLH-1, a constitutive P granule component of embryos and adults, is regulated by the novel JNK KGB-1. When compared to N2, levels of GLH-1 are drastically increased in *kgb-1* worms grown at the non-permissive temperature of 26°C, and are increased to a lesser extent in *kgb-1* worms grown at 20°C. We also see elevated levels of GLH-1 in old *kgb-1* worms (greater than three days past L4), and this corresponds to an increase in PGL-1, a P granule component that depends on GLH-1 for its localization (Kawasaki et al. 1998).

Previous studies with KGB-1 revealed its role in temperature stress and response to heavy metals; the MEK-1 pathway, in which KGB-1 can participate, also mediates innate immunity (Smith et al. 2002; Kim et al. 2004; Mizuno et al. 2004). This suggests that KGB-1 may play many roles in *C. elegans* development. Our work shows that a crucial role of KGB-1 in the germline is to regulate GLH-1 protein levels. The conserved MAPK docking site found in the C-terminus of GLH-1 may be required for this regulation. In GST pull downs, we find that elimination of the D site strongly inhibits KGB-1 binding GLH-1 (Figure 2.14 and 2.15). The presence of a phosphodegron also points to possible regulation of GLH-1 through phospho-mediated degradation. A construct has

been created for baculoviral expression where the conserved phosphorylation site (threonine 425) has been changed to an alanine. This construct will be useful both in kinase assays, to examine the ability of KGB-1 to phosphorylate GLH-1 without a consensus phosphodegron, and for examining the ability of KGB-1 to target GLH-1 for degradation with the phosphodegron perturbed.

Through use of the proteasome inhibitor MG132, we find that KGB-1 can target GLH-1 for degradation by the proteasome in insect cells, and that GLH-1 is less rapidly degraded in N2 adult worm extracts when MG132 is added (Figure 2.17). We also find that KGB-1 can utilize GLH-1 as a phosphorylation substrate through *in vitro* kinase assays. Taken together, the data suggest that phosphorylation of GLH-1 by KGB-1 may normally function to regulate GLH-1 levels in the germline. Yet we do not detect a larger form of GLH-1 in adult extracts. Possible explanations include: phosphorylated GLH-1 is degraded rapidly and is therefore not detectable in our assays, phosphorylation of GLH-1 does not cause a shift in protein migration or the shift is too small to be visualized. Future experiments will involve both the docking site deleted and T425A (phosphodegron inactive) constructs in MG132 assays to determine the role of these motifs in targeting GLH-1 for degradation.

Although increases in GLH-1 levels correlate with sterility at high temperature, it is difficult to determine if excess GLH-1 is the cause of the fertility defects seen in *kgb-1* worms. To partially address this issue, we initiated studies to decrease GLH-1 levels in *kgb-1* worms through *glh-1* RNAi. This resulted in significantly more fertility progeny in *csn-5* RNAi worms of the *kgb-1* background

than non-injected *kgb-1* worms (Table 2.5). This result suggest that, although it may not be the only factor, excess GLH-1 negatively affects fertility in *kgb-1* worms.

We have not detected GLH-1 protein migration differences by western blot between *kgb-1* and N2 worms, but we have found that GLH-1, but not GLH-4 migrates more slowly in embryo extracts than in adults (Figures 2.19, 20 and 21). This shift is observed even in *kgb-1* embryos. If the shift is due to phosphorylation, it is possible that in the *kgb-1* strain other kinases could perform the function of KGB-1, or that a kinase other than KGB-1 (such as KGB-2) is responsible for this modification.

We have observed in the past that GLH-4 levels tend to be higher in the somatic cells of early embryos compared to the other GLHs (Kuznicki et al. 2000). We also find that GLH-1 is more sensitive to degradation in embryo extracts than in adults (Figure 2.21). GLH-4 does not have the consensus phosphodegron site found in GLH-1; this site may play a role in eliminating GLHs from somatic cells during embryonic divisions. One possible explanation for the increased sensitivity of GLH-1 to degradation in embryos may be related to the method for preparing the embryo extracts. In embryos, GLH-1 is found only in the germline progenitor cell; any protein left behind in somatic blastomeres during embryonic divisions would need to be degraded. When embryos are prepared for extracts the cells are disrupted, mixing the contents of the germline and somatic cells. Any proteins responsible for degrading GLH-1 in the somatic cells now freely mix with the GLH-1 that was restricted to only the P lineage.

Without cell barriers to protect it, germline GLH-1 is now susceptible to somatic proteins that might regulate its degradation; one of these proteins may be KGB-1.

Although it has an obvious role in adult germline development, KGB-1 is not germline specific (Smith 2001; Smith et al. 2002). The *C. elegans in situ* database shows that *kgb-1* is found at highest levels in embryos, and is present in both germline and somatic blastomeres (Figure 2.24). It is therefore possible that KGB-1 may play a role degrading GLH-1 in the somatic cells of embryos. Whatever modification of GLH-1 occurs in embryos to cause the migration shift may specifically protect the protein from degradation in the germline or target GLH-1 to the germline cells exclusively; this modification either serves no protective purpose in the soma, or targets GLH-1 for degradation in non-germline cells. The abundance of *kgb-1* transcript in all cells of embryos suggests it could be fulfilling a role for GLH degradation in the soma as well. A functional relationship between KGB-1 and the MAPK kinase MEK-1 has been identified. Previous studies have shown that KGB-1 can be activated by MEK-1 (Figure 2.25) (Kim et al. 2004; Mizuno et al. 2004). *mek-1* RNA is expressed in the same stages and tissues as *kgb-1* in larvae and adult worms (Figure 2.26), with an intriguing exception. The germline lineage seems to be free of *mek-1* RNA in early embryos. The lack of *mek-1* in the early germline could indicate that KGB-1 may be free from MEK-1 activation in these cells, thereby limiting its activity. A genome wide yeast two-hybrid screen also found that KGB-1 binds the MAPK kinase MKK-4, whose RNA expression pattern is similar to *kgb-1* (Figure 2.27) (Li et al. 2004). As no functional relationship has been explored for these two

Figure 2.24: *kgb-1 in situ* hybridizations. In embryos, *kgb-1* is found in all cells. Very little *kgb-1* mRNA is seen until the late larval and adult stages, when it is enriched in the germline. Arrows point to germline. Compiled from the *C. elegans* Nematode Expression Database (NEXTDB).

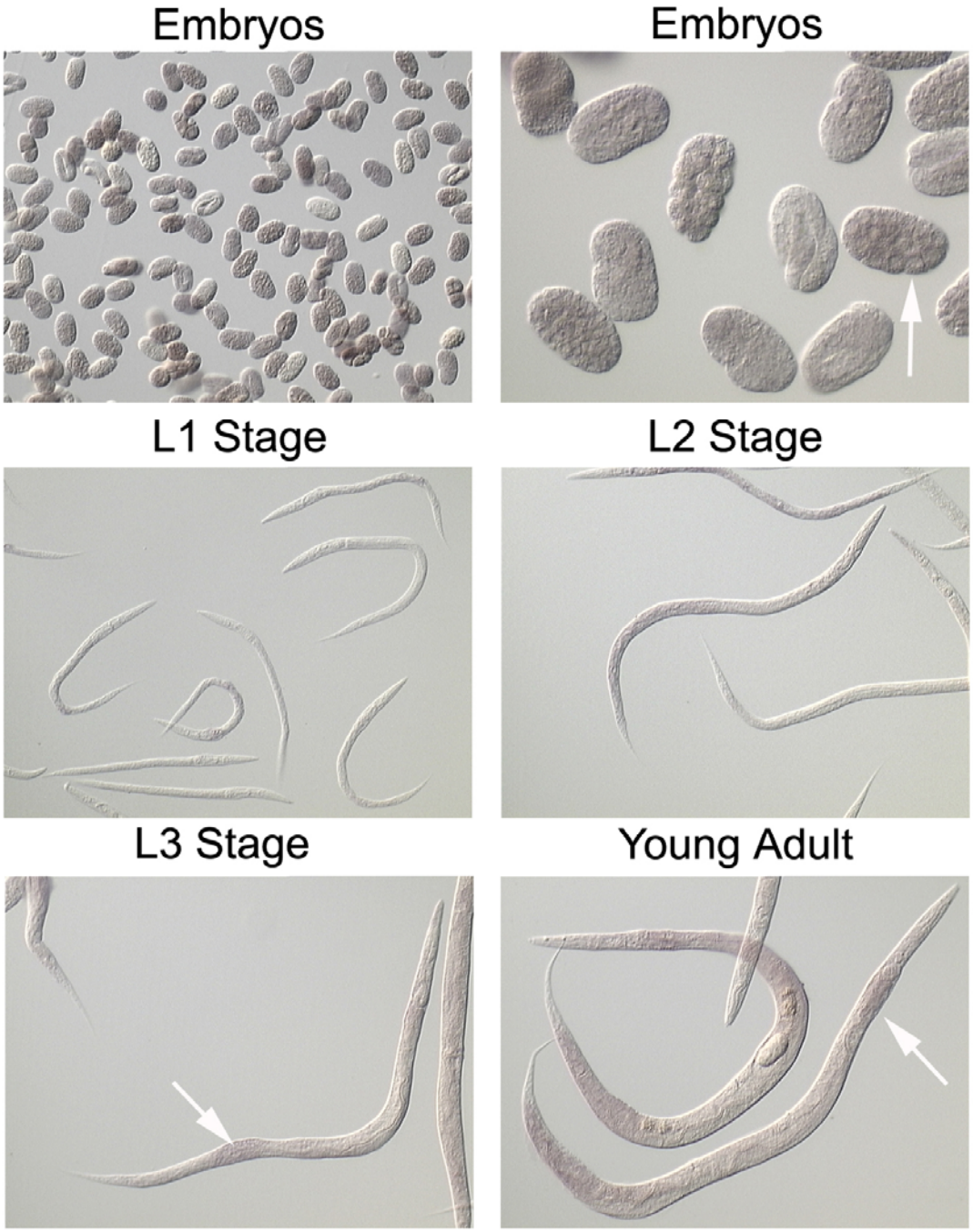

Figure 2.25: Hypothetical JNK pathways in *C. elegans*. Top: Integration of signals in response to kinase signal cascades for stress responses. Modified from (Kim et al. 2004). Bottom: KGB-1 is regulated up stream but a MAPKK MEK-1, which is first activated by the MAPKKK MLK-1. The protein phosphatase VHP-1 negatively regulates KGB-1 function in response to heavy metals. Modified from (Mizuno et al. 2004).

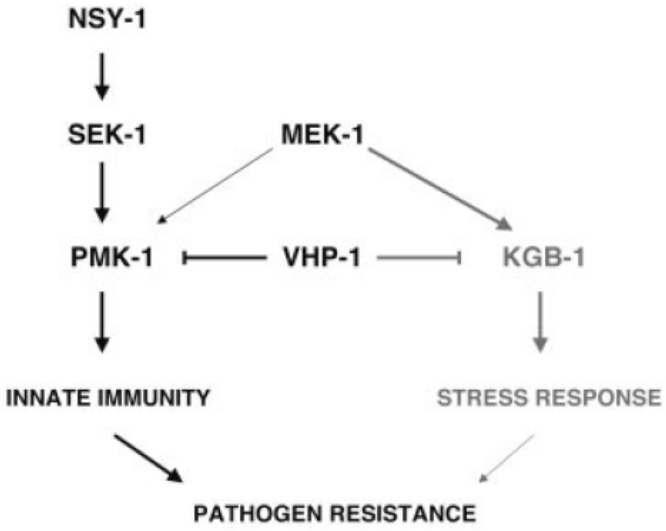

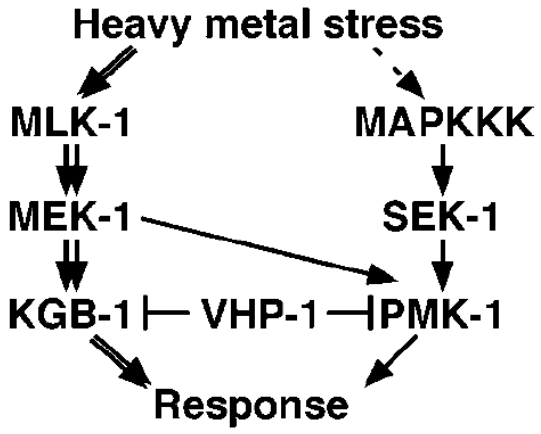

Figure 2.26: *mek-1 in situ* hybridizations. In embryos, *mek-1* mRNA seems enriched in all by the germline blastomere (P cell). In the early larval stages *mek-1* is weak, but by the L4 stage it is enriched in the germline and is increasingly more so in adults. Arrows point to germline (P2 cell in embryo panel). Compiled from the *C. elegans* Nematode Expression Database.

Embryos

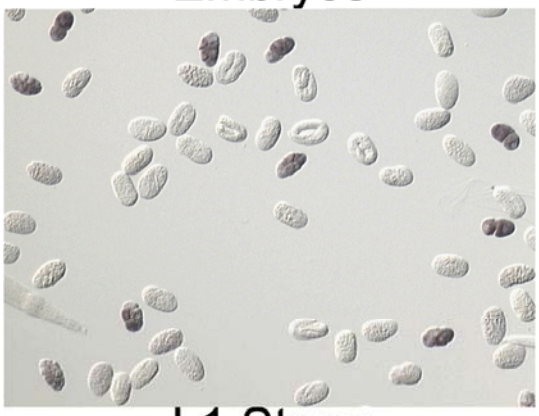

Embryos

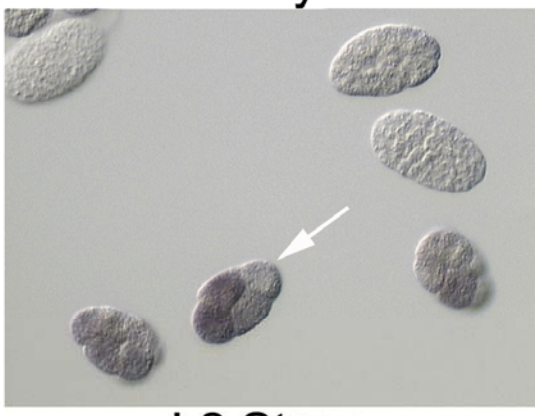

L1 Stage

L2 Stage

L3 Stage

L4 Stage

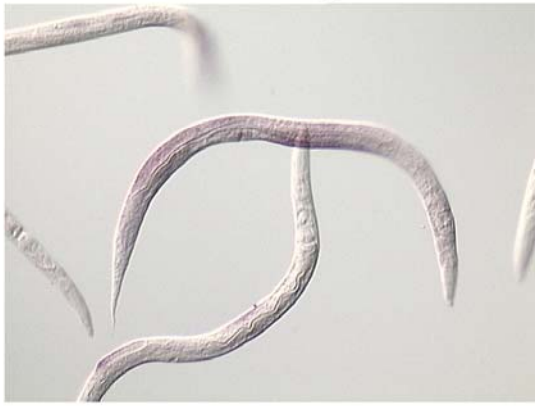

Young Adult

Figure 2.27: *mkk-4 in situ* hybridizations. In early embryos *mkk-4* mRNA expression is particularly strong in all cells. By the L2 stage, *mkk-4* is enriched in the germline progenitors, and this expression grows in strength as the worm gets older. Arrows point to germline. Compiled from *C. elegans* Nematode Expression Database.

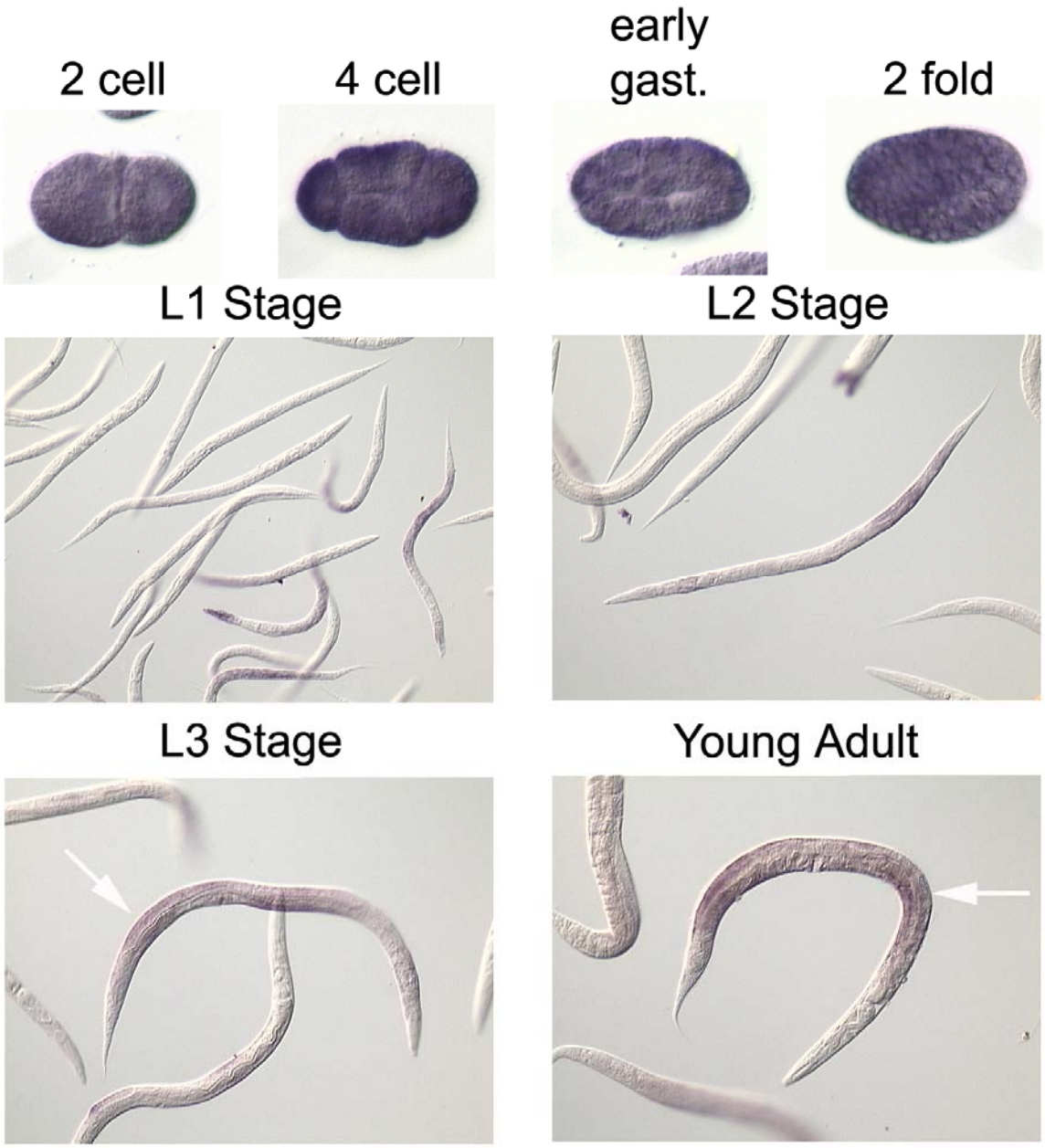

proteins, it is impossible to say if MKK-4 modulates KGB-1 activity, but it is an attractive interpretation due to the fact that lack of MEK-1 does not result in the drastic GLH-1 increase we see in *kgb-1* (Figure 2.18), pointing to roles for other upstream activators to regulate KGB-1.

The same yeast two-hybrid screen that identified MKK-4 as a binding partner for KGB-1 also found that KGB-1 bound to the protein TIR-1, which has been implicated in apoptosis (Aravind et al. 2001; Li et al. 2004) The RNA expression of *tir-1* is found in somewhat ubiquitously, but is definitely present in the germline (Figure 2.28). This is logical, as a great deal of germ cell death occurs during oogenesis (Gumienny et al. 1999). The abnormal acridine orange and SYTO-12 staining seen in *kgb-1* worms may be due to defects in apoptosis (Figure 2.23), perhaps due to a perturbation of the interaction between KGB-1 and TIR-1.

Figure 2.28: *tir-1 in situ* hybridizations. Early embryos (2 cell, 4 cell, early gastrulation, 2 fold), L1, L2, L3, and adult worms are shown. *tir-1* mRNA expression is strong in early embryos. In the L1 and L2 stage *tir-1* expression is limited to somatic tissues such as the pharynx. By the L4 stage, germline expression is seen (arrow). In the adult stage *tir-1* is ubiquitously expressed. Compiled from *C. elegans* expression database.

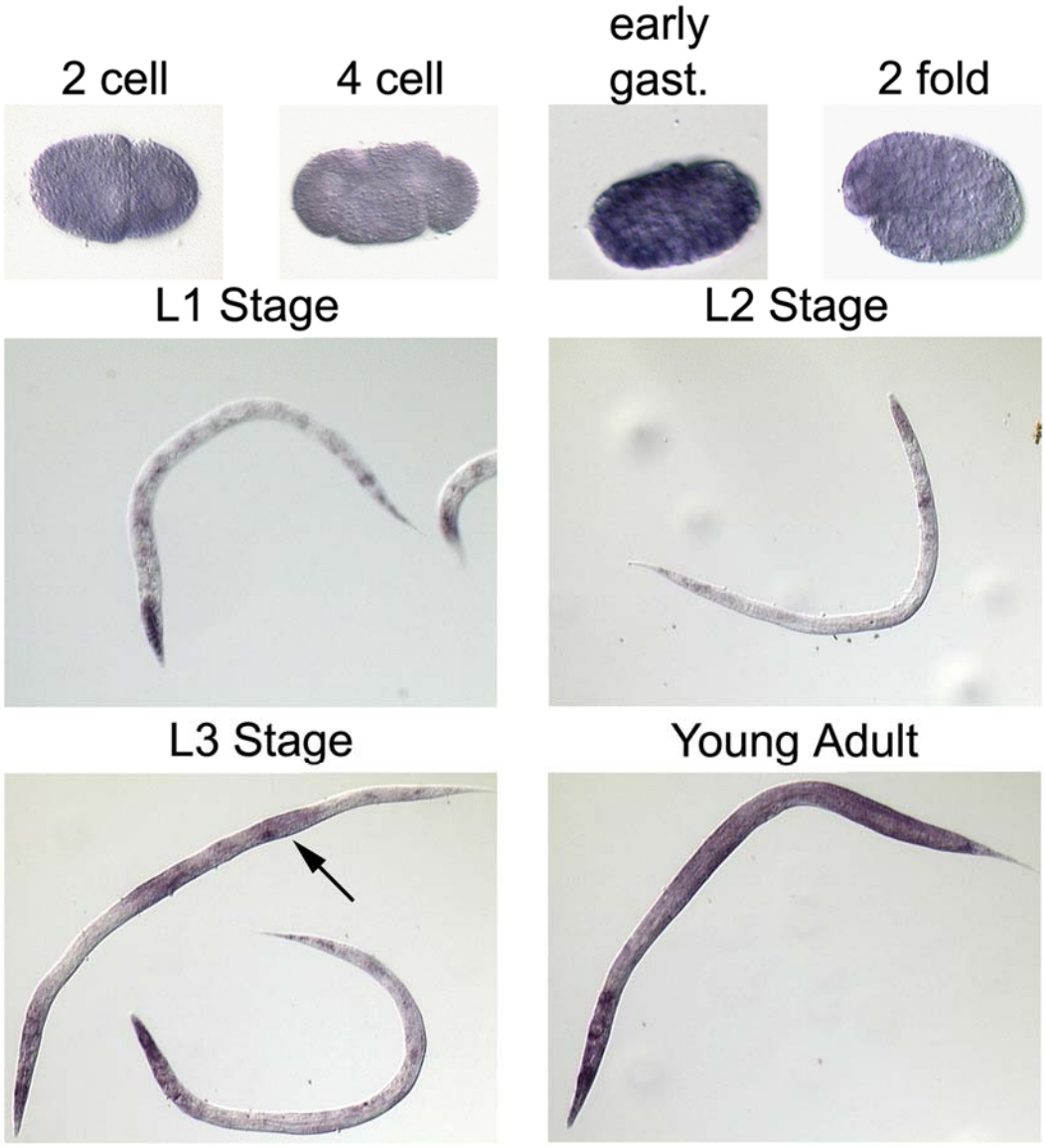

Chapter 3: KGB-1:CSN-5 Interactions

Introduction

The yeast two-hybrid screen performed by the Bennett laboratory identified proteins of diverse functions binding to the GLHs. Studies on the GLH associated kinase, KGB-1, has been facilitated by the identification of the *kgb-1(um3)* deletion strain. Another GLH interactor, CSN-5, has been less well studied. A deletion strain for *csn-5* has only recently been isolated, and therefore little work has been done with these worms. Yet the relationship of CSN-5 with the GLHs is an intriguing one. The phenotype produced by *csn-5* RNA interference (RNAi) is very similar to that seen with combinatorial elimination of *glh-1* and *glh-4* using RNAi. The fact that the loss of CSN-5 results in germlines closely resembling those missing GLH-1 and GLH-4 begs the question: does CSN-5 protect the GLHs? The very small germlines of *csn-5* and *glh-1/4* RNAi animals make assaying amounts of germline proteins difficult because many worms are needed for such experiments and RNAi to produce enough worms is laborious. Once the backcrossing of the *csn-5(vc861)* strain is completed, it will be possible to examine the GLHs in these mutants, which may shed light on the relationship between CSN-5 and the GLHs (Figure 3.1).

The CSN complex contains eight well defined subunits; purified COP9 signalosome complexes have been shown to have associated kinase activity,

Figure 3.1: Schematic depiction of *csn-5* gene and protein. The extent of the deletion in the *csn-5(vc861)* gene is indicated. The location of primers used to screen for the mutation are indicated. Numbers indicate nucleotides in the top image and amino acids in the bottom.

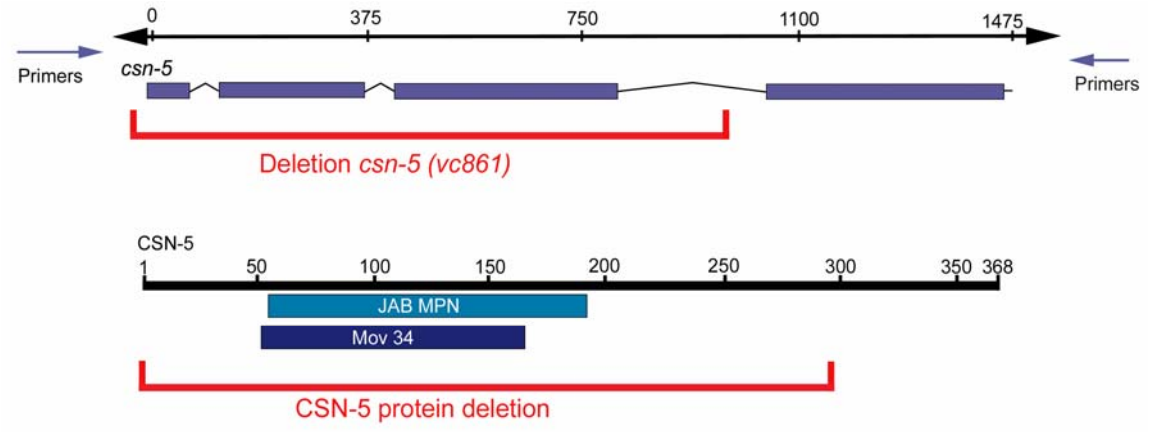

although none of the CSN subunits contains identifiable kinase domains. The kinases CK2, PKD, and inostitol 1,3,4-triphosphate 5/6 kinase have been found associated with the mammalian CSN complex (Sun et al. 2002; Uhle et al. 2003). The *C. elegans* interactome project, involving a genome wide yeast two-hybrid screen, found that the MAPK kinases MPK-1, PMK-1, and PMK-2 interact with CSN-5 (Li et al. 2004). These interactions have yet to be confirmed in any physical or functional studies. Currently, no kinases have been identified in plant or invertebrate CSN complexes, nor has the interaction of a MAP kinase with CSN-5 been verified. As both KGB-1 and CSN-5 associate with GLH proteins, we examined the ability of KGB-1 to interact both functionally and physically with CSN-5. Unlike the GLHs, neither *kgb-1* nor *csn-5* is germline specific (Figure 3.2) (Smith et al. 2002).

Figure 3.2: *csn-5* is germline enriched. Top: by *in situ* analysis *csn-5* mRNA is not present in observable levels until the young adult stage, at which time it is present mostly in the germline (arrow). Compiled from *C. elegans* expression database. Bottom: northern analysis of *csn-5* transcript levels in *glp-1* mutants at permissive and non-permissive temperatures (15°C and 25°C respectively). At non-permissive temperatures, *glp-1* mutants produce very little germline tissue. Adapted from (Smith et al. 2002).

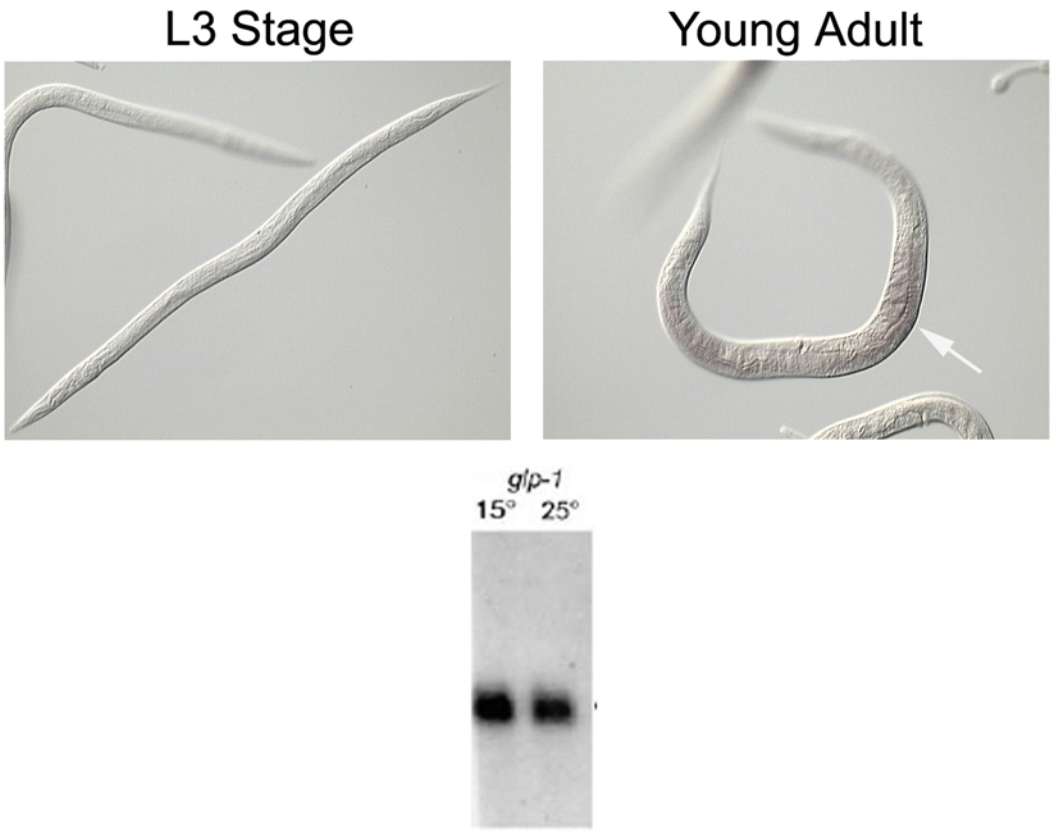

Materials and Methods

Strains

The following strains were used in this work: wild type (N2 variety Bristol), *kgb-1(um3)*, and *csn-5(vc861)*.

GST pull-down analysis

GST pull-downs were performed as described in Chapter 2, Methods, GST pull-down analysis section. High Five cells were co-infected with CSN-5 GST and KGB-1 6-His or eGFP 6-His as a negative control Cells were then either processed as in GST pull-down section of Chapter 2, or lysed in 300mM LiCl, 1% Triton-X 100, 1x Complete Protease Inhibitor (Roche) and 1mM PMSF. Cells were lysed and cleared as above and incubated with beads as described previously. GST beads were blocked with 3% BSA in 300mM LiCl overnight, washed four times with 300mM LiCl, and resuspended in 300mM LiCl to 50:50v. Washes were also performed with 300mM LiCl; proteins were eluted and analyzed as above.

RNA interference

dsRNA was generated using an Ampliscribe T7 transcription kit (Epicentre Technologies), as described in the RNA interference methods section of Chapter 2, from a PCR product produced from the pACT vector containing a *csn-5* cDNA

as identified in a yeast two hybrid screen and pACT primers that had T7 polymerase sites added. *csn-5* dsRNA is ~1.3kb long (Smith et al. 2002). Young adult wild type and *kgb-1* worms were injected with ~1µg/mL dsRNA. The injected worms were allowed to recover at 20°C overnight and the surviving worms moved to new plates. With this process of purging maternal CSN-5 protein, the progeny produced in the first 16-18 hours after injection were not considered. After this time, injected worms were individually plated and the fertility of their F_1 progeny was recorded five-six days later. Sterile F_1 worms are obvious with a dissecting microscope; they display a "clear gonad" phenotype and they produce no F_2 progeny.

Generation of *csn-5(vc861);kgb-1(um3)* double mutant

The *C. elegans* Knock-Out Consortium generated and isolated a strain with a deletion of approximately one kilo-base in the *csn-5* gene on chromosome IV (Figure 3.1). The deletion was sequenced and end-points determined. This strain was backcrossed by undergraduate researcher Holly Boedefeld. As worms homozygous for the *csn-5* deletion are sterile and exhibit the *csn-5* RNAi phenotype, these worms were balanced with gNT1 chromosome (covering a portion of chromosome IV including *csn-5*), which produces eGFP in the pharynx and can be easily screened using a fluorescent stereo-dissecting microscope. To produce the double mutant, two crosses were performed. First *kgb-1(um3)* homozygous males were crossed with *csn-5/*gNT1 heterozygotes. F_1 worms were individually plated and allowed to self fertilize. The F_2 progeny were then

individually plated and their offspring checked at the *kgb-1* allele by PCR as described in the Generation of *kgb-1(um3);kgb-2(km16)* Methods section of Chapter 2 and for the presence of the *csn-5* deletion:

csn-5 (B0547.1) 5' Inner 5'AAGTTGGAGTGTCGTTGTTAG3'

csn-5 (B0547.1) 3' Inner 5'TTGGAACTTGTATCCCTCCTC3'

The cross is completed and the progeny await analysis.

Results

KGB-1 and CSN-5 physically interact

To investigate the ability of CSN-5 and KGB-1 to interact, GST pulldowns followed by western blotting were performed, as in Chapter 2. We found that KGB-1 bound CSN-5 in these assays (Figure 3.3 panel A). To verify this interaction, GST pulldown assays were performed using more stringent conditions. Cells were lysed, and beads were washed with 300mM LiCl with 1% Triton X-100 to determine the specificity of the interaction. Even under these more strict conditions, CSN-5 and KGB-1 bind (Figure 3.3 panel B). Examination of the CSN-5 protein sequence identified a consensus MAPK docking site (Table 3.1). This is consistent with the interactions we have seen between KGB-1 and GLH-1, which also has a consensus MAPK docking site.

kgb-1 worms partially rescue *csn-5* RNAi induced sterility

We have previously shown that reduction of CSN-5 through RNAi results in sterile worms at all temperatures; these worms have very small gonads, with GLH-1 in P granules (Smith et al. 2002) . This sterility phenotype with small gonads and a reduced germline, is very similar to the loss of both GLH-1 and GLH-4; we therefore hypothesize that CSN-5 may somehow protect the GLHs. Our work on KGB-1 suggests that it may regulate GLH-1 degradation. To examine the role of CSN-5 we performed *csn-5* RNAi in *kgb-1* worms. We found

Figure 3.3: CSN-5 and KGB-1 physically interact. GST pull downs were performed with KGB-1 and CSN-5 as in GST pull-down analysis methods section. A. Insect cells were lysed in 1xPBS, 1% Triton X-100, 1mM PMSF and 1x Complete Protease Inhibitor; washes were performed with the 1x PBS with 1% Triton X-100. CSN-5 GST binds to KGB-1 6-His but not eGFP 6-His. B. Cells were lysed in 300mM LiCl, 1% Triton X-100, 1mM PMSF and 1x Complete Protease Inhibitor; washes were performed with 300mM LiCl with 1% Triton X-100. CSN-5 GST binds to KGB-1 6-His but not eGFP 6-His, and GST alone does not bind KGB-1 6-His. Western blots were performed with antibodies to 6-his and GST tags.

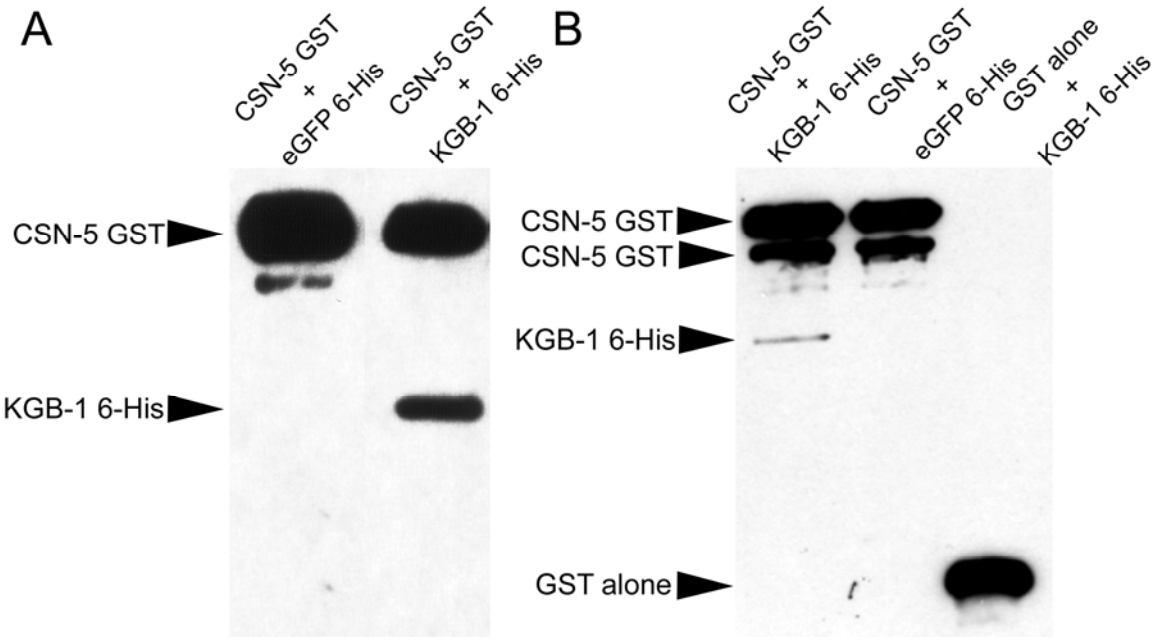

Table 3.1: MAPK docking site in CSN-5

Consensus MAPK Docking Site

K/R-X-X/K/R-K/R-X(1-4)L/I-X-L/I or

K/R-K/R-K/R-X(1-5)L/I-X-L/I

CSN-5 (aa54) KQIKISAIAL Consensus

that elimination of *csn-5* in the *kgb-1* background at 20°C resulted in significantly more fertile offspring than the same experiment performed in N2 worms (Table 3.2).

Initial characterization of the *csn-5(vc861)* strain

Isolation of a deletion in the *csn-5* gene by the *C. elegans* Knockout consortium has occurred relatively recently. An undergraduate researcher, Holly Boedefeld has been backcrossing this strain to wild type and creating a *csn-5(vc861)*;*kgb-1(um3)* double mutant. Analysis of the genetic lesion suggests that the *csn-5(vc861)* strain is a null. Western blot analysis has found that the *csn-5(vc861)* strain does not produce a detectable CSN-5 protein (data not shown).

As *csn-5* RNAi produces sterile worms, we determined that the *csn-5(vc861)* strain would have to be maintained over a chromosomal balancer or the strain would be quickly lost. After balancing the strain, we looked at *csn-5(vc816)* homozygotes and found that they exhibit the same under-proliferated germlines we observed using *csn-5* RNAi. More work will have to be done with the *csn-5(vc816)* strain to examine the role CSN-5 plays in GLH regulation. The *csn-5(vc816)*;*kgb-1(um3)* strain, if viable, should prove useful for understanding the relationship of these two proteins.

Table 3.2: Injection of *csn-5* dsRNA in N2 and *kgb-1* worms. The F_1 progeny from single *csn-5* injected worms (N2 or *kgb-1*) were individually plated and examined 5-6 days after purging maternal CSN-5 protein overnight. Plates were scored as either containing no F_2 progeny or containing some F_2 worms. The difference between the N2 and the *kgb-1* results are highly significant, using the Student's T test ($p<1x10^{-5}$).

csn-5 RNAi	# injected	# with only sterile F_1s.	# with some fertile F_1s	% some fertile F_1s
wild type (N2)	54	43	11	20%
kgb-1(um3)	54	22	32	59%

Discussion

Our interest in CSN-5 began with the finding that it binds the GLH proteins, and that the elimination of CSN-5 results in a phenotype very similar to the combined loss of GLH-1 and GLH-4. Our studies with KGB-1 revealed a different phenotype, with temperature-sensitive sterility, and large gonads. As both proteins interact with the GLHs, we decided to explore possible relationships between the two. Previous studies have shown that the COP9 Signalosome (CSN) has kinase activity and several kinases have been shown to associate with the multi-subunit complex (Sun et al. 2002; Uhle et al. 2003). Here we show that KGB-1, a novel JNK MAP kinase that binds to GLH proteins, also physically interacts with CSN-5; this interaction is able to withstand high salt conditions.

We also find that KGB-1 and CSN-5 interact functionally. The elimination of CSN-5 in N2 worms at 20°C results in sterile worms with small germlines that produce no functional oocytes. The same experiment in *kgb-1* worms results in significantly more fertility (20% in fertile N2 compared to 59% in *kgb-1*, $p<1x10^{-5}$). We postulate that CSN-5 may serve a protective role for the GLHs as the CSN complex does for the transcriptional regulators c-Jun, Id1 and Id3 (Naumann et al. 1999; Berse et al. 2004). This would explain the similarity in phenotypes for the loss of CSN-5 and the combined loss of GLH-1/4. The work discussed in Chapter 2 points to a role for KGB-1 in the targeting of GLH proteins for

degradation, especially GLH-1. Therefore, KGB-1 and CSN-5 may be playing opposing roles in the regulation of GLH-1 protein. The fact that *kgb-1* worms are more fertile when subjected to *csn-5* RNAi suggests that when KGB-1 is missing, perhaps CSN-5 is not as vital for protecting the GLHs.

To explain the data presented here and in Chapter 2, we propose the following model (Figure 3.4). KGB-1 and CSN-5 both physically interact with GLH proteins. KGB-1 requires the MAP kinase docking site to bind GLH-1 efficiently; this site is not conserved in GLH-4. We also find that KGB-1 can phosphorylate GLH-1 in vitro and target it for degradation. Therefore, we propose that KGB-1 binds to GLH-1 at the D site, phosphorylates GLH-1, and in doing so, promotes its degradation. The involvement of CSN-5 is less clear, but it is possible that CSN-5 antagonizes KGB-1 function. CSN-5 could bind GLH proteins and sequester them, preventing KGB-1 interactions. Alternatively, CSN-5 could bind KGB-1 and modulate its function. Either possibility allows for a cooperative system that may regulate GLH proteins to ideal levels during development, ensuring fertility.

We find that the lack of GLH proteins results in sterility; excess GLH proteins (as in the *kgb-1*) mutants also correlates with fertility defects. Therefore, it seems likely that maintaining proper levels of GLHs during development is crucial for fertility. The *C. elegans* germline is a dynamic tissue, with nuclei dividing mitotically and meiotically, oocytes developing, and over half the germ cell nuclei dying by apoptosis (Gumienny et al. 1999). As worms do not have nurse cells to provide nutrients to the developing oocytes, it has been postulated

Figure 3.4: Regulation of GLH proteins by KGB-1 and CSN-5. The model we propose to explain the data presented in Chapters 2 and 3 of this document. KGB-1 binds to GLH-1 by means of the MAPK docking site; this interaction facilitates the phosphorylation of GLH-1 at the phosphodegron (and possibly elsewhere in the protein). The phosphorylation of GLH-1 at the phosphodegron targets it for degradation, most likely through the proteasome. A similar pathway may regulate GLH-4, as we know KGB-1 can bind GLH-4 (Smith et al. 2002). This pathway is not as robust as the GLH-1 pathway, perhaps due to the non-consensus MAPK docking and phosphodegron sites in GLH-4. CSN-5, which also has a MAPK docking site, can bind KGB-1. CSN-5 may regulate KGB-1 through this functional interaction, inhibiting the ability of KGB-1 to target GLH proteins for degradation, serving a protective role for the GLHs. CSN-5 may do this in conjunction with the CSN complex; it is also possible monomeric CSN-5 performs this function.

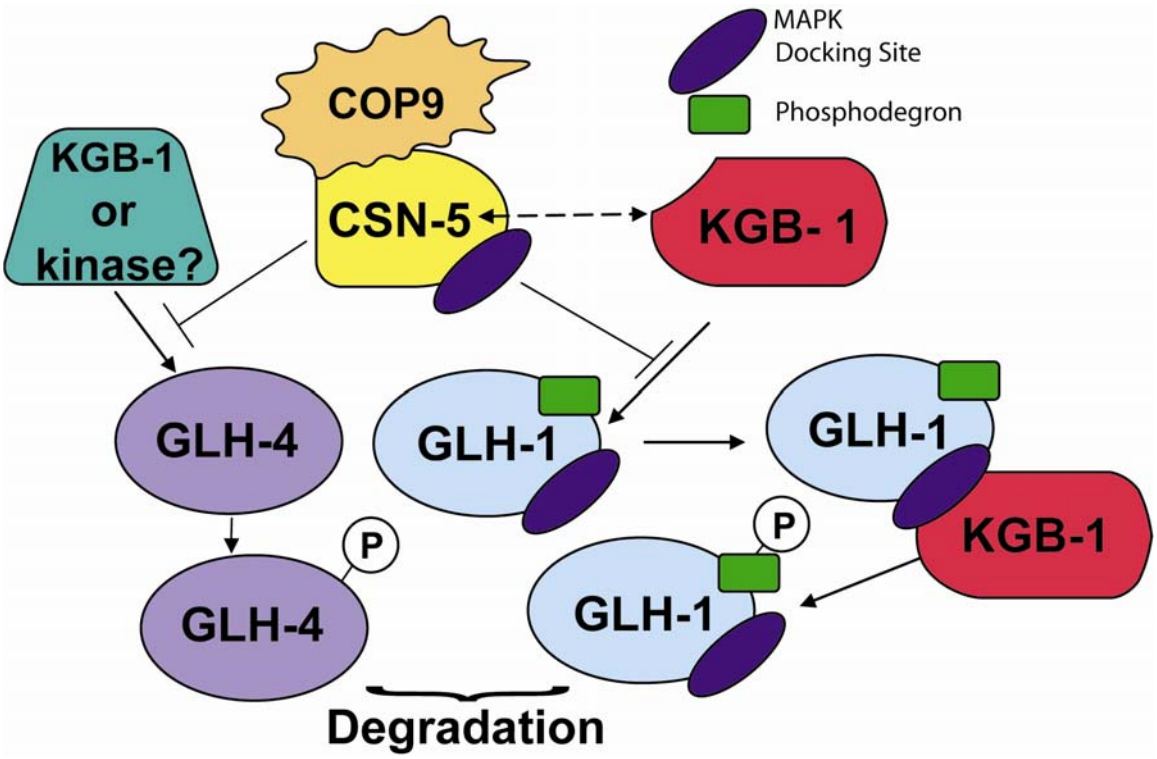
MAPK
Docking Site
Phosphodegron
COP9
KGB-1
or
kinase?
CSN-5
KGB- 1
GLH-4
GLH-1
GLH-1
KGB-1
P
GLH-4
P
GLH-1
Degradation

that the massive cell death in the germline might fill this role, with the dying germ cells donating their cytoplasm to produce functional oocytes. During this time, it is possible that certain proteins may be too abundant to allow their complete accumulation developing oocytes. Under these circumstances, coordinated degradation of certain protein targets could ensure that the amounts of proteins needed for embryogenesis are accurately deposited in the oocytes, as too much protein could be detrimental for the next generation.

Chapter 4: *glh* Mutant Characterization

Introduction

Previous studies in the Bennett laboratory explored the impact of GLH proteins on fertility (Kuznicki 2000; Kuznicki et al. 2000). Although the biochemical function of GLH proteins remains unclear to us, they are necessary for fertility. The elimination of GLH-1 at restrictive temperatures (26°C) causes sterility, and the elimination of GLH-1 and GLH-4 by RNAi results in sterile worms even at permissive temperatures (Table 1.2). The importance of GLH-2 and GLH-3 for fertility seems negligible in RNAi experiments, but this procedure does not usually eliminate all production of the target protein. Therefore, to fully understand the function of GLH proteins, null alleles are necessary.

A previous graduate student, Kathleen Kuznicki, isolated mutations in *glh-2* and *glh-3* that are protein nulls, as determined by western blot analysis. The *C. elegans* Knock-Out Consortium, a group of researchers who generate large deletion libraries and screen for mutations in requested genes, isolated two deletion alleles in *glh-1* (*glh-1(ok439)* and *glh-1(gk100)*). Unfortunately, neither of these alleles is a protein null, though they both seem to be functional nulls, resulting in sterility at 26°C. Our collaborators in the Strome laboratory also isolated two *glh-1* mutant alleles, *glh-1(bn103)* which is the result of a Tc1 transposon insertion in the *glh-1* gene and *glh-1(bn125)*, a small C terminal

deletion allele. The *glh-1(bn103)* allele produces GLH-1, but at very low levels (Nicole Meyer, personal communication); we have not examined the *glh-1(bn125)* strain.

The *C. elegans* Knock-Out Consortium has also isolated a deletion in the *glh-4* gene (allele *glh-4(gk225)*) which is a protein null by western blot analysis and we have used to construct a *glh-1(ok439);glh-4(gk225)* double mutant. The maximum affect on fertility is seen when both GLH-1 and GLH-4 are eliminated at permissive temperatures. Since the *glh-1(ok439)* strain is not a protein null, the interpretation of this data is clouded, but it is clear that the truncated GLH-1 produced by *glh-1(ok439)* worms is non-functional, as these worms are sterile at 26°C.

To use these available strains to analyze GLH function, we first performed western blots to determine if the strains were protein nulls; we then carried out brood counts and fertility assessments to examined the roles of GLH proteins on fertility.

Materials and Methods

Strains

The following strains were used in this work: wild type (N2 variety Bristol), *glh-1(ok439)*, *glh-1(gk100)*, *glh-1(bn103)*, *glh-2(um2)*, *glh-3(um1)*, and *glh-4(gk225)*.

Deletion Library Screening

Using a reverse genetics approach, we screened mutagenized libraries of worms for deletions in GLH genes as in (Yandell et al. 1994) (Figure 4.1). Starved L1 worms on 60x15mm NGM plates were used and agar cut into four pieces. One-fourth of the plate was put onto a 150X15mm NGM plate seeded with OP50 *E. coli* as described in methods section of Chapter 2. The worms were to grown until gravid, washed off plates with M9 and gravity settled in 15mL conical tubes on ice. The worms were treated with an alkaline hypochlorite solution (0.25M NaOH, 1.5% NaOCl) for three to five minutes to dissolve away the bodies, leaving the eggs behind. These eggs were washed six times in M9, and put onto fresh 150x15mm NGM plates with OP50. The worms grew to the L4 stage and were washed off the plates as before. The worms were brought up in a solution of 30 µg/mL trimethylpsoralen in M9 and incubated in the dark with this solution for 15 minutes with gentle shaking. We then exposed the worms to 360nm UV light for 90 seconds, shaking gently. The worms were then

Figure 4.1 Scheme of Deletion Library Screening. *C. elegans* worms are grown in synchronous cultures, mutagenized and then plated. After the mutagenized worms have been allowed to have progeny the worms are harvested and screened for deletions in selected genes. Adapted from (Yandell et al. 1994).

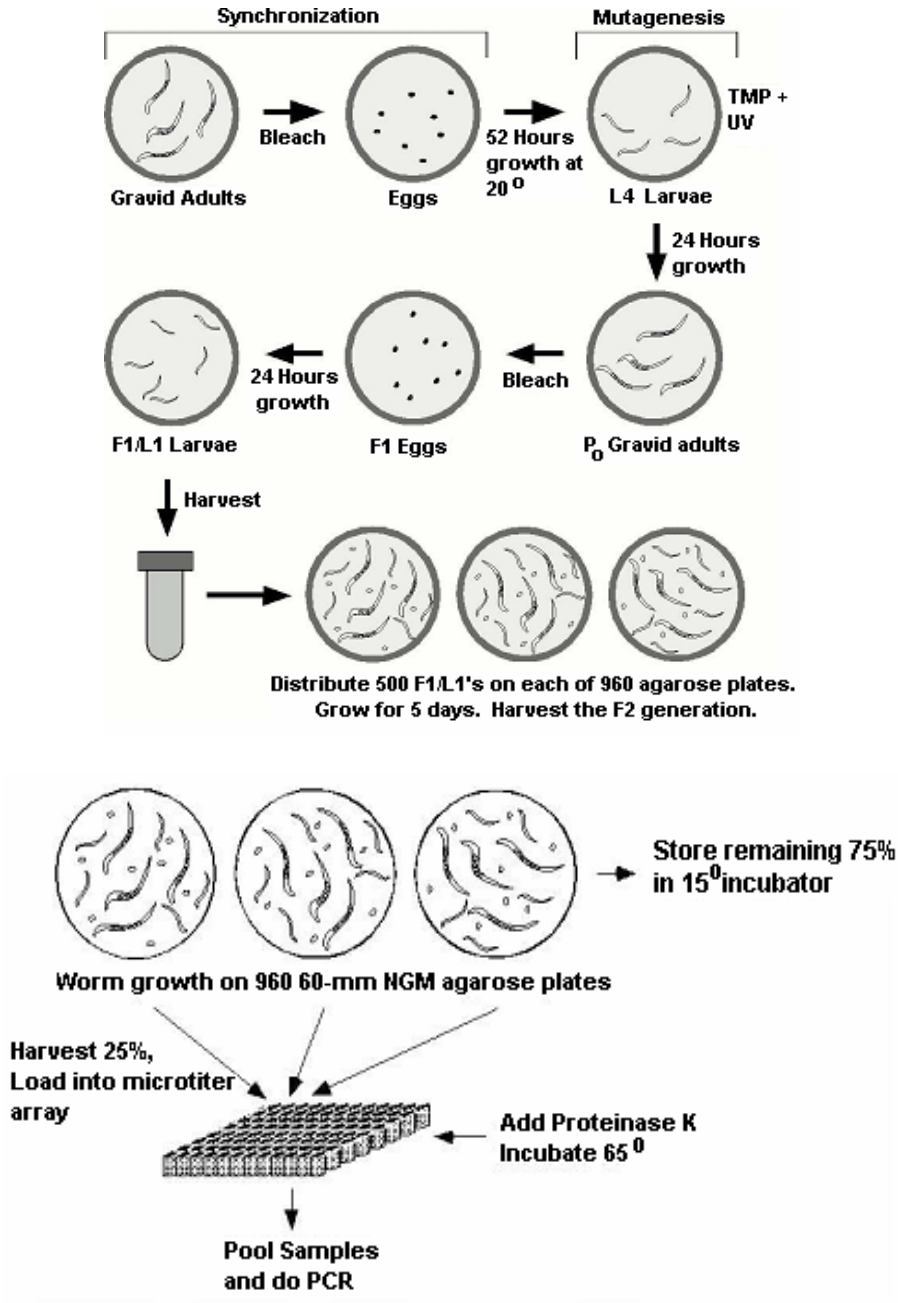

plated onto fresh 150x15mm NGM plates with OP50 and allowed to grow until gravid. Again, the worms were washed off the plates, gravity settled, and embryos harvested by the alkaline hypochlorite solution described above. The embryos were brought up in M9 and allowed to hatch out overnight, with shaking. Each of 960 plates received 500 of the resulting L1 larvae which were allowed to grow up and produce progeny. Once the F_1 generation had started to produce progeny, the worms were harvested as described in the backcrossing section of Chapter 2 Methods. A portion of the DNA was pooled and aliquoted for multiple PCR reactions. Kathleen Kuznicki screened multiple libraries and found deletions in *glh-2* and *glh-3*, alleles *glh-2(um2)* and *glh-3(um1)* respectively (Kuznicki 2000). The *C. elegans* Knock-Out Consortium found two deletion alleles for *glh-1*: *glh-1(ok439)* and *glh-1(gk100)* as well as a deletion in *glh-4*, *glh-4(gk225)*. All alleles were back crossed to wild type worms as described in the Backcrossing section of Chapter 2 Methods. Chris Yee performed the *glh-4(gk225)* backcrossing and screened by PCR using the following primers:

glh-4 inners 5' 5'ATGAACACGTGAAATGCACC3',

glh-4 inners 3' 5'TCCACCGAATCCAGCTTTAGG3',

glh-4 5' deletion 5'CAACTCGAACGGATGCATAA3'

glh-4 3' deletion 5'GACTTCCGAAAGTCTTGCTAG3'

Brood counts

For the *glh* mutants brood counts were performed much as in the Brood Count section of Chapter 2 Methods. The exception to this procedure is the *glh-1(ok439);glh-4(gk225)* double mutant; this mutant exhibits significant sterility when homozygous even at the permissive temperature of 20°C. Therefore, this strain was maintained over the balancer chromosome gHT2. For brood counts, non-gHT2 (non-green) expressing progeny of *glh-1(ok439);glh-4(gk225)*/gHT2 worms were individually plated, these are referred to as maternal + /zygotic – (M+/Z-) because the parent produced wild type GLH-1 and GLH-4 protein and will have transmitted some maternal GLH proteins to the zygote. Some of the M+/Z- worms produced progeny, and these worms were also scored, they are referred to as M-/Z- as neither maternal nor zygotic wild type GLH-1 and GLH-4 proteins are produced in this generation.

Western blot analysis

As in the Methods section of Chapter 2, wild type and *glh* mutant worms were grown at 20°C to the adult stage, washed off to unseeded plates, allowed to clean for approximately 30 minutes and then 100 worms were individually picked into 70 µL M9. To the worm solution was added 25 µL of 4x protein loading dye and 5 µL 50x Complete Protease Inhibitor (Roche). The tubes were flash frozen in liquid N_2, boiled 10 minutes and the proteins analyzed by SDS-PAGE using 10% acrylamide gels. The mutants were analyzed for protein expression, using αGLH-1 and αGLH-4 as described above.

Generation of *glh-1(ok439);glh-4(gk225)* strain

As the worms treated with of *glh-1;glh-4* combinatorial RNAi had the most severe phenotype, we wanted to produce a *glh-1;glh-4* double mutant. As we have had no null *glh-1* mutant, we chose the *glh-1(ok439)* allele as it lacks the majority of the protein. Undergraduate researcher Christopher Yee performed the following experiment. To create the double mutant, we crossed homozygous *glh-1(ok439)* hermaphrodites with *glh-4(gk225)* homozygous males. The resulting cross progeny should be heterozygous at both alleles. These *glh-1(ok439)*/+;*glh-4(gk225)*/+ hermaphrodites were mated with gHT2 heterozygous males. The *glh-1* and *glh-4* genes are both on chromosome one, approximately four map units apart; therefore 4% of the progeny from this cross could be expected to have a recombination event bringing both *glh-1(o439)* and *glh-4(gk225)* to the same chromosome. Hundreds of progeny were screened by PCR for the presence of both alleles. The *glh-4(gk225)* allele was screened by PCR using the primers in the Deletion Library Screening section above. The following primers were used to screen for the *glh-1(ok439)* deletion:

glh-1 inner left 5'CGATCGAGTGACTGTCCAGA3'

glh-1 inner right 5'TTCAATTGCAGACTTCGTCG3'

ok439 5' deletion 5' 5'ACGTGATGATTGCAATCGACAGGATTGGAGC3'

ok439 3' deletion 3' 5'CTCCGTAATTGCCTCCAGCAGCACCTTGCAT3'

Results

Sequencing of the different deletion alleles for *glh* genes gave predictions as to whether the mutants would produce any protein. It was hypothesized that the *glh-2(um2)* and *glh-3(um1)* worms would produce no GLH-2 or GLH-3 respectively and this was confirmed in (Kuznicki et al. 2000). The *glh-1* mutants were not complete deletions of the entire *glh-1* gene and sequencing suggested that both *glh-1(ok439)* and *glh-1(gk100)* would produce modified GLH-1 protein (Figure 4.2); *glh-1(ok439)* lacks three of the eight conserved DEAD-box helicase motifs, while *glh-1(gk100)* is missing three of four CCHC zinc fingers and four of 19 glycine rich repeats. Additionally, the *glh-4(gk225)* allele was predicted to be a protein null by sequence analysis.

All the *glh* mutants available to us were analyzed by western blot analysis for the presence of GLH-1 and GLH-4 proteins (Figure 4.3). As predicted, we find that *glh-1(ok439)* produces a truncated GLH-1 protein, about 45 kDa in size. This truncated GLH-1 is less abundant and only detectable in larger number of worms (500 worms loaded for *glh-1(ok439)* lane compared to 100 worms in all other lanes) (Figure 4.3 lane 7). The *glh-1(gk100)* strain also produces a smaller GLH-1, approximately 50 kDa (Figure 4.3 lane 6). The *glh-1(bn103);glh-3(um1)* allele produces no detectable GLH-1 protein (lane 5). All of the *glh-1* alleles do produce GLH-4 protein. Both *glh-2(um2)* and *glh-3(um1)* produce both GLH-1 and GLH-4 as predicted (Figure 4.3 lanes 4 and 3 respectively). We also find the *glh-4(gk225)* strain produced wild type GLH-1, but no detectable GLH-4 protein.

Figure 4.2: Diagram of GLH-1 protein deletions in *glh-1* mutants. The GLH-1 protein is composed of glycine rich repeats (yellow), CCHC zinc fingers (red), and a portion containing the eight conserved DEAD-box helicase motifs (green). The *glh-1(gk100)* allele is lacking three of four Zn fingers, and a portion of the glycine rich repeats (indicated by the solid bent lines). The *glh-1(ok439)* results in a truncated protein (missing the region indicated by the dotted line). The location of the Tc1 transposon insertion in the *glh-1(bn103)* allele is indicated by an arrowhead. The number of residues predicted to be produced is indicated.

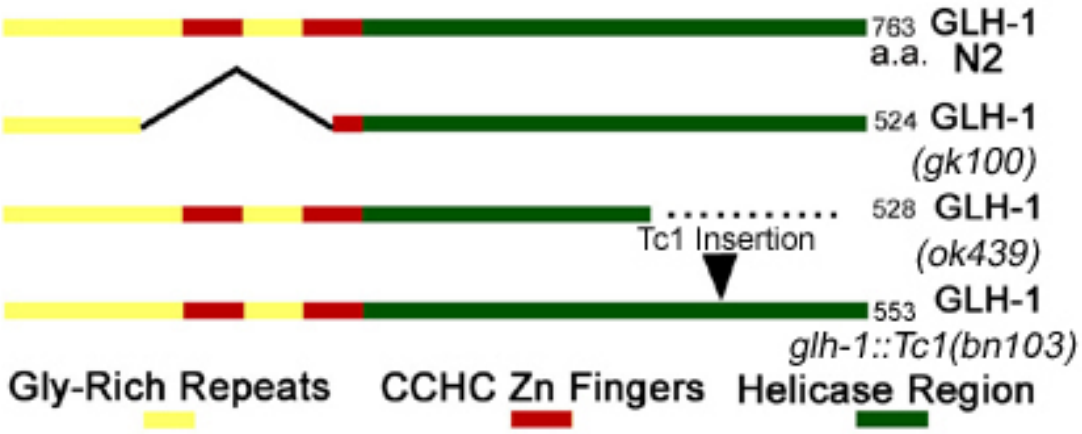

Figure 4.3: GLH-1 and GLH-4 in *glh* mutants. N2 and *glh* mutants were raised at 20°C, and 100 adult worms for each sample (except *glh-1(ok439)* where 500 worms were used because this truncated GLH-1 is less abundant) analyzed by western blot with antibodies generated against GLH-1 and GLH-4 (Kuznicki et al. 2000). Asterisk indicates GLH-4 break down product.

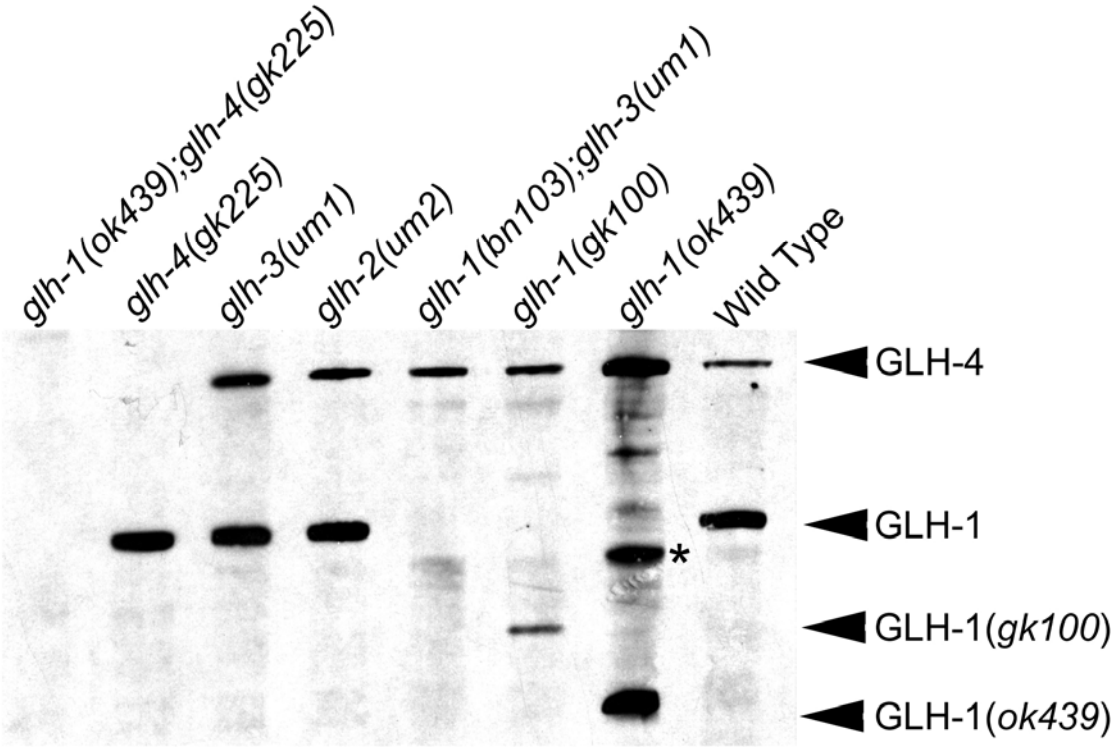

A double mutant of *glh-1(ok439);glh-4(gk225)* shows no GLH-1 or GLH-4 (Figure 4.3 lane 1) (this lane contained only 100 worms, the truncated GLH-1 in the *glh-1(ok439)* strain would be evident with more worms as above). This work shows that *glh-4(gk225)* is a protein null strain and that *glh-1(ok439)* and *glh-1(gk100)* produce smaller GLH-1 proteins, while the Tc1 insertion strain *glh-1(bn103)* produces no detectable protein in our assays. This work also shows that the GLHs are produced independently, as the absence of a single GLH protein does not preclude the presence of the remaining GLHs.

To examine the effects of mutations in *glh* genes on fertility brood counts were performed on *glh-2(um2)*, *glh-3(um1)* and N2 worms at 15°C, 20°C, and 26°C. Brood sizes of mutants were compared to wild type and significant differences determined using a Student's T test (Table 4.1). We found *glh-2(um2)* worms are significantly less fertile that N2 at 15°C and 20°C, with 75% and 80% of wild type brood size respectively, but not 26°C. Additionally, *glh-3(um1)* worms are less fertile than N2 at 15°C (brood size is 70% of N2), but there is no significant difference in these worms at 20°C or 26°C.

Studies of the *glh-1* mutants brood counts and sterility has been a collaboration with the Strome laboratory. All *glh-1* mutant alleles are fertile at 15°C and 20°C but the brood size is significantly reduced for *glh-1(ok439)*, *glh-1(gk100)*, and *glh-1(bn103);glh-3(um1)*. Additionally all *glh-1* alleles show significant sterility at 26°C (Table 4.2). This is consistent with the RNAi phenotype for *glh-1* which showed the most significant reduction in fertility at 25°C and 26°C (Kuznicki et al. 2000). N2 and *glh-1(gk100)*, *glh-1(ok439)*, *glh-*

Table 4.1: Brood counts of N2, *glh-2(um2)*, *glh-3(um1)* worms. N2, *glh-2(um2)*, and *glh-3(um1)* worms were raised at 15°C, 20°C, or 26°C and brood size analyzed. Significance was determined by comparing mutant values to N2 using Student's T test.

Strain	Growth Temp.	Total # F_1 progeny/ # P_0 worms counted	Average Progeny ± s.d	% of wild type at same temperature	P value
glh-2(um2)	15°C	2065/12	172±27	75%	<0.001
	20°C	2009/10	201±71	80%	<0.006
	26°C	952/11	86±36	100%	0.973
glh-3(um1)	15°C	1766/11	161±49	70%	<0.001
	20°C	3095/12	258±26	103%	0.454
	26°C	1119/11	102±40	116%	0.321
N2	15°C	2510/11	228±26		
(wild type)	20°C	3007/12	251±21		
	26°C	783/9	87±19		

Table 4.2: *glh-1* mutant brood counts at 15°C, 20°C, and 26°C. Hermaphrodites for each strain were placed at the appropriate temperature and the brood size of their progeny examined.

Strain	Growth Temp.	Average Progeny ± Standard Dev.	% Wild Type at same Temp	P value
N2	15°C	173±16		
	20°C	219±23		
	26°C	78±49		
glh-1(ok439)	15°C	106±63	61%	<0.05
	20°C	84±14	38%	<0.01
	26°C	0	0%	<0.01
		100% sterile		
glh-1(gk100)	15°C	48±42	28%	<0.01
	20°C	56±37	27%	<0.01
	26°C	0	0%	<0.01
		100% Sterile		
glh-1(bn103); glh-3(um1)	15°C	45±29**	26%	<0.01
	20°C	49±39**	22%	<0.01
	26°C	3±5**	4%	<0.01
		70% Sterile		

1(bn103), and *glh-1(bn125)* were raised at 16°C, 20°C and 26°C and the percentage of sterile worms determined (Table 4.3). The first generation of worms raised at 16°C results in between 6.5% and 13% sterility in the *glh-1* mutant worms (the variation depending on the strain examined); the second generation does not show increased sterility. At 20°C, *glh-1* mutants are about 10% sterile. In contrast, when raised at 25°C, the first generation of *glh-1* mutants is between 8% and 48% sterile, and the second generation is 26% to 100% sterile. An increase to 26°C results in even greater sterility; in the first generation *glh-1* mutants raised at 26°C were between 26 and 36% sterile, but in the second generation all alleles were 100% sterile. This data suggests that although the *glh-1* mutants may produce portions of GLH-1, these proteins are poorly functional or non-functional.

To further examine the *glh-1* mutants, *glh-1(ok439)* and *glh-1(gk100)* worms were raised at 20°C and extruded gonads and embryos were reacted with antibodies generated against GLH-1 (Figure 4.4). GLH-1 protein localization in the *glh-1(ok439)* strain is severely abrogated; although a truncated GLH-1 is produced, it does not show punctate, P granular staining, but is rather present in a honeycomb pattern in the gonad and seems to be in all cells of early embryos. In contrast, *glh-1(gk100)* shows more or less normal P granule staining for GLH-1, both in extruded gonads and embryos. This suggests that although the helicase motifs, zinc fingers and glycine-rich repeats are necessary for protein function, the C terminus containing the helicase region may play a role in protein localization.

Table 4.3: Percentage of sterile progeny produced by N2 and *glh-1* mutants at various temperatures. St=sterile. F_1 worms were the first generation raised at that temperature, F_2 were progeny of the F_1 generation. From Nicole Meyer, Strome laboratory.

Genotype	16°C		20°C		25°C		26°C	
	% St F1	% St F2	% St F1	% St F2	% St F1	% St F2	% St F1	% St F2
N2	0	0	0	0	0	0	0	0
glh-1(gk100)	6.7	11	10	14	48	100	46	100
glh-1(ok439)	15	10	11	11	46	99	45	100
glh-1(bn103) unc-13	12	13	12	10	46	100	44	100
glh-1(bn125)	6	6	10	8	8	26	34	100

Figure 4.4: GLH-1 in *glh-1(ok439)* and *glh-1(gk100)* worms raised at 20°C. Top: *glh-1(ok439)* extruded gonad (left) and embryos (right) reacted with αGLH-1 antibodies. GLH-1 is not in P granules, but diffuse. Bottom: *glh-1(gk100)* extruded gonad (left) and embryos (right) reacted with with αGLH-1 antibodies. GLH-1 localization is more or less normal.

Top

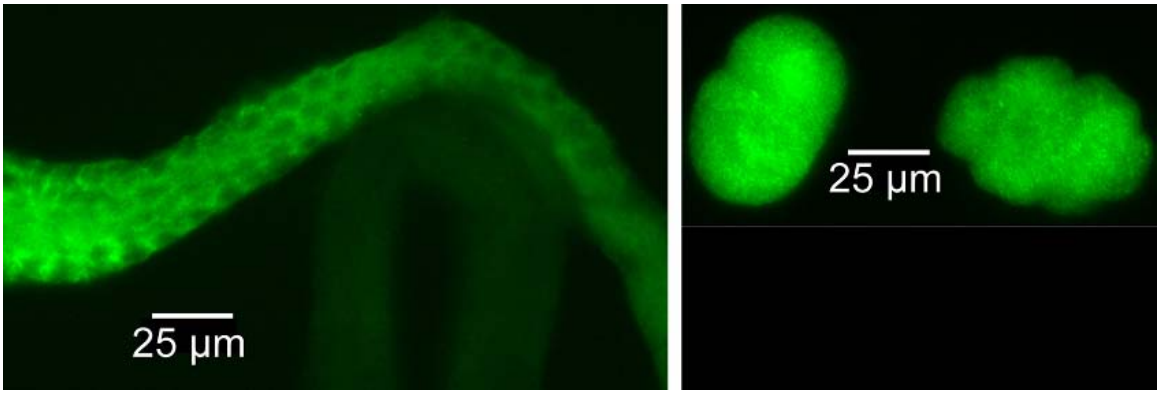

Bottom

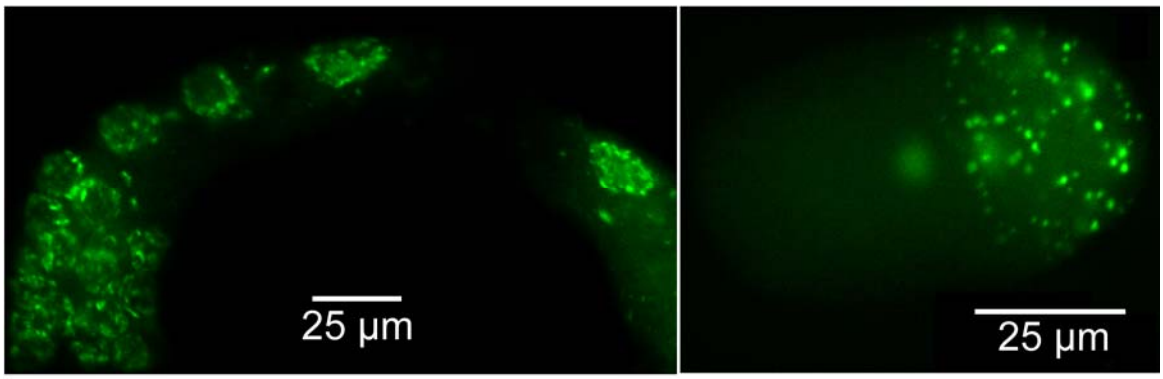

Both *glh-1(ok439)* and *glh-1(gk100)* worms were also raised at 26°C and extruded gonads stained with DAPI to examine the germlines of these sterile worms (Figure 4.5). Both *glh-1(ok439)* and *glh-1(gk100)* worms had germlines of normal size, with sperm, and evidence of diakinesis by the presence of bivalent chromosomes. Yet neither strain produced functional oocytes; in fact EMO oocytes were sometimes seen. These results were unexpected, as *glh-1* RNAi at 26°C results in sterile worms with an under-proliferated gonads (Kuznicki et al. 2000). As neither *glh-1(ok439)* nor *glh-1(gk100)* worms are protein nulls, this could suggest that the presence of non-functional GLH-1 protein may lead to additional phenotypes, such as EMO.

Another set of brood counts was performed with *glh-4(gk225)* and N2 worms raised at 20°C and no significant difference was seen in this case, with the brood size of *glh-4(gk225)* worms being 95% of wild type (Table 4.4). Brood counts at 26°C have not yet been carried out, but will be critical for understanding the importance of GLH-4 at elevated temperatures. To corroborate the western blot analysis which shows *glh-4(gk225)* is a protein null, immunocytochemistry of *glh-4(gk225)* extruded gonads reacted with antibodies generated against GLH-4 also shows no detectable GLH-4 protein (Figure 4.6).

As the most severe fertility defect is seen when both GLH-1 and GLH-4 are lacking, we decided to construct a double mutant with the *glh-1(ok439)* and *glh-4(gk225)* alleles. As the two genes are within four map units, chromosomal recombination was necessary and many worms had to be screened to isolate the double mutant. The RNAi effect of combinatorial *glh-1/4* elimination results in

Figure 4.5: DAPI staining of *glh-1(ok439)* and *glh-1(gk100)* mutants raised at 26°C. Top: Extruded gonad from *glh-1(ok439)* worms raised at 26°C from the L1 stage. Bottom: Extruded gonad from *glh-1(gk100)* raised at 26°C from the L1 stage. Arrowheads point to oocytes in diakinesis, arrows point to EMO oocytes, and asterisk indicates sperm.

Top

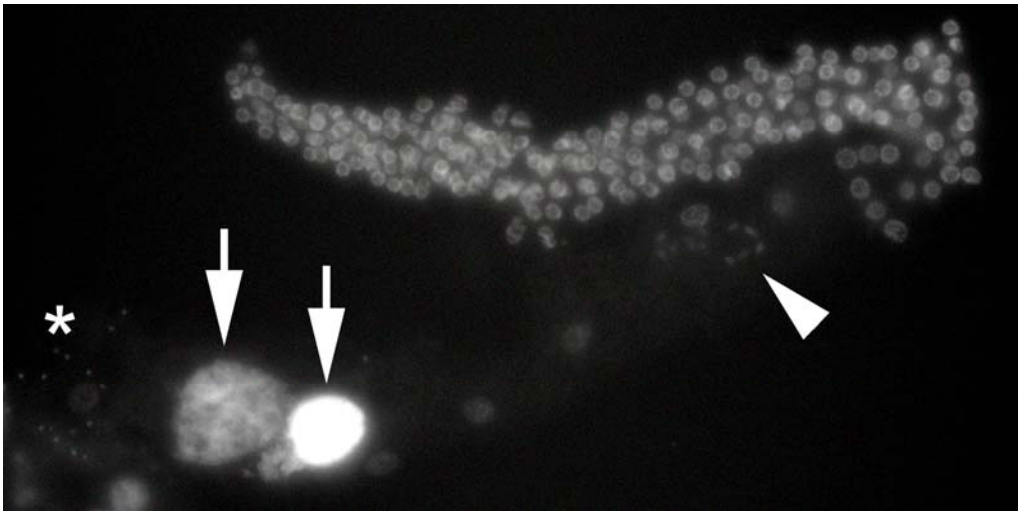

Bottom

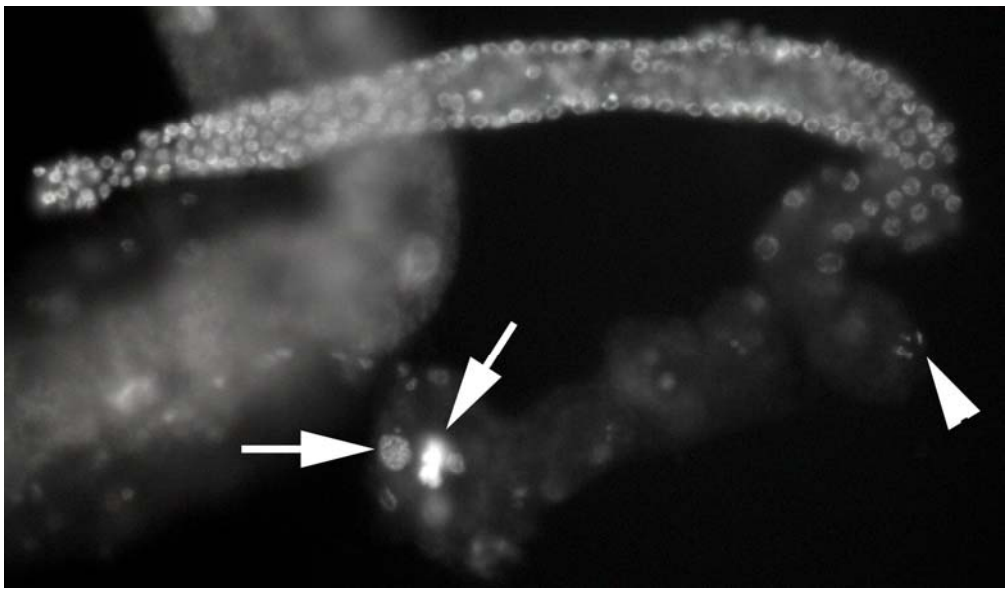

Table 4.4: *glh-4(gk225)* brood counts. Brood sizes for *glh-4(gk225)* and N2 mutants raised at 20°C were determined. No significant difference was observed ($p<0.17$).

Strain	Growth Temp.	Total # F_1 progeny/ # P_0 worms counted	Average Progeny ± s.d	% of wild type at same temperature
glh-4(gk225)	20°C	4659/18	259±38	95%
N2	20°C	6794/25	272±37	

Figure 4.6: Extruded gonads of N2 and *glh-4(gk225)* with GLH-4. Top: N2 extruded gonad reacted with antibodies generated against GLH-4 showing P granule staining. Bottom: Extruded gonad from *glh-4(gk225)* worm reacted with αGLH-4 antibodies.

Top

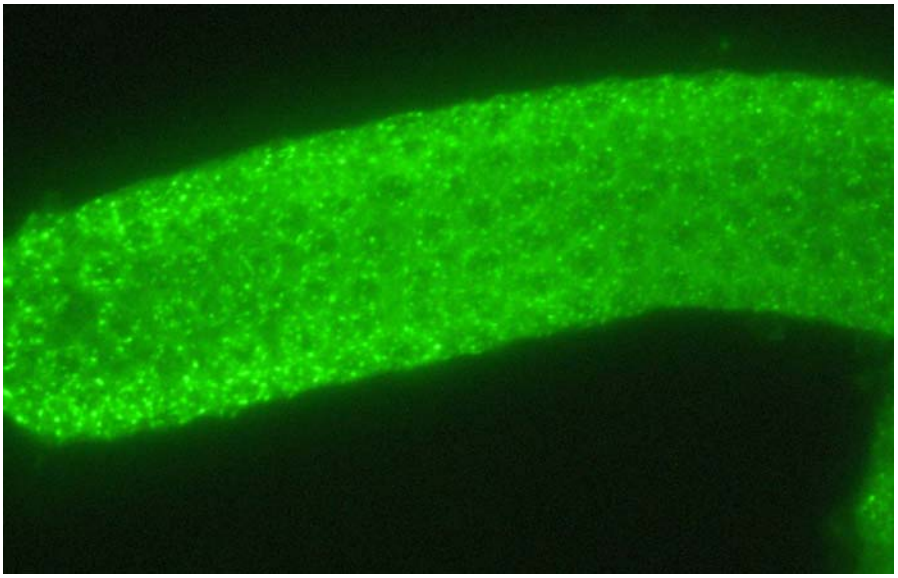

Bottom

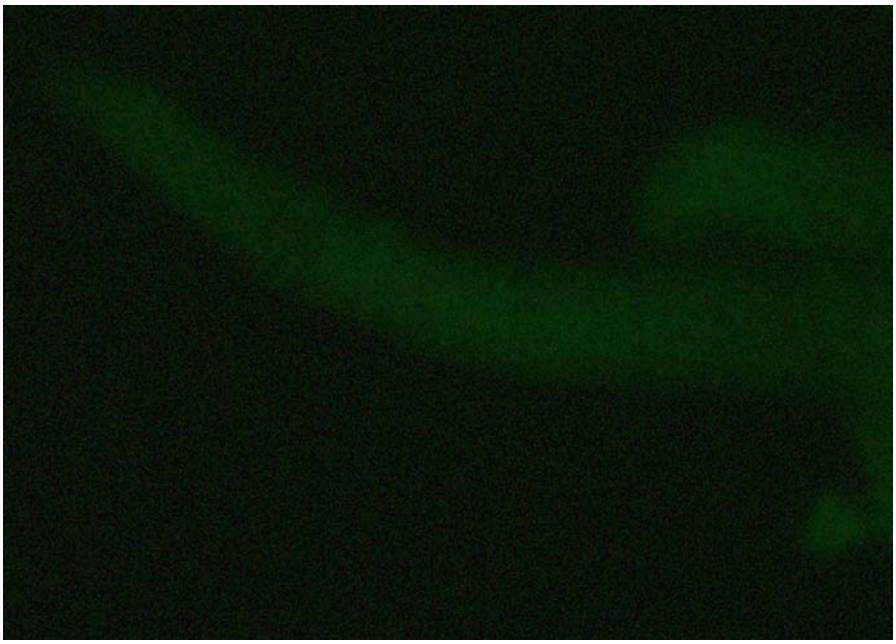

sterility at permissive temperatures; therefore, we balanced the double mutant with the chromosomal balancer gHT2 which covers both *glh-1* and *glh-4*. Homozygous double mutants were examined; the first generation off the balancer is referred to as M+/Z- (for maternal positive, zygotic negative for GLH-1 and GLH-4), any progeny of the M+/Z- worms are referred to as M-/Z- (being negative for both maternal and zygotic GLH-1 and GLH-4). Extruded gonads from N2 and *glh-1(ok439);glh-4(gk225)* double mutants were stained with DAPI to examine the morphology of these defective gonads (Figure 4.7). Like the gonads from *glh-1/4* RNAi worms, *glh-1(ok439);glh-4(gk225)* are much smaller than their wild type counterparts (Kuznicki et al. 2000).

The sterility phenotype we observe in the *glh-1(ok439);glh-4(gk225)* worms is not completely penetrant so we performed fertility assessments of these worms. Only 32% of M-/Z- *glh-1(ok439);glh-4(gk225)* worms were sterile (Table 4.5), compared to 97% of *glh-1/4* RNAi worms at the same temperature (Kuznicki et al. 2000). This suggests that at permissive temperatures, *glh-1(ok439)* mutant GLH-1 may be able to perform some of its normal functions, allowing for some fertility.

Figure 4.7: Comparison of wild type and *glh-1(ok439);glh-4(gk225)* mutant. Top: wild type worms were raised at 20°C, splayed, and stained with DAPI to visualize nuclei. Bottom: homozygous *glh-1(ok439);glh-4(gk225)* worms were raised at 20°C and treated as above. The phenotype of homozygous *glh-1(ok439);glh-4(gk225)* worms is similar to *glh-1/4* combinatorial RNAi. Sperm indicated by arrowheads.

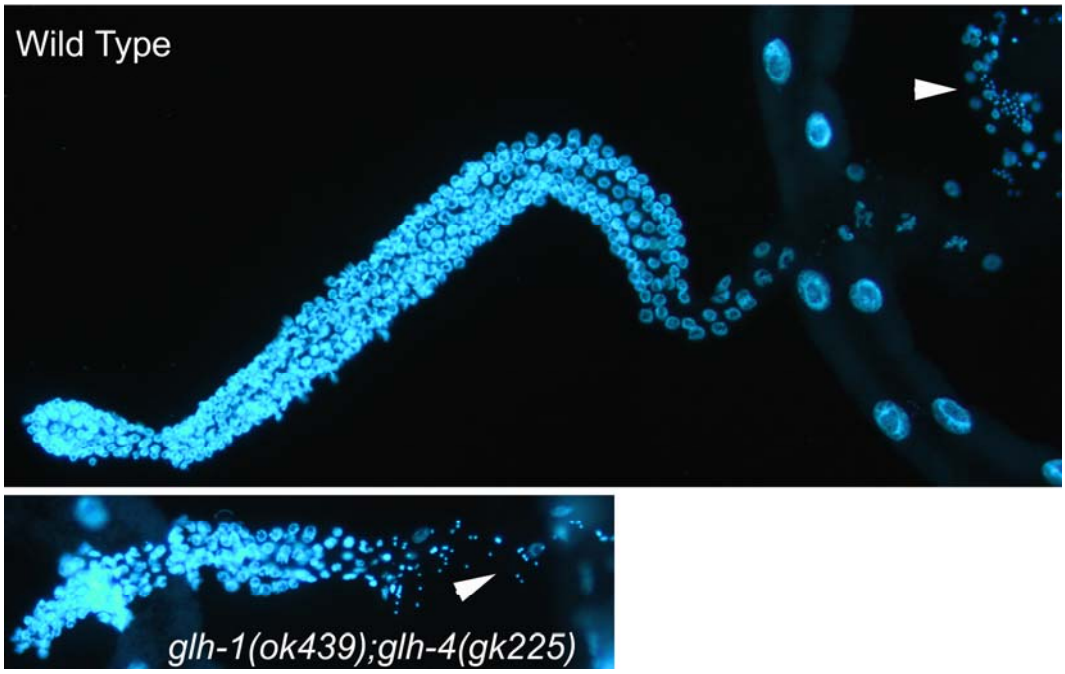

Table 4.5: *glh-1(ok439);glh-4(gk225)* fertility. Brood counts for N2 and *glh-1(ok439);glh-4(gk225)* (M+/Z- or M-/Z-) were determined at 20°C.

Strain	Avg. # Progeny ± Standard Dev.	% Wild type at Same Temp.	P value
N2	186±17		
glh-1(ok439);glh-4(gk225) M+/Z-	133±25	72%	$p<0.001$
glh-1(ok439);glh-4(gk225) M-/Z-	86±72	46% 32% Sterile	$p<0.001$

Discussion

The results presented in this chapter draw heavily upon the combinatorial RNAi experiments performed previously (Kuznicki et al. 2000). Our work with the single *glh* mutants (*glh-1(ok439), glh-1(gk100), glh-1(bn103); glh-2(um2), glh-3(um1),* and *glh-4(gk225)*) is consistent with previous results that find at the permissive temperature, the elimination of any one GLH does not cause sterility. We did find in the experiments presented here, that although the single mutants at permissive temperatures are fertile, all but *glh-4(gk225)* have some reduction in brood size at 15°C or 20°C. Like *glh-1* RNAi, the effects of the *glh-1* mutations are most evident at 26°C resulting in 100% sterility. Our *glh-1(ok439);glh-4(gk225)* mutant does not have as penetrant a sterility defect at *glh-1/4* RNAi at 20°C (32% compared to 97% respectively). The fact that *glh-1(ok439)* does produce a truncated protein may explain this observation.

Although the fact that *glh-1(ok439)* and *glh-1(gk100)* worms produce altered GLH-1 proteins makes interpretation of results related to these alleles difficult, the localization patterns of these two mutants sheds some light on the roles of portions of the GLH-1 protein. The *glh-1(ok439)* worms are lacking three of the eight conserved DEAD-box helicase motifs, consisting of a large portion of the C-terminus of the protein. When we examine GLH-1 localization in these mutants, we find that there is no obvious P granular staining, with the mutant GLH-1 seemingly present in all cells of early embryos and staining the gonad diffusely. This suggests the C-terminus is important for protein function and may play a role in protein localization. The *glh-1(gk100)* allele shows more or less

normal P granule staining for GLH-1; this suggest the zinc fingers and FGG repeats are involved in protein function but not crucial for localization. Both of these alleles seem to be functional nulls, as the sterility at 26°C is complete, and the worms are less fertile than wild type at permissive temperatures. An interesting aspect of the *glh-1(ok439)* and *glh-1(gk100)* phenotype is the presence of EMO oocytes in some of the mutants raised at 26°C. The data presented in Chapter 2 suggests that too much GLH-1 is detrimental for fertility and that the phosphodegron may play a role in regulation of GLH-1 protein levels. The *glh-1(ok439)* truncated protein lacks the MAPK docking site and the protein seems to accumulate in non-P granular structures in the germline and in embryos. This could be due to the inability of KGB-1 to target this truncated GLH-1 protein for degradation. We find, however, that *glh-1(ok439)* GLH-1 protein is not very abundant at permissive temperatures. This could be due to problems with translation of this truncated allele or the disturbance of regulatory elements in the 3' region of the gene that would be missing because of the deletion. Therefore assessing the effect of KGB-1 on the *glh-1(ok439)* truncated GLH-1 is difficult. Analysis of GLH-1 migration in *glh-1(ok439)* embryos and adults was attempted, but there was too little truncated GLH-1 in the *glh-1(ok439)* embryos to detected in our assays. Unfortunately, the use of this allele for studying KGB-1 function will be limited due to the low expression of GLH-1.

Future Directions

The data presented in this document only begins to scratch the surface of GLH function. The relationships between the GLHs and their binding partners, KGB-1 and CSN-5 are intriguing and deserving of further study. The full understanding of the regulation of GLH-1 levels by KGB-1 may require technology that is currently unavailable or impractical for use in the germline of *C. elegans*.

To further understand how KGB-1 regulates GLH-1 levels more proteasome inhibitor studies could be performed. Using the GLH-1 construct lacking the docking site and examining the ability of KGB-1 to regulate GLH-1 when the putative interaction site is missing would add to our understanding of physical requirements for KGB-1 mediated regulation. A baculoviral construct has also been generated that prevents the phosphorylation of the phosphodegron by mutating a threonine to an alanine. This construct could also be used in proteasome inhibitor experiments to determine if phosphorylation at the phosphodegron is necessary for KGB-1 mediated regulation of GLH-1.

Additionally, *in vivo* studies with proteasome inhibitors would be very useful for understanding GLH-1 regulation in the worm. Soaking worms in proteasome inhibitors revealed no changes in GLH-1 protein levels (data not shown), but injection of MG132 into the germline and subsequent western blot analysis of injected worms may allow us to visualize changes in GLH-1 levels.

Both N2 and *kgb-1(um3)* worms could be employed in these experiments to determine the requirement of KGB-1 for GLH-1 regulation.

Understanding the exact function of the GLH proteins in germline development is an on-going goal of the Bennett laboratory. Further analysis of *glh* mutants may shed more light on this field. One of the most intriguing discoveries of the work presented in this document is the shift in GLH-1 size when proteins from adult and embryos are compared. The nature of this shift is still a mystery. Based on our KGB-1 data, the shift could be due to a phosphorylation event, or other protein modification. The elucidation of this size shift may provide valuable insight into the regulation of GLH-1 during development.

In addition, the isolation of a deletion mutant in *csn-5* will allow for further work understanding the function of CSN-5 as it relates to fertility and the GLHs in particular. The interaction between KGB-1 and CSN-5 is also of interest. If there is a system by which these two proteins regulate GLH levels, either cooperatively or antagonistically it will help us to understand protein regulation in the germline of *C. elegans*, and perhaps on a larger scale.

Appendix 1 ZYX-1

Introduction

The yeast two-hybrid screen carried out by the Bennett laboratory to identify proteins that interact with the GLHs found, in addition to CSN-5 and KGB-1, the protein ZYX-1, which interacted robustly (Figure A.1 and 2.6) (Smith et al. 2002). ZYX-1 contains three conserved LIM domains, protein motifs thought to facilitate protein binding (Figure A.2) (Michelsen et al. 1993). The vertebrate homologue Zyxin is found in focal adhesions and associated with the actin cytoskeleton; Zyxin is thought to facilitate cell divisions, cell identity, and development (Sanchez-Garcia and Rabbitts 1993).

Like *kgb-1* and *csn-5*, *zyx-1* RNA is not restricted to the germline (Figure A.3) (Smith 2001). We also saw little effect of *zyx-1* RNAi on fertility with only a modest 9% sterility observed in worms raised at 26°C (Smith et al. 2002). As RNAi does not always reveal the requirements for a protein (as was the case for KGB-1), we screened deletion libraries for a mutant in *zyx-1*. Two alternate transcripts for *zyx-1* have been identified and we screened for a mutation in the region conserved in both transcripts (*zyx-1a* and *zyx-1b*) (Figure A.2). We isolated, backcrossed, and examined the fertility of the *zyx-1(um4)* mutant. Western-blot analysis was also performed to see if *zyx-1(um4)* worms produce any ZYX-1 protein.

Figure A1.1: GST pull-downs with GLHs and ZYX-1. ZYX-1 6-His and either GST alone, GLH-1 GST, or GLH-3 GST were co-expressed and ability to bind assayed with GST pull-down analysis. Lane 1: ZYX-1 6-His does not bind GST alone. Lane 2: ZYX-1 6-His does bind GLH-1 GST. Lane 3: ZYX-1 6-His also binds GLH-3 GST. Adapted from (Smith et al. 2002).

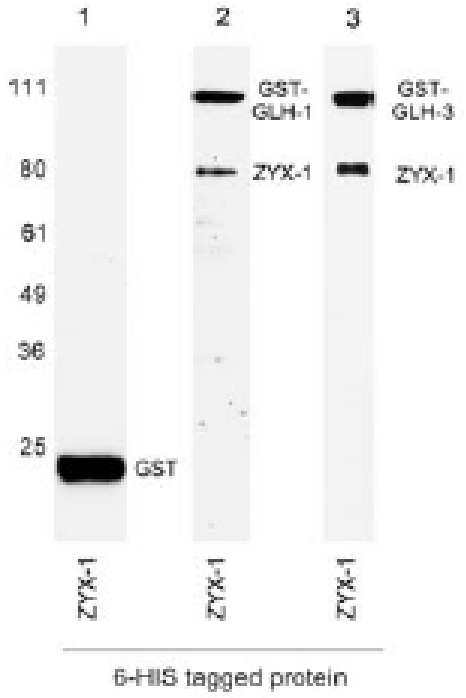

Figure A1.2: Depiction of *zyx-1* gene and protein. Extent of deletion allele *zyx-1(um4)* indicated in both gene and protein. There are two alternate transcripts for *zyx-1* (a and b); exons are indicated by blue boxes, introns by lines connecting exons. The proline rich region of ZYX-1a is indicated by a green box, and the conserved LIM domains are indicated by red boxes, a predicted nuclear export signal is indicated in purple. Adapted from (Smith et al. 2002).

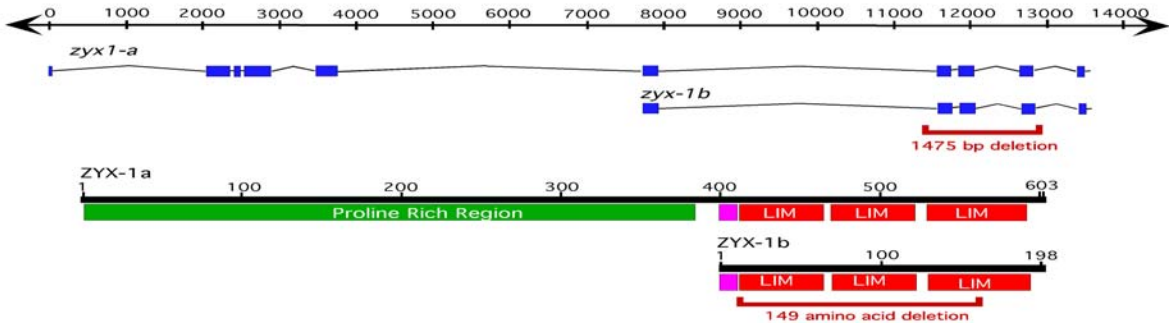

Figure A1.3: *zyx-1 in situ* hybridizations. Expression of *zyx-1* is seen in early embryos in hypodermal regions, which persists in larvae and young adults. Additional germline expression is seen in late larval stages and adult worms.

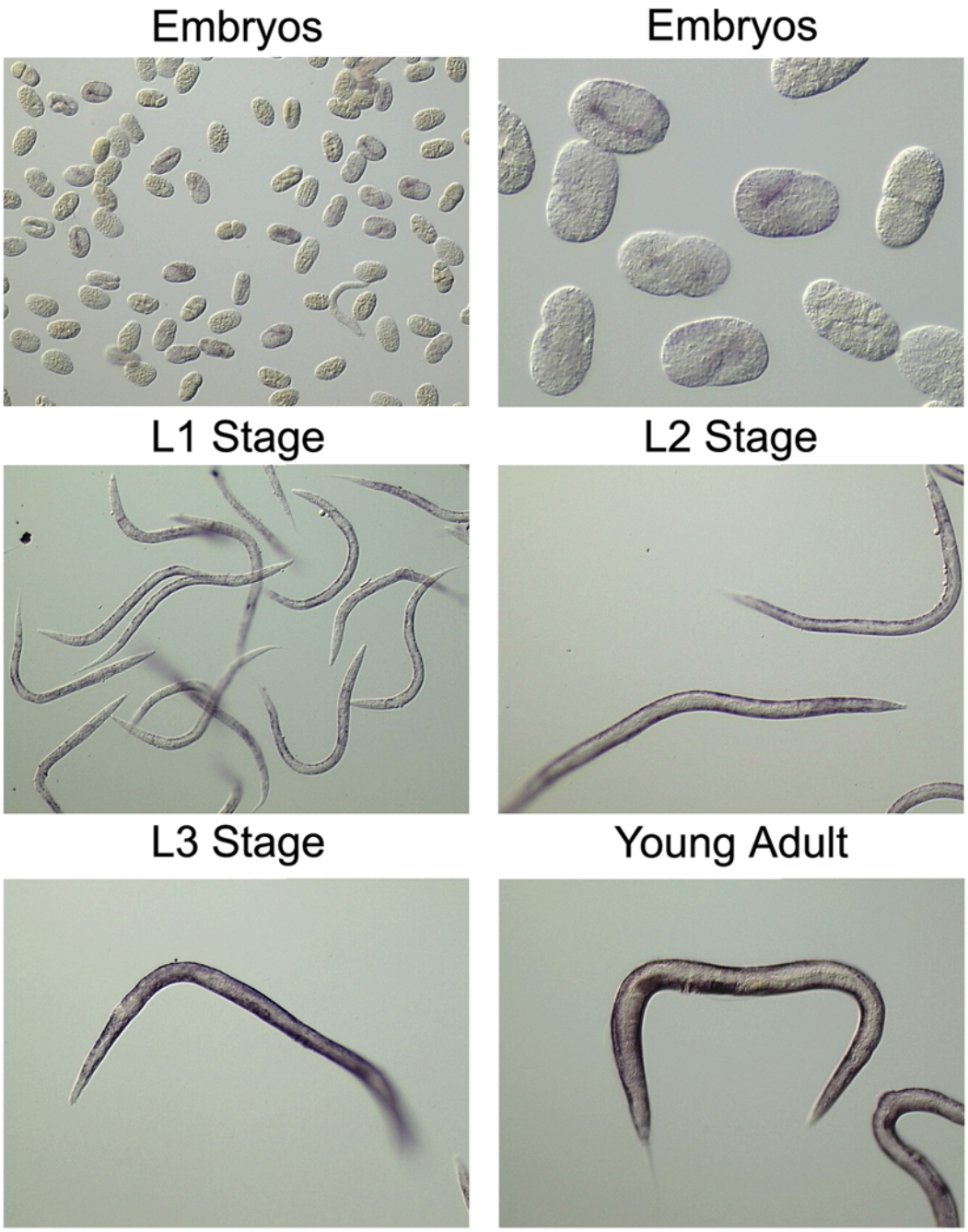

Materials and Methods

Strains

The following strains were used in this work: wild type (N2 variety Bristol), *zyx-1(um4)* (Smith et al. 2002).

Deletion library screening

This screening was performed essentially as in Chapter 3 Methods section. In addition to the *glh* genes mentioned above, we also screened libraries for deletions in genes known to encode GLH binding partners. After Emily Coberly *kgb-1(um3)* deletion, we screened for *csn-5* and *zyx-1* (cosmid identifier F42G4.3b). A *csn-5* mutant was found but it was unable to be recovered. Ruth Montgomery and Regan Barnes helped me find a deletion in *zyx-1* (Figure A.4). Primers used were:

zyx-1 (F42G4.2b) 5' Inner 5'TTTGCATCAACGCTGTAGAAG3'

zyx-1 (F42G4.2b) 3' Inner 5'GCACACCTCACTGGCACGC3'

zyx-1 3' 42 Deletion Long 5'GCAATTATTACCCCTAACCAGTTTCCCTCC3'

zyx-1 5' 42 Deletion Long 5'CAAATGTGGTCAGTGCTCGAAGACACTTGC3'

Western blot analysis

To determine if *zyx-1(um4)* is a protein null, western blot analysis was carried out essentially as above. Instead of picking individual worms, *zyx-1(um4)*

Figure A1.4: Screening for *zyx-1(um4)* mutation. Top: In the first set of PCR reactions on pooled DNA from a mutagenized library using primers designed for the LIM of ZYX-1 protein domain, a band smaller than the wild type size is found. Pooled DNA from 10 plates (each with 500 progenitor worms) was used in each lane. Middle: The pooled DNA from the lane in the top panel was rescreened along with other control DNA, and six out of six reactions show the smaller band and wild type band, and control reactions have only the wild type band. Bottom: Each of the 10 pooled plates from the reaction in the top panel that showed the smaller band are screened by PCR to determine which plate contains the mutation, each plate is examined by triplicate PCR reactions. One plate shows three out of three reactions with the smaller band.

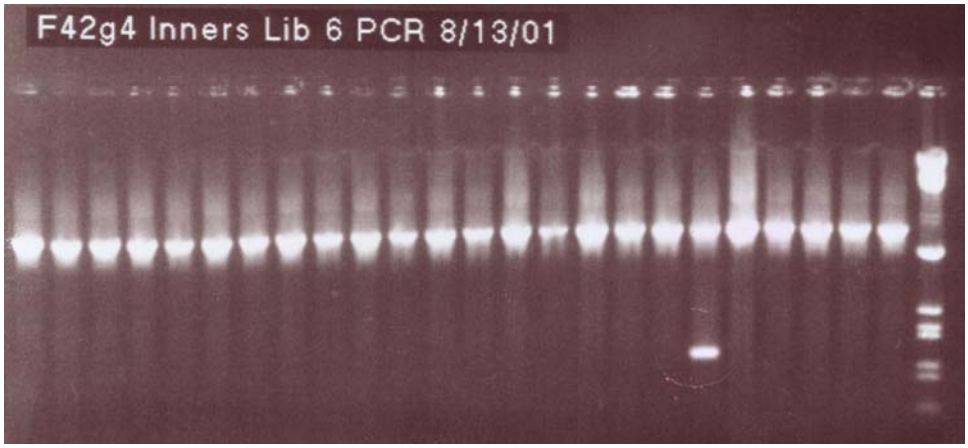
F42g4 Inners Lib 6 PCR 8/13/01

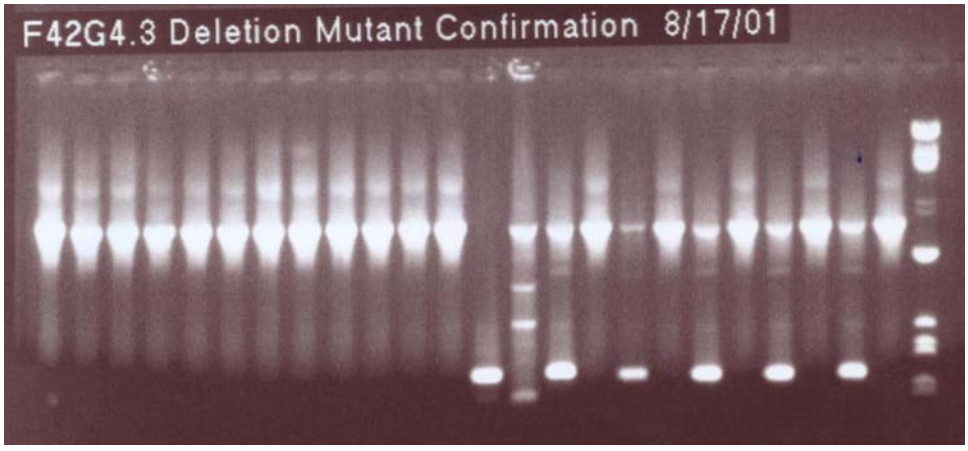
F42G4.3 Deletion Mutant Confirmation 8/17/01

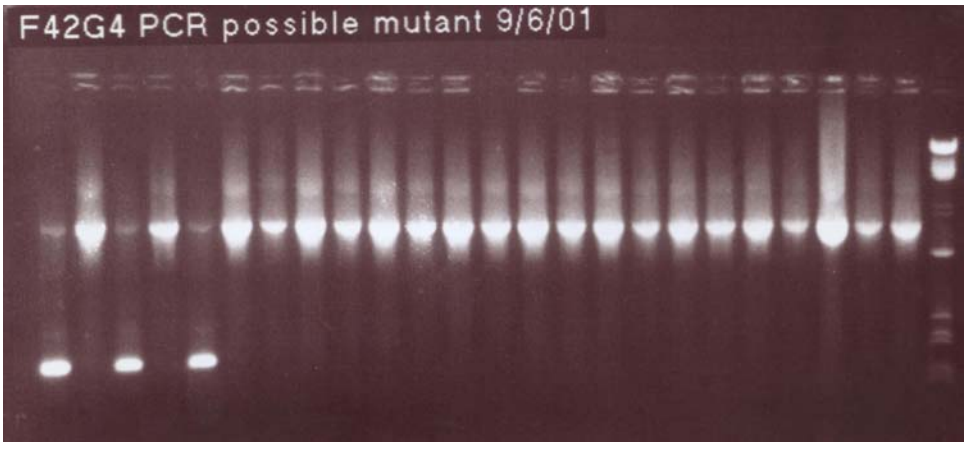
F42G4 PCR possible mutant 9/6/01

worms were grown in liquid culture with 5% X1666 *E. coli* to adult stage, harvested by gravity settling on ice. The worms were washed in M9 for one hour to clear their guts and frozen in 1% β mercaptoethanol, 2x Complete Protease Inhibitor (Roche), 1mM EDTA and 2x protein loading dye in liquid N_2. The tubes were then boiled for 10 minutes and centrifuged for two minutes to pellet worm bodies. The proteins were then analyzed by SDS-PAGE and western blot analysis on 10% acrylamide gels as described previously. An antibody was raised to the C-terminus (CSKPIVPQDGEKESVRVVAMD) of the ZYX-1 protein in mice and used at 1:1000.

Backcrossing and brood counts

Backcrossing was performed with wild type males as described in Chapter 2 Methods Backcrossing section. Primers from Library Screening section were used to select homozygous mutants. Brood counts were performed as described in Brood Counds section of Chapter 2 Methods using *zyx-1(um4)* worms.

Results

Screening of mutagenized libraries resulted in the isolation of a mutation in the *zyx-1* gene; this deletion eliminates 1475 base pairs of DNA corresponding to the three conserved LIM domains of ZYX-1. To examine *zyx-1(um4)* fertility, we performed brood counts at 15°C, 20°C, and 26°C (Table A.1). We found at 15°C that *zyx-1(um4)* worms produced 12% more progeny than their wild type counterparts; this difference is statistically significant. We observed no significant change in *zyx-1(um4)* fertility at 20°C, but did find an increased sterility at 26°C with 29% sterility for *zyx-1(um4)* worms raised at 26°C compared to 7% of N2 worms. There was also a significant decrease in brood size for *zyx-1(um4)* worms at 26°C, with these worms producing broods on 68% that of wild type. Due to their infrequency, we have not yet characterized the phenotype of sterile *zyx-1(um4)* worms.

We predicted that the deletion of the LIM domains in the *zyx-1* gene would result in no *zyx-1* mRNA production due to nonsense mediated degradation and thereby no ZYX-1 protein. To examine this possibility, we raised *zyx-1(um4)* worms at 20°C and analyzed them by western blot for the presence of ZYX-1 protein (Figure A.5). We find that, although the antibody we raised to ZYX-1 is specific (Figure A.5 lanes 2, 3, 5 and 6), *zyx-1(um4)* worms do not produce full-lengthZYX-1 protein of either isoform (Figure A.5 lane 4).

Table A1.1: Brood counts for *zyx-1(um4)* mutants and N2. Worms were grown as for brood counts in Chapter 2. Individual L4 worms from each strain were age matched and individually plated. F_1 offspring were counted four to seven days after plating depending on temperature. *P_0 L4 animals were shifted to 26°C; the F_2 broods of F_1 adults were determined. P value was determined by comparing brood counts of *zyx-1* with N2 worms grown at same temperature using a Student's T Test. s.d.= standard deviation

Strain	Growth Temp.	Total # F_1 progeny/ # P_0 worms counted	Average progeny ± s.d	% of wild type at same temperature	% Sterility	P value
zyx-1(um4)	15°C	1997/14	143±12	112%	0%	<0.02
	20°C	1693/15	113±10	94%	0%	0.21
	26°C*	984/29	34±28	68%	29%	<0.02
N2	15°C	1903/15	127±23		0%	
(wild type)	20°C	1794/15	119±29		0%	
	26°C*	1413/28	50±27		7%	

Figure A1.5: *zyx-1(um4)* worms are protein nulls. Lane 1, αGLH-1 was used as a positive control; lane 2, pre-immune sera from an αZXY-immunized mouse; lanes 3-5, hyper-immune sera from the same mouse were tested. Lanes 1-3 contain N2 protein; lane 4 contains protein from the *zyx-1(um4)* strain; lane 5 contains ~0.1μg of baculoviral-produced full-length ZYX-1 protein and lane 6 contains an equal amount of baculoviral-produced eGFP protein, a negative control. The *zyx-1(um4*) protein homogenate was not degraded when tested with several other antibodies, not shown. Protein sizes were estimated using Benchmark pre-stained protein markers (GIBCO).

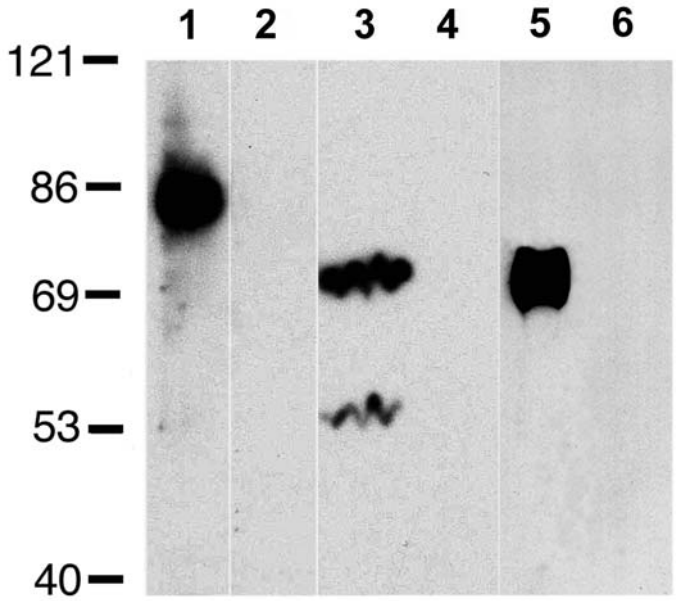

Discussion

The role of ZYX-1 in *C. elegans* development has not been well studied. Our results show that the *zyx-1(um4)* strain produced no detectable levels of ZYX-1 full-length protein. Unfortunately, though our antibodies are suitable for western blot analysis, they have not been useful in immunocytochemistry. Therefore, on a cellular level, there is more work to be done examining ZYX-1 in worms.

We also find that *zyx-1(um4)* worms are less fertile than N2 worms at 26°C, with 29% of *zyx-1(um4)* exhibiting sterility at this non-permissive temperature. The low penetrance of this phenotype makes its characterization somewhat difficult, as isolating significant numbers of sterile *zyx-1(um4)* worms would require large scale experiments. We are perplexed by the significant increase in brood size (12%) in *zyx-1(um4)* worms when raised at 15°C. It is possible that the deletion in this strain is somehow favorable for fertility at lower temperatures, perhaps due to the role of ZYX-1 or other genes whose regulation could be affected by the deletion. Yet, *zyx-1(um4)* worms are less fertile than N2 at higher temperatures, implying ZYX-1 must have some role in fertility. As a putative cytoskeletal protein, it is possible that other proteins maybe able to compensate for the loss of ZYX-1 at permissive temperatures but not high temperatures, as is often the case for germline genes, like the GLHs. We have postulated that the role of ZYX-1 in relation to the GLHs may be in movement of

P granules. Through the LIM domains, ZYX-1 may associate with GLH proteins and tether them to the cytoskeleton, possibly helping to transport P granules to the germline progenitors in embryos and helping them associate with the nuclear membrane. However, P granules are intact in the *zyx-1(um4)* mutant strain. To fully understand the function of ZYX-1, further work will have to be done examining the phenotype of *zyx-1(um4)* sterile worms.

Appendix 2 H27M09.1

Introduction

The GLHs are belong to the family of DEAD-box RNA helicases. Though very similar to proteins like *Drosophila Vasa*, the GLHs are characterized by the presence of CCHC, retroviral like zinc fingers. To date, the only DEAD-box helicases identified in *C. elegans* are the GLHs (Roussell and Bennett 1993; Gruidl et al. 1996; Kuznicki et al. 2000). The *C. elegans* genome was published in 1998, the first animal genome to be completed (Consortium 1998; Hodgkin et al. 1998). Completion of the *C. elegans* genome annotation is still on-going. An analysis of the region of chromosome I up-stream of *glh-1* identified a putative DEAD-box helicase with CCHC zinc fingers. Only 0.01 map units, approximately 570 nucleotides from the 5' end of *glh-1* is a putative open reading frame (H27M09.1) that encodes a protein 35% identical and 54% similar to GLH-1. As the only other proteins identified in the *C. elegans* genome with CCHC zinc fingers and the nine conserved DEAD-box RNA helicase motifs are the GLHs, we reasoned that H27M09.1 protein could be related to the GLHs due to its proximity to *glh-1* and the presence of the characteristic protein sequences. To examine this possibility we eliminated H27M09.1 using RNAi, examined the levels of H27M09.1 transcription in germline defective mutants, and compiled data from the *in situ* database detailing the expression of H27M09.1 RNA.

Materials and Methods

Strains

The following strains were used in this work: wild type (N2 variety Bristol), *fem-1(hc17), fem-3(q24), glp-4(bn2)* (Kuznicki et al. 2000; Smith et al. 2002)

RNA interference

To generate dsRNA for H29M09.1 a cDNA was obtained from the Kohara laboratory (National Institute of Genetics, Japan). Primers were designed for the cDNA with T7 polymerase sites and PCR was performed as described in RNA interference section of Chapter 2, Methods. The primers are:
H27M09.15' T7 5'GTAATACGACTCACTATAGGGCGGAGCAAGAGATGAAAC3'
H27M09.13' T7 5'GTAATACGACTCACTATAGGGCTCCGGTACGACCAATTC3'
Transcription of dsRNA was as described above. Young adult wild type worms grown at 20°C were injected and placed at 20°C or 26°C. The worms were purged overnight, transferred to new plates and their F_1 progeny individually plated and examined.

Northern blot analysis

To determine if H27M09.1 RNA is germline enriched, a northern blot was performed. Poly A+ RNA from *fem-3(q24)* (a strain that over-produces sperm, and makes no oocytes), *fem-1(hc17)* (makes oocytes, but no sperm), and *glp-*

4(bn2) (few germ cells, no oocytes, no sperm produced) mutant worms was used. For each strain, worms grown at permissive and non-permissive temperatures were used, and 3 µg of total RNA was used. The RNA was run on a 1% agarose MOPS gel with 12.7% formaldehyde. The RNA was transferred to nitrocellulose, baked at 80°C in a vacuum oven for two hours, and pre-hybridized using 5x SSPE, 4x Denhardt's solution, 0.1 SDS, 200 µg/mL herring DNA, 50% formamide, and 200 µg/mL *E. coli* RNA. Random-primed riboprobes were generated from H27M09.1 using 25 ng of purified PCR product used to produce dsRNA described above. The DNA was heated to greater than 95°C for five minutes, placed on ice for two minutes, and then kept at room temperature for five minutes. To the DNA was added 10 µL 80 µM each dCTP, dGTP, dTTP (in OLB), 37% BSA, 1µL Klenow DNA polymerase and 5 µL [α-^{32}P] dATP. The reaction was incubated overnight at room temperature, and the probe cleaned through G-50 sepharose filtration. The probe was then boiled and ^{32}P incorporation determined using PEI paper. To the blot was added 90 million counts; the blot was incubated for 48 hours at 42°C, and then washed thoroughly with a solution of 5x SSPE, 0.5% SDS, and 50% formamide at 42°C, followed by 2x SSPE, 0.2% SDS, and 0.5x SSPE, 0.2% SDS both at 65°C. The blot was then exposed to autoradiography film at -80°C for ten hours. The film was scanned and processed in Adobe Photoshop.

Results

To examine any requirement for H27M09.1 in fertility, we generated dsRNA from an H27M09.1 cDNA and injected this dsRNA into N2 worms at 20°C and 26°C. We examined the F_1 progeny of the injected worms for fertility and found that at 20°C and 26°C, worms lacking H27M09.1 were significantly more sterile than mock-injected controls (Table A.2). At 20°C, only 87.5% of worms lacking H27M09.1 were fertile, compared to 100% of mock-injected worms. The brood size of H27M09.1 F_1 RNAi worms was examined, and found to be significantly reduced, at only 42% that of mock-injected controls raised at the same temperature. The sterility of H27M09.1 RNAi is exacerbated by high temperature; at 26°C, only 5% of H27M09.1 RNAi worms were fertile. Combinatorial RNAi of H27M09.1 and *glh-1* showed the similar levels of fertility defects seen with either gene alone.

As the RNAi phenotype of H27M09.1 was very similar to that of *glh-1*, we examined the transcript levels of H27M09.1 in germline mutants, a common way of determining germline specificity of RNAs in *C. elegans* (Kuznicki et al. 2000) (Figure A.6). We saw little difference in H27M09.1 transcript levels in *glp-4(bn2)* (a strain that makes few germ cells, no oocytes, no sperm produced at 25°C), *fem-1(hc17)* (makes oocytes, but no sperm at 25°C), or *fem-3(q24)* (over-produces sperm, and makes no oocytes at 25°C) raised at permissive versus non-permissive temperatures. This suggests that H27M09.1 RNA is not germline

specific. We also made use of the *C. elegans* expression database to examine the localization of H27M09.1 RNA during different stages of *C. elegans* development (FigureA.7). We only observed H27M09.1 transcript in the germline of L3 and older worms, but levels seem low even in these tissues. It is possible that H27M09.1 RNA is present in the soma, but at levels not detectable in these *in situ* assays.

Table A2.1: RNAi of H27M09.1. N2 worms were injected with dsRNA from H27M09.1 cDNA, a combination of dsRNA *glh-1* and H27M09.1, or TE (mock injection). The progeny of the injected worms were assayed for fertility at 20°C or 26°C. Brood size of N2 and H27M09.1 injected worms were determined, and analyzed using a Student's T test.

RNAi	**20°C**	**26°C**
Mock injection	100% Fertile	100% Fertile
	n=18	n=6
H27M09.1	87.5% Fertile	5% Fertile
	n=64	n=20
Brood size	42%	
(% of WT)	(p<.001)	
glh-1/H27M09.1	92% Fertile	3% Fertile
	n=41	n=94

Figure A2.1: Northern analysis of H27M09.1 RNA in germline mutants. Levels of H27M09.1 RNA were analyzed in *glp-4(bn2)* (a strain that makes few germ cells, no oocytes, no sperm produced at 25°C), *fem-1(hc17)* (make oocytes, but no sperm at 25°C), and *fem-3(q24)* (over-produces sperm, and makes no oocytes at 25°C). Samples were compared of the same strain raised and permissive versus non-permissive temperatures.

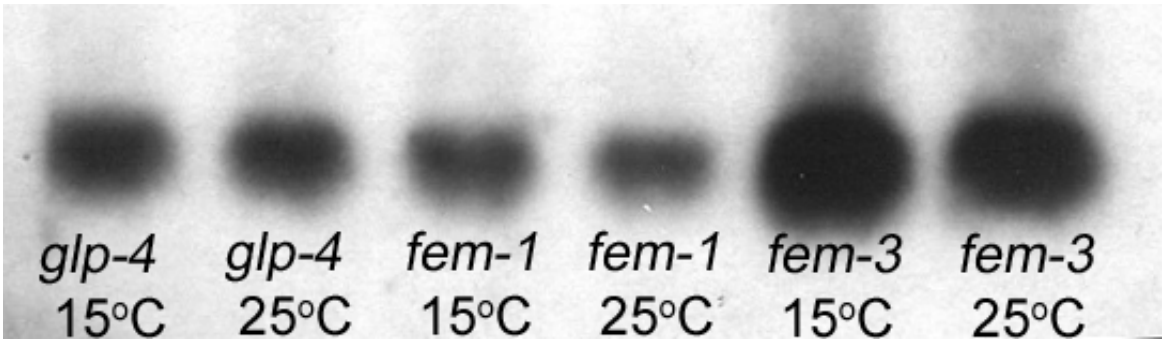

Figure A2.2: *In situ* hybridization of H27M09.1. Embryos, L1, L2, L3, and young adult worms were assayed for H27M09.1 RNA expression. Embryos show diffuse expression; by the L3 stage worms are showing germline expression which is stronger in young adults. No somatic expression is evident. Compiled from the *C. elegans* expression database.

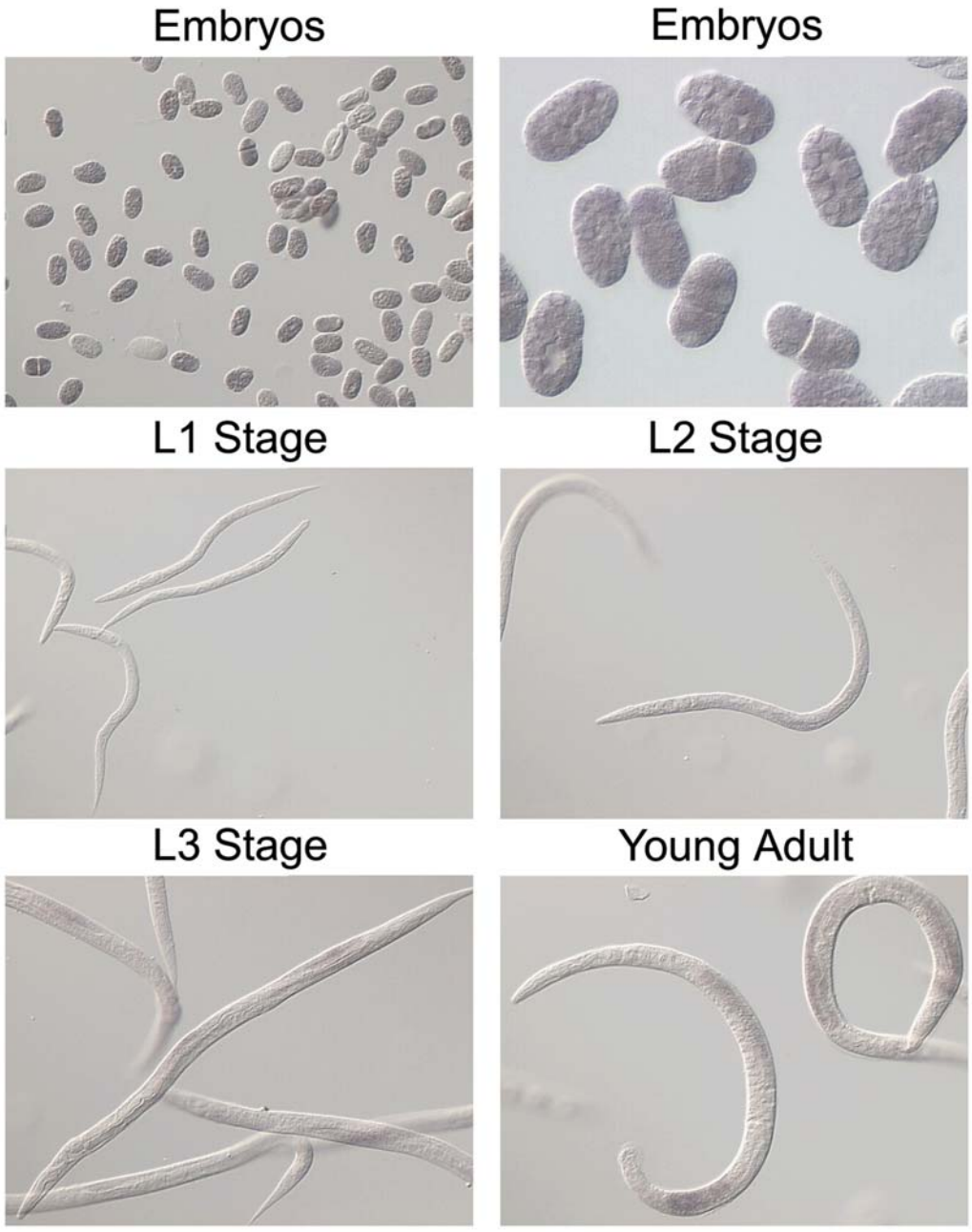

Discussion

Our analysis of H27M09.1 reveals it plays a role in germline development. Elimination of H27M09.1 results in sterility at high temperatures and reduced brood size at permissive temperatures, much like the effects seen when *glh-1* is eliminated. The *in situ* data suggests that H27M09.1 RNA is present in the germline from the later larval stages, which corresponds with the fertility defects we see upon its elimination. Our northern data suggest that H27M09.1 RNA, though it may be enhanced in the germline, is probably found in somatic tissues as well. Therefore, despite its similarity to GLH proteins, proximity to *glh-1*, and sterility phenotype, we cannot call H27M09.1 a germline RNA helicase (GLH).

Sequence comparisons find that H27M09.1 similar to the *Drosophila* protein *Abstrakt* (*Abs-1*) having 94% similarity to that protein. We therefore think it is more appropriate to name H27M09.1 *abs-1*. Though Abstrakt has not yet been shown to have any role in *Drosophila* germline development, it has not been ruled out. In flies, *Abstrakt* plays a role in development of the visual system, a tissue not found in *C. elegans* (Irion and Leptin 1999; Schmucker et al. 2000; Irion et al. 2004). It is therefore possible that ABS-1 in worms and *Abstakt* in flies may have similar functions, perhaps with their main biochemical functions being carried out in different tissues in these two model organisms.

Appendix 3 CYE-1

Introduction

Our work examining the phenotype of *kgb-1(um3)* mutant worms has left many unanswered questions. As we do not know the precise function of the GLH proteins, it is difficult to rationalize how excess GLH could lead to sterility, specifically endoreplication of oocytes, a phenotype that would suggest defects in the cell cycle. As possible transcriptional regulators, a scenario could be envisioned in which the translation of a cell cycle regulator is perturbed because of too much GLH. An alternative explanation could be that KGB-1 may have other targets along with the GLHs, possibly including cell cycle regulators.

JNK kinases have been shown to have roles in life span regulation, response to heavy metals, body movement, innate immunity, and temperature stress (Villanueva et al. 2001; Mizuno et al. 2004; Mattila et al. 2005; Wang et al. 2005). The regulation by these varied stimuli must require coordination of signals by upstream activators. As the *C. elegans* genome contains relatively few MAP kinases, the presence of MAPKKs, and MAPKKs may add to the diversity, with the number of signaling pathways feeding into any one MAPK could be many and varied though combinations of different MAPKs, MAPKKs, and MAPKKKs (Stronach 2005).

In our search to understand the *kgb-1(um3)* phenotype of temperature sensitive sterility, we began to explore other possible germline targets of KGB-1 regulation. Cyclin E (CYE-1), a well conserved regulator of cell cycle progression is present in the *C. elegans* germline and elsewhere (Fay and Han 2000). CYE-1 is found in the nucleus of germ cells in mitosis, levels of CYE-1 fall off and the CYE-1 protein reappears in germ cell nuclei around diakinesis (Brodigan et al. 2003). This later expression corresponds well to the stage at which we see problems developing in *kgb-1(um3)* worms. It has also been shown in *Drosophila* that the over-expression of one copy of cyclin E can cause an extra round of DNA replication (Richardson et al. 1995). Certain cells normally endoreplicate during development, such as the gut cells of *C. elegans*, giant cells of the vertebrate trophoblast, and salivary glands of flies; all of these functions require cyclin E (Sauer et al. 1995; Fay and Han 2000; Brodigan et al. 2003; Geng et al. 2003; Parisi et al. 2003). Regulation of cyclin proteins by degradation has been well established in many organisms (Whitfield et al. 1990; Kobayashi et al. 1991; Doronkin et al. 2003; Ye et al. 2004). Therefore, we decided to examine CYE-1 in *kgb-1(um3)* mutants to see if increases in CYE-1 could be responsible for the endoreplication phenotype we see in these mutants.

Materials and Methods

Strains

C. elegans strains used for this section inclue N2 Bristol (wild type) strain and *kgb-1(um3)* (Smith et al. 2002).

Cloning into pFastBac and baculovirus generation

For future use in pull-down analysis, CYE-1 was cloned into pFastBac in frame with a GST tag. We obtained the CYE-1 cDNA from Ed Kipreos in the pCR2.1 plasmid; which was digested with with EcoRI. A pFastBac vector with GST was created by Pliny Smith and named DEG 8-6; this vector was also digested with EcoRI and ligated to the CYE-1 EcoRI purified fragment. The resulting plasmid was sequenced to confirm that the CYE-1 coding sequence was in frame with the GST tag. Recombinant baculovirus was then produced as described in the Baculovirus Generation section of Chapter 2 Methods.

Results

To determine the effects of the *kgb-1(um3)* deletion on CYE-1 we first performed immunocytochemistry with αCYE-1 antibodies on N2 and sterile *kgb-1* worms raised at 26°C (Figure A.8). We found that CYE-1 seemed to be present earlier in the *kgb-1* gonad compared to wild type and there seemed to be more CYE-1 positive nuclei in the *kgb-1* gonad. We found that clusters of CYE-1-positive nuclei were found near large EMO nuclei (Figure A.8 arrow).

To validate the increased CYE-1 observed in *kgb-1* gonads, we performed western blot analysis to examine CYE-1 levels in N2 and *kgb-1* worms (Figure A.9). We find that there is more CYE-1 in *kgb-1* raised at 26°C compared to N2s, when equal numbers of worms are examined. Analysis of the CYE-1 protein sequence identified a consensus MAPK docking site and a phosphodegron with a serine substituted for the consensus threonine.

If the increased CYE-1 is the cause of EMO in *kgb-1* worms, we reasoned that decreasing CYE-1 levels in *kgb-1* worms might eliminate EMO, perhaps restoring fertility. We attempted *cye-1* RNAi by injection and soaking of worms. Even using dilute RNA, both of these types of experiments resulted in complete lethality in N2 and *kgb-1* worms treated with *cye-1* dsRNA. Therefore we were unable to assess the role excess CYE-1 has on fertility. Cloning of *cye-1* into an RNAi feeding vector may allow for this analysis, but it is not certain this experiment would be any more fruitful than those we have already attempted.

Figure A3.1: CYE-1 in N2 and *kgb-1* extruded gonads. N2 and *kgb-1* worms were stained for CYE-1 and DAPI, the two channels were merged, bottom. More CYE-1 positive nuclei are present in *kgb-1* worms.

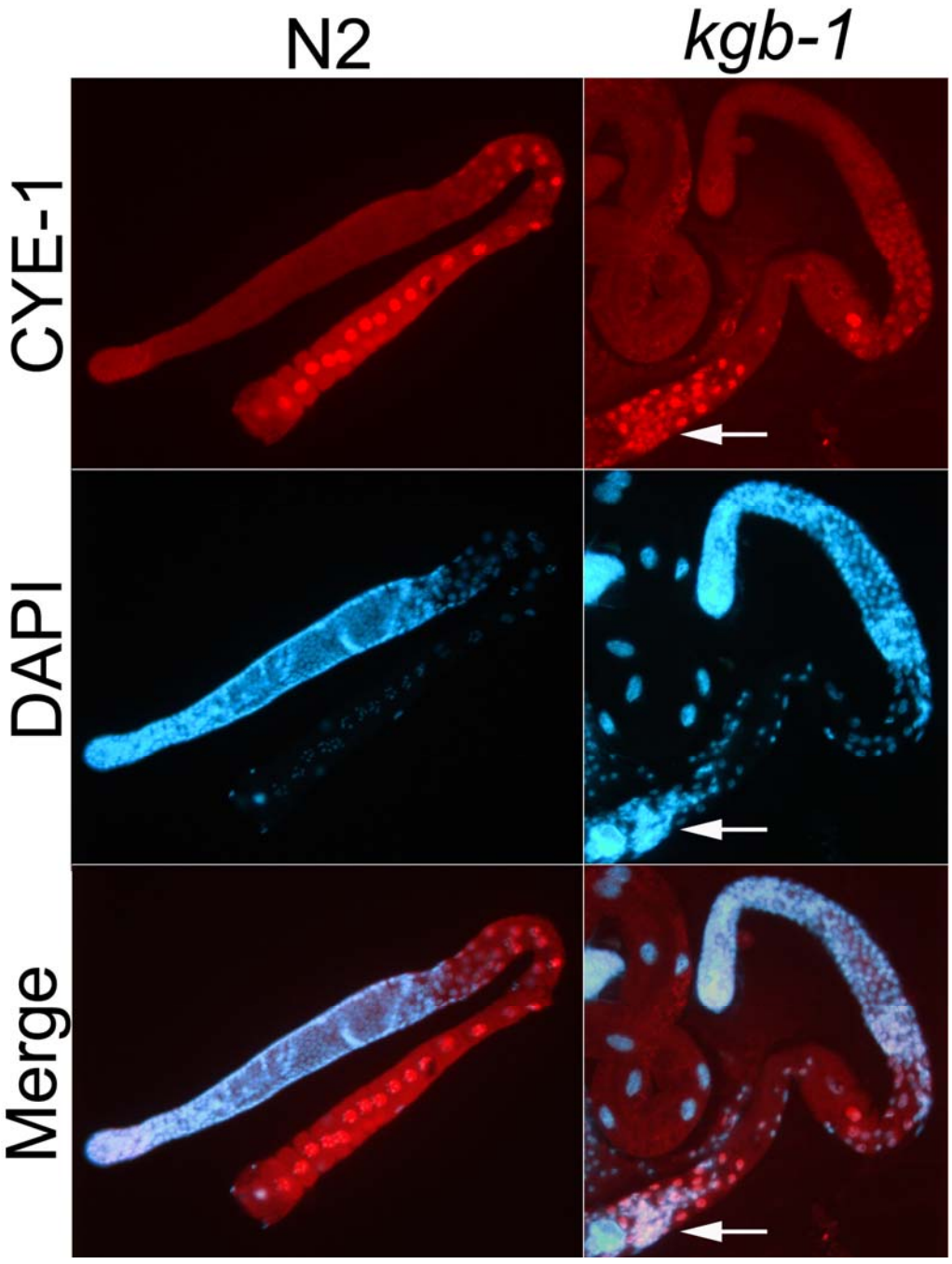

Figure A3.2: CYE-1 is elevated in *kgb-1* worms. Top: western blot analysis of 100 N2 or *kgb-1* worms raised at 26°C, with levels of CYE-1 analyzed. Bottom: CYE-1 protein sequence. Putative phosphodegron in yellow, non-consensus site with the substitution of a serine for consensus threonine. Serine could still serve as a phosphorylation for dual specificity kinases such as KGB-1 (serine/threonine kinase). Consensus MAPK docking site indicated in red.

Top

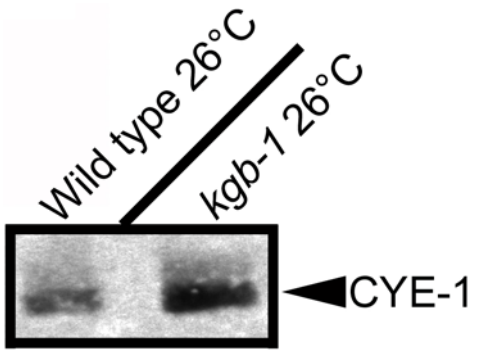

Bottom

MAGRKSSRTA ERVPTTQKPE RKSAILSPHD ELRERLLETA IDMKENIPQR NTRNSSVGSQ KSDCSETRKR RSTKEGPAAK
RHSGEKHRNG SREDSLEYIS EYSDDREVGS SSSQSSRTRG QPLPAMPEEE EVFDKSSSSD NLAESEESHE MVRLEERQDI
EEEIEDDFDD EEEDVVNDKE EYEEIESEDE DDYPVQNEGF AVTKRLMNDE HMVTAPTFLS TAKCDGIGSP TKVWSLMVKR

$X_{(1-4)}$
V

DEIPRATRFL LGNHPDMDDE KRRILIDWMM EVCESEKLHR ETFHLAVDYV DRYLESSNVE CSTDNFQLVG TAALFIAAKY
EEIYPPKCID FAHLTDSAFT CDNIRTMEVL IVKYIGWSLG PITSIQWLST YLQLLGTGKK NKSDHYEEQN MYVPELLRSE
YLEMCKILDF LLFEIDSFTF SYRTIAAAVL FVNYEPTCAV EKATGFMQAQ LEKVIEYVEP VCRAFAKQRQ LLDDVIPKHE
SIKSDDSHNI QVYVKRSSME PIVKSERERI QHLKARRLHP QRLF

With the presence of a D site and phosphodegron in CYE-1, and an increase in CYE-1 levels in *kgb-1* worms, we would like to determine if CYE-1 and KGB-1 physically interact. To this end, CYE-1 has been cloned in frame with a 6-His tag in pFastBac vector, and recombinant baculovirus produced. This construct will allow for GST pull-downs with KGB-1 to determine if the two proteins physically interact.

Discussion

Here we present evidence that CYE-1 levels are increased in the *kgb-1(um3)* mutant background. We find increased numbers of CYE-1 positive nuclei in extruded gonads from *kgb-1* worms, corresponding with EMO nuclei. Western blot analysis also shows increased levels of CYE-1 in *kgb-1* worms raised at 26°C compared to their wild type counterparts. CYE-1 has both a MAPK docking site and a possible phosphodegron; although the phosphodegron has a threonine to serine substitution thereby not perfectly matching consensus, it is still possible this site could function with kinases like KGB-1 that can phosphorylate both serine and threonine residues.

Our attempt to knock-down CYE-1 levels in both N2 and *kgb-1* worms resulted in lethality, suggesting a vital role for CYE-1 in *C. elegans*. We were, therefore, unable to determine if the EMO phenotype of *kgb-1* worms could be averted if CYE-1 levels were decreased. In *Drosophila*, Cyclin E levels are regulated through ubiquitination mediated by the COP9 signalosome (Doronkin et al. 2003). As KGB-1 has been shown to associate with CSN-5 in *C. elegans* and cyclin E has been shown to associate with the CSN in *Drosophila*, KGB-1 and CSN-5 could cooperatively regulate protein levels of CYE-1 in *C. elegans* as they are proposed to do for GLH-1.

References Cited

Aravind, L., V. M. Dixit and E. V. Koonin (2001). "Apoptotic molecular machinery: vastly increased complexity in vertebrates revealed by genome comparisons." Science **291**(5507): 1279-84.

Bech-Otschir, D., R. Kraft, X. Huang, P. Henklein, B. Kapelari, C. Pollmann and W. Dubiel (2001). "COP9 signalosome-specific phosphorylation targets p53 to degradation by the ubiquitin system." EMBO Journal **20**: 1630-1639.

Berse, M., M. Bounpheng, X. Huang, B. Christy, C. Pollmann and W. Dubiel (2004). "Ubiquitin-dependent degradation of Id1 and Id3 is mediated by the COP9 signalosome." Journal of Molecular Biology **343**: 361-370.

Brenner, S. (1974). "The genetics of *Caenorhabditis elegans*." Genetics **77**: 71-94.

Brodigan, T. M., J. Liu, M. Park, E. T. Kipreos and M. Krause (2003). "Cyclin E expression during development in *Caenorhabditis elegans*." Developmental Biology **254**: 102-115.

Chomczynski, P. and N. Sacchi (1987). "Single-step method of RNA isolation by acid guanidinium thiocyanate-phenol-chloroform extraction." Annals of Biochemistry **162**: 156-159.

Consortium, *C. e.* S. (1998). "Genome sequence of the nematode *C. elegans*: a platform for investigating biology." Science **282**: 2012-2018.

Cope, G. A. and R. J. Deshaies (2003). "COP9 signalosome: a multifunctional regulator of SCF and other cullin-based ubiquitin ligases." Cell **114**: 663-671.

Cordin, O., J. Banroques, N. K. Tanner and P. Linder (2006). "The DEAD-box protein family of RNA helicases." Gene **367**: 17-37.

Crittenden, S. L., C. R. Eckmann, L. Wang, D. S. Bernstein, M. Wickens and J. Kimble (2003). "Regulation of the mitosis/meiosis decision in the *Caenorhabditis elegans* germline." Philos Trans R Soc Lond B Biol Sci **358**(1436): 1359-62.

Doronkin, S., I. Djagaeva and S. K. Beckendorf (2002). "*CSN5/Jab1* mutations affect axis formation in the *Drosophila* oocyte by activating a meiotic checkpoint." Development **129**: 5053-5064.

Doronkin, S., I. Djagaeva and S. K. Beckendorf (2003). "The COP9 signalosome promotes degradation of cyclin E during early *Drosophila* oogenesis." Developmental Cell **4**: 699-710.

El-Shemerly, M., P. Janscak, D. Hess, J. Jiricny and S. Ferrari (2005). "Degradation of human exonuclease 1b upon DNA synthesis inhibition." Cancer Res **65**(9): 3604-9.

Epstein, H. F. and D. C. Shakes (1995). *Caenorhabditis elegans*: Modern Biological Analysis of an Organism. Methods in Cell Biology. San Diego, CA, Academic Press.

Fay, D. S. and M. Han (2000). "Mutations in *cye-1*, a *Caenorhabditis elegans* cyclin E homolog, reveal coordination between cell-cycle control and vulval development." Development **127**(18): 4049-60.

Gavis, E. R., L. Lunsford, S. E. Bergsten and R. Lehmann (1996). "A conserved 90 nucleotide element mediates translational repression of *nanos* RNA." Development **122**: 2791-2800.

Geng, Y., Q. Yu, E. Sicinska, M. Das, J. E. Schneider, S. Bhattacharya, W. M. Rideout, R. T. Bronson, H. Gardner and P. Sicinski (2003). "Cyclin E ablation in the mouse." Cell **114**(4): 431-43.

Gruidl, M. E., P. A. Smith, K. A. Kuznicki, J. S. McCrone, J. Kirchner, S. Strome and K. L. Bennett (1996). "Multiple potential germline helicases are components of the germline-specific P granules of *Caenorhabditis elegans*." Proceedings of the National Academy of Sciences USA **93**: 13837-13842.

Gumienny, T. L., E. Lambie, E. Hartwieg, H. R. Horvitz and M. O. Hengartner (1999). "Genetic control of programmed cell death in the *Caenorhabditis elegans* hermaphrodite germline." Development **126** 1011-1022.

Hay, B., L. Ackerman, S. Barbel, L. Y. Jan and Y. N. Jan (1988). "Identification of a component of *Drosophila* polar granules." Development **103**: 625-640.

Hay, B., L. Y. Jan and Y. N. Jan (1988). "A protein component of *Drosophila* polar granules is encoded by *vasa* and has extensive sequence similarity to ATP-dependent helicases." Cell **55**: 577-587.

Hermann, G. J., L. K. Schroeder, C. A. Hieb, A. M. Kershner, B. M. Rabbitts, P. Fonarev, B. D. Grant and J. R. Priess (2005). "Genetic analysis of lysosomal trafficking in *Caenorhabditis elegans*." Molecular Biology of the Cell **16**(7): 3273-88.

Hodgkin, J., H. R. Horvitz, B. R. Jasny and J. Kimble (1998). "*C. elegans*: sequence to biology." Science **282**: 2011.

Illmensee, K. and A. P. Mahowald (1975). "The autonomous function of germ plasm in a somatic region of the *Drosophila* egg." Experimental Cell Research **97**: 127-140.

Irion, U. and M. Leptin (1999). "Developmental and cell biological functions of the *Drosophila* DEAD-box protein *abstrakt*." Current Biology **9**(23): 1373-81.

Irion, U., M. Leptin, K. Siller, S. Fuerstenberg, Y. Cai, C. Q. Doe, W. Chia and X. Yang (2004). "*Abstrakt*, a DEAD box protein, regulates Insc levels and asymmetric division of neural and mesodermal progenitors." Curr Biol **14**(2): 138-44.

Jacobs, D., D. Glossip, H. Xing, A. J. Muslin and K. Kornfeld (1999). "Multiple docking sites on substrate proteins form a modular system that mediates recognition by ERK MAP kinase." Genes & Development **13**: 163-175.

Jonas, B. A. and M. L. Privalsky (2004). "SMRT and N-CoR corepressors are regulated by distinct kinase signaling pathways." Journal of Biological Chemistry **279**(52): 54676-86.

Kawasaki, I., Y. H. Shim, J. Kirchner, J. Kaminker, W. B. Wood and S. Strome (1998). "PGL-1, a predicted RNA-binding component of germ granules, is essential for fertility in *C. elegans*." Cell **94**: 635-645.

Kim, D. H., R. Feinbaum, G. Alloing, F. E. Emerson, D. A. Garsin, H. Inoue, M. Tanaka-Hino, N. Hisamoto, K. Matsumoto, M. W. Tan and F. M. Ausubel (2002).

"A conserved p38 MAP kinase pathway in *Caenorhabditis elegans* innate immunity." Science **297**: 623-626.

Kim, D. H., N. T. Liberati, T. Mizuno, H. Inoue, N. Hisamoto, K. Matsumoto and F. M. Ausubel (2004). "Integration of *Caenorhabditis elegans* MAPK pathways mediating immunity and stress resistance by MEK-1 MAPK kinase and VHP-1 MAPK phosphatase." Proceedings of the National Academy of Sciences **101**: 10990-10994.

Kobayashi, H., J. Minshull, C. Ford, R. Golsteyn, R. Poon and T. Hunt (1991). "On the synthesis and destruction of A- and B-type cyclins during oogenesis and meiotic maturation in *Xenopus laevis* " Journal of Cell Biology **114**: 755-765.

Koga, M., R. Zwaal, K. L. Guan, L. Avery and Y. Ohshima (2000). "A *Caenorhabditis elegans* MAP kinase kinase, MEK-1, is involved in stress responses." EMBO J. **19**: 5148-5156.

Kuznicki, K. A. (2000). The function of the germline RNA helicase (GLHs) genes in *Caenorhabditis elegans*. PhD Dissertation University of Missouri-Columbia.

Kuznicki, K. A., P. A. Smith, W. M. Leung-Chiu, A. O. Estevez, H. C. Scott and K. L. Bennett (2000). "Combinatorial RNA interference indicates GLH-4 can compensate for GLH-1; these two P granule components are critical for fertility in *C. elegans* " Development **127**: 2907-2916.

Kwok, S. F., R. Solano, T. Tsuge, D. A. Chamovitz, J. R. Ecker, M. Matsui and X. W. Deng (1998). "*Arabidopsis* homologs of a c-Jun coactivator are present both in monomeric form and in the COP9 complex, and their abundance is differentially affected by the pleiotropic *cop/det/fus* mutations." The Plant Cell **10** 1779-1790.

Lasko, P. F. and M. Ashburner (1988). "The product of the *Drosophila* gene *vasa* is very similar to eukaryotic initiation factor-4A." Nature **335**: 611-617.

Lee, S. W., G. Dai, Z. Hu, X. Wang, J. Du and W. E. Mitch (2004). "Regulation of muscle protein degradation: coordinated control of apoptotic and ubiquitin-proteasome systems by phosphatidylinositol 3 kinase." Journal of the American Society of Nephrology **15**(6): 1537-1545.

Li, S., C. M. Armstrong, N. Bertin, H. Ge, S. Milstein, M. Boxem, P. O. Vidalain, J. D. Han, A. Chesneau, T. Hao, D. S. Goldberg, N. Li, M. Martinez, J. F. Rual, P. Lamesch, L. Xu, M. Tewari, S. L. Wong, L. V. Zhang, G. F. Berriz, L. Jacotot, P. Vaglio, J. Reboul, T. Hirozane-Kishikawa, Q. Li, H. W. Gabel, A. Elewa, B. Baumgartner, D. J. Rose, H. Yu, S. Bosak, R. Sequerra, A. Fraser, S. E. Mango, W. M. Saxton, S. Strome, S. Van Den Heuvel, F. Piano, J. Vandenhaute, C. Sardet, M. Gerstein, L. Doucette-Stamm, K. C. Gunsalus, J. W. Harper, M. E. Cusick, F. P. Roth, D. E. Hill and M. Vidal (2004). "A map of the interactome network of the metazoan *C. elegans*." Science **303**(5657): 540-543.

Maeda, I., Y. Kohara, M. Yamamoto and A. Sugimoto (2001). "Large-scale analysis of gene function in *Caenorhabditis elegans* by high-throughput RNAi." Current Biology **11**: 171-176.

Mahowald, A. P. (1971). "Polar granules of *Drosophila*. IV. Cytochemical studies showing loss of RNA from polar granules during early stages of embryogenesis." Journal of Experimental Zoology **176**: 345-352.

Mattila, J., L. Omelyanchuk, S. Kyttala, H. Turunen and S. Nokkala (2005). "Role of Jun N-terminal kinase (JNK) signaling in the wound healing and regeneration of a *Drosophila melanogaster* wing imaginal disc." International Journal of Developmental Biology **49**: 391-399.

Michelsen, J. W., K. L. Schmeichel, M. C. Beckerle and D. R. Winge (1993). "The LIM motif defines a specific zinc-binding protein domain." Proceedings of the National Academy of Sciences USA **90**: 4404-4408.

Mizuno, T., N. Hisamoto, T. Terada, T. Kondo, M. Adachi, E. Nishida, D. H. Kim, F. M. Ausubel and K. Matsumoto (2004). "The *Caenorhabditis elegans* MAPK phosphatase VHP-1 mediates a novel JNK-like signaling pathway in stress response." EMBO J.: 1-9.

Naumann, M., D. Bech-Otschir, X. Huang, K. Ferrell and W. Dubiel (1999). "COP9 signalosome-directed c-Jun activation/stabilization is independent of JNK." Journal of Biological Chemistry **274**: 35297-35300.

Nishi, Y. and R. Lin (2005). "DYRK2 and GSK-3 phosphorylate and promote the timely degradation of OMA-1, a key regulator of the oocyte-to-embryo transition in *C. elegans*." Developmental Biology **288**(1): 139-149.

Orlicky, S., X. Tang, A. Willems, M. Tyers and F. Sicheri (2003). "Structural basis for phosphodependent substrate selection and orientation by the SCF Cdc4 ubiquitin ligase." Cell **112**: 243-256.

Oron, E., M. Mannervik, S. Rencus, O. Harari-Steinberg, S. Neuman-Silberberg, D. Segal and D. A. Chamovitz (2002). "COP9 signalosome subunits 4 and 5 regulate multiple pleiotropic pathways in *Drosophila melanogaster* " Development **129**: 4399-4409.

Oron, E., M. Mannervik, S. Rencus, O. Harari-Steinberg, S. Neuman-Silberberg, D. Segal and D. A. Chamovitz (2002). "COP9 signalosome subunits 4 and 5 regulate multiple pleiotropic pathways in *Drosophila melanogaster*." Development **129**(19): 4399-4409.

Parisi, T., A. R. Beck, N. Rougier, T. McNeil, L. Lucian, Z. Werb and B. Amati (2003). "Cyclins E1 and E2 are required for endoreplication in placental trophoblast giant cells." EMBO J **22**(18): 4794-4803.

Pellettieri, J., V. Reinke, S. K. Kim and G. Seydoux (2003). "Coordinate activation of maternal protein degradation during the egg-to-embryo transition in *C. elegans*." Developmental Cell **5** 451-462.

Pintard, L., T. Kurz, S. Glaser, J. H. Willis, M. Peter and B. Bowerman (2003). "Neddylation and deneddylation of CUL-3 is required to target MEI-1/katanin for degradation at the meiosis-to-mitosis transition in *C. elegans*." Current Biology **13**: 911-921.

Pitt, J. N., J. A. Schisa and J. R. Priess (2000). "P granules in the germ cells of *Caenorhabditis elegans* adults are associated with clusters of nuclear pores and contain RNA." Developmental Biology **219**: 315-333.

Ramaswamy, N. T., B. K. Dalley and J. F. Cannon (1998). "Analysis of protein interactions between protein phosphatase 1 and noncatalytic subunits using the yeast two-hybrid assay." Methods Mol Biol **93**: 251-61.

Reese, K. J., M. A. Dunn, J. A. Waddle and G. Seydoux (2000). "Asymmetric segregation of PIE-1 in *C. elegans* is mediated by two complementary mechanisms that act through separate PIE-1 protein domains." Mol.Cell **6**: 445-455.

Reinke, V., H. E. Smith, J. Nance, J. Wang, C. Van Doren, R. Begley, S. J. Jones, E. B. Davis, S. Scherer, S. Ward and S. K. Kim (2000). "A global profile of germline gene expression in *C. elegans*." Molecular Cell **6**: 605-616.

Richardson, H., L. V. O'Keefe, T. Marty and R. Saint (1995). "Ectopic cyclin E expression induces premature entry into S phase and disrupts pattern formation in the *Drosophila* eye imaginal disc." Development **121**(10): 3371-3379.

Rocak, S. and P. Linder (2004). "DEAD-box proteins: the driving forces behind RNA metabolism." Nature Reviews. Molecular Cell Biology **5**(3): 232-241.

Roussell, D. L. and K. L. Bennett (1993). "*glh-1*: A germline putative RNA helicase from *Caenorhabditis* has four zinc fingers." Proceedings of the National Academy of Sciences USA **90**: 9300-9304.

Sakaguchi, A., K. Matsumoto and N. Hisamoto (2004). "Roles of MAP kinase cascades in *Caenorhabditis elegans*." J Biochem (Tokyo) **136**(1): 7-11.

Sanchez-Garcia, I. and T. H. Rabbitts (1993). "LIM domain proteins in leukemia and development." Seminars in Cancer Biology **4**: 349-358.

Sauer, K., J. A. Knoblich, H. Richardson and C. F. Lehner (1995). "Distinct modes of cyclin E/cdc2c kinase regulation and S-phase control in mitotic and endoreduplication cycles of *Drosophila* embryogenesis." Genes and Development **9**(11): 1327-1339.

Schisa, J. A., J. N. Pitt and J. R. Priess (2001). "Analysis of RNA associated with P granules in germ cells of *C. elegans* adults." Development **128**: 1287-1298.

Schmucker, D., G. Vorbruggen, P. Yeghiayan, H. Q. Fan, H. Jackle and U. Gaul (2000). "The Drosophila gene abstrakt, required for visual system development, encodes a putative RNA helicase of the DEAD box protein family." Mech Dev **91**(1-2): 189-96.

Seeger, M., R. Kraft, K. Ferrell, D. Bech-Otschir, R. Dumdey, R. Schade, C. Gordon and M. Naumann (1998). "A novel protein complex involved in signal transduction possessing similarities to 26S proteasome subunits." FASEB Journal **12**: 469-478.

Smith, P. A. (2001). Physical properties of the germ line RNA helicases (GLHs) in *Caenorhabditis elegans*. PhD Dissertation. , University of Missouri-Columbia.

Smith, P. A., W. M. Leung-Chiu, R. Montgomery, A. Orsborn, K. A. Kuznicki, E. Gressman-Coberly, L. Mutapcic and K. L. Bennett (2002). "The GLH proteins, *Caenorhabditis elegans* P granule components, associate with CSN-5 and KGB-1, proteins necessary for fertility, and with ZYX-1, a predicted cytoskeletal protein." Developmental Biology **251**: 333-347.

Stronach, B. (2005). "Dissecting JNK signaling, one KKKinase at a time." Developmental Dynamics **232**: 575-584.

Styhler, S., A. Nakamura, A. Swan, B. Suter and P. Lasko (1998). "*vasa* is required for GURKEN accumulation in the oocyte, and is involved in oocyte differentiation and germline cyst development." Development **125**: 1569-1578.

Sulston, J. E., E. Schierenberg, J. G. White and J. N. Thomson (1983). "The embryonic cell lineage of the nematode *Caenorhabditis elegans*." Developmental Biology **100**: 64-119.

Sun, Y., M. P. Wilson and P. W. Majerus (2002). "Inositol 1,3,4-trisphosphate 5/6-kinase associates with the COP9 signalosome by binding to CSN1." Journal of Biological Chemistry **277**: 45759-45764.

Tomancak, P., A. Guichet, P. Zavorszky and A. Ephrussi (1998). "Oocyte polarity depends on regulation of *gurken* by *Vasa*." Development **125**(9): 1723-1732.

Tomoda, K., Y. Kubota and J. Kato (1999). "Degradation of the cyclin-dependent-kinase inhibitor p27Kip1 is instigated by Jab1." Nature **398**: 160-165.

Uhle, S., O. Medalia, R. Waldron, R. Dumdey, P. Henklein, D. Bech-Otschir, X. Huang, M. Berse, J. Sperling, R. Schade and W. Dubiel (2003). "Protein kinase CK2 and protein kinase D are associated with the COP9 signalosome." Embo Journal **22**: 1302-1312.

Villanueva, A., J. Lozano, A. Morales, X. Lin, X. Deng, M. O. Hengartner and R. N. Kolesnick (2001). "*jkk-1* and *mek-1* regulate body movement coordination and response to heavy metals through *jnk-1* in *Caenorhabditis elegans* " The EMBO Journal **20**: 5114-5128.

Wang, M. C., D. Bohmann and H. Jasper (2005). "JNK extends life span and limits growth by antagonizing cellular and organism-wide responses to insulin signaling." Cell **121**: 115-125.

Watanabe, N., H. Arai, Y. Nishihara, M. Taniguchi, N. Watanabe, T. Hunter and H. Osada (2004). "M-phase kinases induce phospho-dependent ubiquitination of somatic Wee1 by SCFbeta-TrCP." Proceedings of the National Academy of Sciences USA **101**(13): 4419-24.

Whitfield, W. G., C. Gonzalez, G. Maldonado-Codina and D. M. Glover (1990). "The A- and B-type cyclins of *Drosophila* are accumulated and destroyed in temporally distinct events that define separable phases of the G2-M transition. ." EMBO Journal **9**: 2563-2572.

Wolf, N., J. Priess and D. Hirsh (1983). "Segregation of germline granules in early embryos of *Caenorhabditis elegans*: an electron microscopic analysis." Journal of Embryology & Experimental Morphology **73**: 297-306.

Wood, W. B. (1988). The Nematode *Caenorhabditis elegans*. Cold Spring Harbor, NY, Cold Spring Harbor Laboratory.

Yandell, M. D., L. G. Edgar and W. B. Wood (1994). "Trimethylpsoralen induces small deletion mutations in *Caenorhabditis elegans*." Proceedings of the National Academy of Sciences USA **91**: 1381-1385.

Ye, X., G. Nalepa, M. Welcker, B. M. Kessler, E. Spooner, J. Qin, S. J. Elledge, B. E. Clurman and J. W. Harper (2004). "Recognition of phosphodegron motifs in human cyclin E by the SCF Fbw7 ubiquitin ligase." Journal of Biological Chemistry **279**: 50110-50119.

VITA

Born March 6, 1978 in O'Neill, Nebraska to parents Pamela and Robert, April Marie Orsborn attended elementary schools in Nebraska, Illinois, Michigan and Kentucky. At the age of 12 April moved with her family to Missouri and attended Warrenton Junior High school. After moving once again, April graduated from Jefferson City High School in 1996. April received B.A. and B.S. degrees in Biology from Truman State University in Kirksville, Missouri. April was accepted to the PhD program in Molecular Microbiology and Immunology at the University of Missouri-Columbia in 2000. On April 10, 2006, April successfully defended her dissertation and was subsequently awarded her PhD.